

ANTAL KERPELY DOCTORAL SCHOOL OF MATERIALS SCIENCE & TECHNOLOGY



Polymer Composites for Energy Applications (Polyurethanes of Increased Heat Conductivity)

A PhD dissertation submitted to Antal Kerpely Doctoral School for the degree of
Doctor of Philosophy in the subject of Materials Science and Technology

By

Patcharapon Somdee

Supervisors

Dr. Kálmán Marossy

Professor Emeritus

Dr. János Erdélyi

Associate Professor

Head of the Doctoral School

Prof. Gacsi Zoltan

Institute of Ceramic and Polymer Engineering

Faculty of Materials Science and Engineering

University of Miskolc

Hungary, 2020

ACKNOWLEDGMENTS

First and foremost, I would like to express my deep and sincere gratitude to my supervisor Prof. Dr. Kálmán Marossy who gave me the feeling of the very good teacher for his teach throughout the course of this study, guidance in everything, encouragement and support. Apart from my Ph.D. works, he also gave me a wide knowledge and experience in the polymer industrial. He always makes me stress less by his great sense of humor that made me learn more about European jokes.

I am also grateful to my co-supervisor Assoc. Prof. Dr. János Erdélyi for his advice and support for my work and dissertation. He provided me good advice to make my work better and complete. My sincere thanks also go to Assoc. Prof. Dr. Tamás József Szabó for always give me insightful comments about my report and some interest questions.

I would like to express my special thanks to my colleagues, Tímea Lassú-Kuknyó, Csaba Kónya and José Trujillo Vilaboy at BosodChem Zrt., for provided me professional guidance, support and generous advice at several stages of my research. They were so helpful and provided me completed guidance about Hungary which has a different culture with my country. I was fortunate to work with all of them.

My thanks go to the faculty and staff members of the Institute of Ceramic and Polymer Engineering, University of Miskolc for their help and suggestion. Special thanks to Ágnes Solczi for her friendship and empathy not only about the Ph.D. study.

I am extending my thanks to Rajamangala University of Technology Isan (Nakhon Ratchasima) for giving me this good opportunity and financial support to study Ph.D. in Hungary.

Special thanks are extended for all friends for their kindness, help, and encouragement.

Finally, I owe my loving thanks and deep sense of gratitude to my sibling and my parents, Mr. Pamorn and Mrs. Boasorn Somdee, for their loving support and encouragement me throughout the course of Ph.D. at the University of Miskolc.

TABLE OF CONTENTS

ACKNOWLEDGMENTS	I
TABLE OF CONTENTS	II
LIST OF FIGURES AND TABLES	VI
LIST OF ABBREVIATIONS AND NOTATIONS	XII
CHAPTERS	
1 Introduction	1
2 Theoretical Background and Literature Overview	3
2.1 Fundamental on thermal conductivity.....	3
2.1.1 Thermal conductivity of polymer and its composites.....	5
2.2 Fundamental on polyurethanes.....	8
2.2.1 Polyols.....	11
2.2.1.1 Polyethers.....	12
2.2.1.2 Polyesters.....	12
2.2.2 Diisocyanates.....	13
2.2.3 Chain extender.....	13
2.3 Inorganic fillers with high thermal conductivity	14
2.3.1 Silicon carbide (SiC).....	14
2.3.2 Magnesium oxide (MgO).....	15
2.3.3 Zinc oxide (ZnO).....	16
2.4 Metallic fillers with high thermal conductivity.....	16
2.4.1 Copper (Cu).....	17
2.4.1.1 Electrolytic copper.....	17
2.5 Polymer and high thermal conductive composites.....	18
3 Experiment and Methodology	22
3.1 Materials.....	22
3.2 Preparation methods.....	24
3.3 Testing methods.....	27

4 Results and discussion	31
4.1 Polyurethane elastomers with different chain extender contents.....	31
4.1.1 Thermal conductivity and density.....	31
4.1.2 Mechanical properties.....	32
4.1.2.1 Hardness.....	33
4.1.2.2 Tensile properties.....	33
4.1.3 Thermal properties.....	35
4.1.4 Dynamic mechanical properties.....	37
4.1.5 Infrared spectroscopy (IR).....	39
4.1.6 Thermal stimulated discharge (TSD).....	41
4.1.7 Swelling properties.....	42
4.2 Flexible and rigid polyurethane elastomer with silicon carbide Composites.....	44
4.2.1 Thermal conductivity and density.....	44
4.2.2 Mechanical properties.....	47
4.2.2.1 Hardness.....	47
4.2.2.2 Tensile properties.....	49
4.2.3 Thermal properties.....	51
4.2.4 Dynamic mechanical properties.....	52
4.2.5 Infrared spectroscopy.....	56
4.2.6 Morphology.....	57
4.2.6.1 Particle size distribution and morphology of SiC particles....	57
4.2.6.2 Morphology of flexible and rigid polyurethane elastomers with SiC fillers.....	58
4.3 Flexible and rigid polyurethane elastomer with magnesium oxide composites.....	61
4.3.1 Thermal conductivity and density.....	61
4.3.2 Mechanical properties.....	62
4.3.2.1 Hardness.....	62
4.3.2.2 Tensile properties.....	64
4.3.3 Thermal properties.....	64

4.3.4	Dynamic mechanical properties.....	66
4.3.5	Infrared spectroscopy.....	66
4.3.6	Morphology.....	68
4.3.6.1	Particle size distribution and morphology of MgO particles..	68
4.3.6.2	Morphology of flexible and rigid polyurethane elastomers with MgO fillers.....	69
4.4	Flexible and rigid polyurethane elastomer with zinc oxide composites.....	71
4.4.1	Thermal conductivity and density.....	71
4.4.2	Mechanical properties.....	72
4.4.2.1	Hardness.....	72
4.4.2.2	Tensile properties.....	74
4.4.3	Thermal properties.....	75
4.4.4	Dynamic mechanical properties.....	76
4.4.5	Infrared spectroscopy.....	76
4.4.6	Morphology.....	77
4.4.6.1	Particle size distribution and morphology of ZnO particles...	77
4.4.6.2	Morphology of flexible and rigid polyurethane elastomers with ZnO fillers.....	78
4.5	Flexible and rigid polyurethane elastomer with copper composites.....	81
4.5.1	Thermal conductivity and density.....	81
4.5.2	Mechanical properties.....	83
4.5.2.1	Hardness.....	83
4.5.2.2	Tensile properties.....	83
4.5.3	Thermal properties.....	85
4.5.4	Dynamic mechanical properties.....	85
4.5.5	Infrared spectroscopy.....	88
4.5.6	Morphology.....	88
4.5.6.1	Particle size distribution and morphology of Cu particles.....	88
4.5.6.2	Morphology of flexible and rigid polyurethane elastomers with electrolytic Cu fillers.....	88

4.6 Comparing properties of polyurethane elastomers with different types and contents of fillers.....	91
5 Conclusions.....	95
5.1 Effect of chain extender content on polyurethane elastomers matrix.....	95
5.2 Flexible and rigid polyurethane elastomer with silicon carbide composites.....	95
5.3 Flexible and rigid polyurethane elastomer with magnesium oxide Composites.....	96
5.4 Flexible and rigid polyurethane elastomer with zinc oxide composites.....	96
5.5 Flexible and rigid polyurethane elastomer with copper composites.....	97
5.6 Comparing properties of polyurethane elastomers with different types and contents of fillers.....	97
NEW SCIENTIFIC RESULTS.....	99
LIST OF PUBLICATIONS.....	100
REFERENCES.....	102
APPENDIX A.....	112
APPENDIX B.....	117
APPENDIX C.....	122
APPENDIX D.....	127

LIST OF FIGURES AND TABLES

Figure 2.1 The schematic of thermal conductance in a crystalline material.....	6
Figure 2.2 Basic urethane group.....	9
Figure 2.3 Polyurethane alternating hard- and soft segment structure.....	10
Figure 3.1 SEM images of high thermal conductive fillers.....	24
Figure 3.2 Preparation diagram of polyurethane elastomers sheet.....	25
Figure 3.3 Preparation diagram of polyurethane elastomer composites sheet.....	26
Figure 3.4 SEM images of SiC (a), MgO (b), ZnO (c) and Cu with flexible PUR composites (nominal magnification of 150×).....	27
Figure 3.5 Show tensile specimens according to ISO 527 standard.....	29
Figure 3.6 Show typical stress-strain curve and tensile modulus determination.....	29
Figure 4.1 Thermal conductivity (a) and density (b) of polyurethane elastomers with different chain extender contents and thermal conductivity as a function of density (c).....	32
Figure 4.2 Shore A hardness (a) and Shore D hardness (b) of polyurethane elastomers with different chain extender contents.....	34
Figure 4.3 Tensile strength and elongation at break (a) and tensile modulus (b) of polyurethane elastomers with different chain extender contents.....	35
Figure 4.4 DSC curve of polyurethane elastomers with different chain extender contents...	36
Figure 4.5 E' and $\tan\delta$ of polyurethane elastomers with different chain extender contents...	38
Figure 4.6 IR spectra of polyurethane elastomers with different chain extender contents...	40
Figure 4.7 TSD spectra of pure polyurethane elastomers with different chain extender of 10 and 30 phr.....	42
Figure 4.8 Swelling degree of pure polyurethane elastomers with different chain extender of 10 and 30 phr (Independent variable is the solubility parameter of the solvent).....	43
Figure 4.9 Schematic arrangement of equal temperature gradient (a), equal heat flow Models (b) and represents a real dispersed two-phases system (c).....	45
Figure 4.10 Thermal conductivity of flexible (a) and rigid (b) polyurethane elastomers with different SiC contents.....	47

Figure 4.11 Thermal conductivity modelling of flexible (a) and rigid (b) polyurethane elastomers with different SiC contents.....	48
Figure 4.12 Density of flexible (a) and rigid (b) polyurethane elastomers with different SiC contents.....	48
Figure 4.13 Shore A and D hardness of flexible (a) and rigid (b) polyurethane elastomers with different SiC contents.....	49
Figure 4.14 Tensile strength and elongation at break (a) and tensile modulus (b) of flexible polyurethane elastomers with different SiC contents.....	50
Figure 4.15 Tensile strength and elongation at break (a) and tensile modulus (b) of rigid polyurethane elastomers with different SiC contents.....	50
Figure 4.16 DSC curve of flexible polyurethane elastomers with different SiC contents.....	52
Figure 4.17 DSC curve of rigid polyurethane elastomers with different SiC contents.....	53
Figure 4.18 Storage modulus and mechanical loss factor from DMA of flexible PUR with different SiC contents.....	54
Figure 4.19 Storage modulus and mechanical loss factor from DMA of rigid PUR with different SiC contents.....	55
Figure 4.20 IR spectra of flexible polyurethane elastomers with different SiC contents.....	57
Figure 4.21 IR spectra of rigid polyurethane elastomers with different SiC contents.....	58
Figure 4.22 Particle size distribution of silicon carbide particles.....	59
Figure 4.23 SEM image of silicon carbide particles (nominal magnification of 1000× and 5000×).....	59
Figure 4.24 SEM image of flexible PUR with different SiC contents (a) SiC 0 v/v%, (b) SiC 3.79 v/v%, (c) SiC 13.18 v/v% (nominal magnification of 500×) and (d) EDS chart.....	60
Figure 4.25 SEM image of rigid PUR with different SiC contents (a) SiC 0 v/v%, (b) SiC 3.97 v/v%, (c) SiC 13.75 v/v% (nominal magnification of 500×) and (d) EDS chart.....	60
Figure 4.26 Thermal conductivity of flexible (a) and rigid (b) polyurethane elastomers with different MgO contents.....	62
Figure 4.27 Thermal conductivity modelling of flexible (a) and rigid (b) polyurethane elastomers with different MgO contents.....	63

Figure 4.28 Density of flexible (a) and rigid (b) polyurethane elastomers with different MgO contents.....	63
Figure 4.29 Shore A and D hardness of flexible (a) and rigid (b) polyurethane elastomers with different MgO contents.....	64
Figure 4.30 Tensile strength, elongation at break (a) and tensile modulus (b) of flexible polyurethane elastomers with different MgO contents.....	65
Figure 4.31 Tensile strength, elongation at break (a) and tensile modulus (b) of rigid polyurethane elastomers with different MgO contents.....	65
Figure 4.32 Storage modulus and mechanical loss factor from DMA of flexible PUR with different MgO contents.....	67
Figure 4.33 Storage modulus and mechanical loss factor from DMA of rigid PUR with different MgO contents.....	68
Figure 4.34 SEM image of flexible PUR with different MgO contents (a) MgO 0 m/m%, (b) MgO 10 m/m%, (c) MgO 30 m/m% (nominal magnification of 500×) and (d) EDS chart.....	70
Figure 4.35 SEM image of rigid PUR with different MgO contents (a) MgO 0 m/m%, (b) MgO 10 m/m%, (c) MgO 26 m/m% (nominal magnification of 500×) and (d) EDS chart.....	70
Figure 4.36 Thermal conductivity of flexible (a) and rigid (b) polyurethane elastomers with different ZnO contents.....	72
Figure 4.37 Thermal conductivity modelling of flexible (a) and rigid (b) polyurethane elastomers with different ZnO contents.....	73
Figure 4.38 Density of flexible (a) and rigid (b) polyurethane elastomers with different ZnO contents.....	73
Figure 4.39 Shore A and D hardness of flexible (a) and rigid (b) polyurethane elastomers with different ZnO contents.....	74
Figure 4.40 Tensile strength, elongation at break (a) and tensile modulus (b) of flexible polyurethane elastomers with different ZnO contents.....	75
Figure 4.41 Tensile strength, elongation at break (a) and tensile modulus (b) of rigid polyurethane elastomers with different ZnO contents.....	75

Figure 4.42 Storage modulus and mechanical loss factor from DMA of flexible PUR with different ZnO contents.....	77
Figure 4.43 Storage modulus and mechanical loss factor from DMA of rigid PUR with different ZnO contents.....	78
Figure 4.44 SEM image of flexible PUR with different ZnO contents (a) ZnO 0 v/v%, (b) ZnO 2.20 v/v%, (c) ZnO 7.99 v/v% (nominal magnification of 500×) and (d) EDS chart.....	79
Figure 4.45 SEM image of rigid PUR with different ZnO contents (a) ZnO 0 v/v%, (b) ZnO 2.31 v/v%, (c) ZnO 6.96 v/v% (nominal magnification of 500×) and (d) EDS chart.....	80
Figure 4.46 Thermal conductivity of flexible (a) and rigid (b) PUR with different Cu Contents.....	82
Figure 4.47 Thermal conductivity modelling of flexible (a) and rigid (b) polyurethane elastomers with different electrolytic Cu contents.....	82
Figure 4.48 Density of flexible (a) and rigid (b) PUR with different Cu contents.....	83
Figure 4.49 Shore A and D hardness of flexible (a) and rigid (b) PUR with different Cu Contents.....	84
Figure 4.50 Tensile strength and elongation at break (a) and tensile modulus (b) of flexible PUR with different Cu contents.....	84
Figure 4.51 Tensile strength and elongation at break (a) and tensile modulus (b) of rigid PUR with different Cu contents.....	85
Figure 4.52 Storage modulus and mechanical loss factor from DMA of flexible PUR with different Cu contents.....	86
Figure 4.53 Storage modulus and mechanical loss factor from DMA of rigid PUR with different Cu contents.....	87
Figure 4.54 SEM image of flexible PUR with different Cu contents (a) Cu 0 v/v%, (b) Cu 0.39 v/v%, (c) Cu 1.71 v/v% (nominal magnification of 500×) and (d) EDS chart.....	89
Figure 4.55 SEM image of rigid PUR with different Cu contents (a) Cu 0 v/v%, (b) Cu 0.41 v/v%, (c) Cu 1.79 v/v% (nominal magnification of 500×) and (d) EDS chart.....	90

Figure 4.56 Comparing thermal conductivity of flexible PUR (a) and rigid PUR (b) with different the high thermal conductive fillers	92
Figure 4.57 Comparing density of flexible PUR (a) and rigid PUR (b) with different the high thermal conductive fillers	92
Figure 4.58 Comparing Shore A (a), Shore D hardness of flexible PUR and Shore A (c) and Shore D (d) of rigid PUR with different the high thermal conductive fillers.....	93
Figure 4.59 Comparing tensile strength of flexible PUR (a) and rigid PUR (b) with different the high thermal conductive fillers.....	94
Figure 4.60 Comparing tensile modulus of flexible PUR (a) and rigid PUR (b) with different the high thermal conductive fillers.....	94
Figure 4.61 Comparing elongation at break of flexible PUR (a) and rigid PUR (b) with different the high thermal conductive fillers.....	94
Table 2.1 Thermal conductivity of various electrically insulating materials at room temperatures.....	7
Table 3.1 Components of polyurethane elastomer composites formula.....	22
Table 4.1 Thermal conductivity and density of polyurethane elastomers with different chain extender contents.....	33
Table 4.2 Shore A and D hardness of polyurethane elastomers with different chain extender contents.....	34
Table 4.3 Tensile strength, elongation at break and tensile modulus of polyurethane elastomers with different chain extender contents.....	35
Table 4.4 Thermal properties of polyurethane elastomers with different chain extender Contents.....	37
Table 4.5 The glass transition temperature of the soft and hard segment of polyurethane elastomers with different chain extender contents from DMA technique.....	39
Table 4.6 Maximum temperature, maximum current and energy of polyurethane elastomers with different chain extender contents from TDS measurement.....	42

Table 4.7 Thermal conductivity and density of flexible and rigid polyurethane elastomers with different SiC contents.....	47
Table 4.8 Mechanical properties of flexible PUR with different SiC contents.....	50
Table 4.9 Mechanical properties of rigid PUR with different SiC contents.....	51
Table 4.10 Thermal properties of flexible and rigid polyurethane elastomers with different SiC contents.....	53
Table 4.11 The glass transition temperature of the soft and hard segment of polyurethane elastomers with different SiC contents from DMA technique.....	57

LIST OF ABBREVIATIONS AND NOTATIONS

Ag	Silver
AlN	Aluminum nitride
Au	Gold
Al ₂ O ₃	Aluminum oxide
BaTiO ₃	Barium titanate
BDO, BD, BG	1,4-butanediol
BeO	Beryllium oxide
BN	Boron nitride
Cu	Copper
CO ₂	Carbon dioxide
CH _x	Hydrocarbon group
DEG	Diethylene glycol
DMA	Dynamic mechanical analysis
DSC	Differential scanning calorimetry
EDS	Energy- dispersive X-ray spectroscopy
EG	Ethylene glycol
EO	Ethylene oxide
HDPE	High-density polyethylene
HG	1,6-hexanediol
HS	Hard segment
IR	Infrared spectroscopy
LDPE	Low-density polyethylene
LLDPE	Linear low-density polyethylene
mEG	Monoethylene glycol
MDI	Diphenylmethane-4,4' -diisocyanate
MgO	Magnesium oxide
NCO	Isocyanate group
NH	Amine group
OH	Hydroxyl group

PEG	Polypropylene ether glycol
PEO	Polyethylene oxide
PEP	Polyether polyol
PMMA	Poly(methyl methacrylate)
PO	Propylene oxide
PP	Polypropylene
PPG	Polypropylene glycol
PPO	Polypropylene oxide
PS	Polystyrene
PTMO	Polytetrahydrofuran
PTMEG	Polytetramethylene glycol
PVC	Polyvinyl chloride
PU	Polyurethane
PUR	Polyurethane elastomers
SEM	Scanning electron microscopy
SiC	Silicon carbide
SiCNWs	Silicon carbide nanowires
SiO ₂	Silicon dioxide
Si ₃ N ₄	Silicon nitride
SS	Soft segment
TDI	2,4-tolylene diisocyanate
TSD	Thermally stimulated discharge
ZnO	Zinc oxide
phr	Part per hundred resin

a	[mg]	Mass of specimen in air
b	[mg]	Mass of specimen
w	[mg]	Mass of totally immersed sinker
A	[mm ²]	Area
A _e	[kJ/mol]	Apparent energy of activation

E	[Pa]	Young's modulus
E', G'	[Pa]	Storage modulus
E''	[Pa]	Loss modulus
F	[N]	Force
I_{\max}	[pA]	Maximum peak current
L_0	[mm]	Initial length
ΔL	[-]	Elongation
M	[Pa]	Modulus of the composite
M_u	[Pa]	Upper limit of modulus
M_l	[Pa]	Lower limit of modulus
T	[K]	Temperature
T_g	[°C]	Glass transition temperature
T_m	[°C]	Melting temperature
$T_{g,SS}$	[°C]	Glass transition temperature of the soft segment
$T_{g,HS}$	[°C]	Glass transition temperature of the hard segment
T_{endo}	[°C]	Endothermic temperature
V	[v/v%]	Percent by volume
W	[m/m%]	Percent by mass
W	[mg]	Sample weight after swelling
W_i	[mg]	Sample weight before swelling
$\tan\delta$	[-]	Tan delta (mechanical loss factor)
ϑ_{\max}	[°C]	Maximum temperature of β and α relaxation
σ	[Pa]	Stress
ε	[-]	Strain
λ	[W / mK]	Thermal conductivity
λ_c	[W / mK]	Thermal conductivity of the composite
λ_p	[W / mK]	Thermal conductivity of the particle
λ_m	[W / mK]	Thermal conductivity of the matrix
λ_u	[W / mK]	Thermal conductivity of the composite of upper limit
λ_l	[W / mK]	Thermal conductivity of the composite of lower limit
λ_l	[W / mK]	Thermal conductivity of component 1

λ_2	[W / mK]	Thermal conductivity of component 2
ϕ	[-]	Volume fraction of filler
ϕ_1	[-]	Volume fraction of components 1
ϕ_2	[-]	Volume fraction of components 2
ϕ_H	[-]	Volume fraction of the hard phase
ϕ_S	[-]	Volume fraction of the soft phase
Φ_p	[-]	Volume fractions of particles
Φ_m	[-]	Volume fractions of matrix
q	[W/m ²]	Heat flux
x	[mm]	Thickness of material
C_p	[J/gK]	Specific heat capacity per unit volume
v	[-]	Average phonon velocity
l	[-]	Phonon mean free path
a	[m ² /s]	Thermal diffusivity
ρ	[g/cm ³]	Density
n	[-]	Characteristic exponent
∞	[-]	Characteristic exponent = 100

CHAPTER 1

Introduction

Polymers are usually electrical and thermal insulating materials; they display unusual electronic properties such as low energy optical transition, low ionization potentials and high electron affinities. Polymers have long-chain molecules. Their molecular structures vary from highly ordered crystalline structures to random amorphous structures. However, they have some defects which can lead phonon scattering and a significant reduction in phonon mean free path, both factors contribute to the thermal conductivity of polymer (0.1–0.5 W / mK) [1]. Polymer can be used for engineering applications. They have several advantages such as lightweight, low cost, easy processability, resistance against corrosions, good vibration-damping [2, 3] and so on. The lightweight polymer with good thermal conductivity in the range 1-30 W / mK [4, 5] can be applied in heat management and processability are highly required for the construction of miniaturized electronic devices to smoothly transfer the heat generated from various sources integrated in its limited space. Therefore, only few polymers have high thermal conductivity to fulfill these requirements, but their processability and properties are insufficient. Therefore, polymer composites are absolutely essential for modern electronic applications. There are many kinds of polymer which can be used as matrix materials. For example, polypropylene (PP), polystyrene (PS), low and high density polyethylene (LDPE and HDPE), epoxy, polyurethane (PU), etc.

Polyurethane (PU) is versatile polymeric material that has been used in a wide range of applications such as elastomers, coatings, footwear, furniture, foams, packaging, adhesives, automotive finishes and electronics. It has several advantages including high impact strength, good elasticity, high elongation, abrasion-resistant, excellent resistance to oil and solvent, good tear-resistant, etc [6]. Polyurethane elastomers (PUR) are a very important group of urethane products although their consumption is much lower than urethane foams. Structure and properties of PU can be improved by varying diisocyanate, polyol and chain extender. The chain extenders are factor that influences the ratio between the hard and the soft segments. A chain extender may increase the hard segment length to allow hard segment segregation which results in good mechanical properties such as an increase in the modulus as well as an increase in the hard segment glass transition temperature of the polymer. Therefore, the chain extender may also increase

the value of thermal conductivity of PUR. Furthermore, PU composites and blends have wide applications in electronics and optoelectronics. The applications of these include sensors, actuators, electromagnetic interference shielding, electrolytes for supercapacitors, electrostatic dissipation, and shape memory applications [7].

The conductive polymer composites are usually fabricated by incorporating conductive fillers such as carbon black, graphite flakes, fibers, metal powder and ceramic powders into the insulating polymer matrices. Because the conductivity is introduced through the addition of the conducting component, various polymeric materials including both amorphous and crystalline polymers can be turned into electrically conductive polymers. The degree of conductivity of the polymer is decided by the volume fraction of the filler. If the filler volume is high enough, the thermal conductivity will increase from high conductivity fillers form thermally conductive networks. The thermal conductive inorganic fillers are indispensable for achieving high thermal conductivity, stiffness, and strength if the interaction between the filler and the matrix is good. The filler type, loading level, filler size, and filler shape have a strong influence on the thermal conductivity of polymer composites [8]. High thermal conductivity ceramic such as carbonous and metallic materials with different filler content, size and shape were added to enhance thermal conductivity of polymer composites such as aluminum oxide (Al_2O_3) [9-11], silicon dioxide (SiO_2) [12-14], zinc oxide (ZnO) [15-20], boron nitride (BN) [21-29], silicon carbide (SiC) [30-33], beryllium oxide (BeO) [34], magnesium oxide (MgO) [35-40], copper (Cu) [41-47], silver (Ag) [48, 49], gold (Au) [50], etc. Various fillers including carbon black [51-55], carbon nanotubes [56-59], metal [60, 61], and graphene [62-64] have been studied to improve the electrical properties of the PU. Although much work has been done on the improvement of electrical properties of PU, there are barely any works focusing on thermal conductivity of thermosetting polyurethane elastomer composites with inorganic and metallic fillers.

From the discussion above, the goal of this study is to enhance the thermal conductivity of polyurethane elastomers for application of thermal conductive polymer by synthesis new thermosetting polyurethane elastomers with varying the chain extender content and preparing new composites via varying the content of each of silicon carbide, magnesium oxide, zinc oxide, and copper fillers. Effect of the chain extender content, filler types, and filler contents on thermal conductivity, mechanical properties, thermal properties, and morphology of new thermosetting polyurethane elastomer composites are investigated to support their usability in electrical applications.

CHAPTER 2

Theoretical Background and Literature Overview

Theoretical background and literature are reviewed based on polyurethanes structure which consists of polyol, isocyanate and chain extender structure. The fundamental of thermal conductivity is also explained. Furthermore, high thermal conductive fillers consisting of silicon carbide (SiC), magnesium oxide (MgO), zinc oxide (ZnO) and electrolytic copper powder (Cu) are introduced in this chapter.

2.1 Fundamental on thermal conductivity

Thermal conductivity (λ) is the property that determines the working temperature levels of a material, determining the temperature gradient inside the material is considered as an important parameter in the problems involving steady-state heat transfer. This property assumes a critical role in the performance of materials in high-temperature applications. Low values of thermal conductivity are required when the purpose is to minimize heat losses. On the other hand, materials with higher thermal conductivities must be chosen when heat transfer from one site to another is desirable. Therefore, high thermal conductivity values are essential for material selection criteria to get the best performance of the material in a specific application. Moreover, many factors can affect the thermal conductivity of a material such as temperature, density, porosity, moisture, degree of crystallinity, orientation of grains, size of molecules, impurities and so on. Therefore, the average bulk conductivity of a specimen with given geometrical data is measured. The separation of the individual effect of the above mentioned factors is really difficult if possible at all. Thermal conductivity is a specific material property. It represents the heat flow in watts (W) through a 1 m² surface and 1 m thick flat layer of a material when the temperature difference between the two surfaces in the direction of heat flow amounts to 1 Kelvin (K). The unit of measurement for thermal conductivity is W / mK [65]. For one-dimensional and rectilinear heat flow, the steady-state heat transfer in polymeric materials can be described by the Fourier's law of heat conduction (equation (2.1)).

$$q = -\lambda \frac{dt}{dx} \quad (2.1)$$

Where q is the heat flux, x is the thickness of the material, dt/dx is the temperature gradient per unit length and the proportionality constant λ is known as the thermal

conductivity. Heat transfer involves the transport of energy from one place to another by energy carriers. In a gas phase, gas molecules carry energy either by random molecular motion (diffusion) or by an overall drift of the molecules in a certain direction (advection). In liquids, energy can be transported by diffusion and advection of molecules. In solids, phonons, electrons, or photons transport energy. Based on the theoretical prediction, the Debye equation is usually used to calculate the thermal conductivity of polymers as represented in equation (2.2).

$$\lambda = \frac{C_p v l}{3} \quad (2.2)$$

Where C_p is the specific heat capacity per unit volume; v is the average phonon velocity; and l is the phonon mean free path. For amorphous polymers, l is an extremely small constant due to the irregular (not ordered) amorphous structure. A phonon is a quantum of crystal vibrational energy and dominates heat conduction in insulators and semiconductors. Photons are quanta of electromagnetic energy and can transport energy in solids as well as interact with photons and phonons to render radiative properties of solids. At low temperature, the electron mean free path is determined mainly by scattering due to crystal imperfections such as defects, dislocations, grain boundaries, and surfaces. Electron phonon scattering is frozen out at low temperatures. Since the defect concentration is largely temperature independent, the mean free path is a constant in this range. Therefore, the only temperature dependence in the thermal conductivity at low temperature arises from the heat capacity. As the temperature is increased, electron-phonon scattering becomes dominant. The mean free path depends on the material but is independent of the sample, since electron phonon scattering is an intrinsic process. As a result of electron phonon scattering, thermal conductivity of metals decreases at higher temperatures [66]. For amorphous polymers, the mean free path is an extremely small constant due to phonon scattering from numerous defects, leading to a very low thermal conductivity of polymers [67]. Consequently, the thermal conductivity of the amorphous materials is very low. In addition, the crystallinity in crystalline polymers is also low and contains a lot of defects compared to conventional metallic or ceramic crystals, thus the crystalline polymers have also low heat conductivity usually compared to metals and ceramics. Several non-steady state methods have also been developed, including hot wire and hot plate methods, temperature wave method and laser flash techniques. Among these, laser-flash thermal diffusivity measurement is widely used, being a relatively fast method, using small specimens. In this method, the sample surface is irradiated with a

very short laser pulse and the temperature rise is measured on the opposite side of the specimen, permitting calculation of the thermal diffusivity of the material, after proper mathematical elaboration. The thermal conductivity λ is then calculated according to Equation (2.3).

$$\lambda = aC_p\rho \quad (2.3)$$

Where a , C_p and ρ are the thermal diffusivity, heat capacity and density, respectively [65].

2.1.1 Thermal conductivity of polymer and its composites

The thermal conductivity of a polymer depends greatly on its morphology. When amorphous domains are dominant, vibrational modes in the polymer tend to be localized, resulting in a low thermal conductivity. It is therefore natural to expect that thermal conductivity can be enhanced by improving the alignment of polymer chains. Indeed, many efforts have been devoted to align polymer chains to enhance the thermal conductivity, by using mechanical stretching, nanoscale templating and electrospinning [68]. This is because thermal energy transports more efficiently along the polymer chain. Crystalline polymers have ordered structure, and therefore have higher thermal conductivity than amorphous polymers [69]. These lead to phonon scattering and significant reduction in the mean of the phonon's free path. Phonons are usually considered to be the thermal carriers in polymers because there is a free electron. Burger and her colleagues discussed the mechanism of heat transfer in an amorphous polymer and described it using a schematic diagram, which is presented in Figure 2.1. When the surface of the polymer makes contact with the heat source, heat transfers to the first atom of the molecular chain in the form of a vibration and then transfer to the nearest atom. Heat transfer in a molecular chain will also cause the disordered vibration and rotation of atoms which significantly reduces the thermal conductivity of the polymer. A good conductor has a complete lattice structure and atoms accumulate closely. When the heat reaches the first atom, it will quickly transfer to the last one. However, heat transfer in a bad conductor causes the vibration and rotation of atoms, which will significantly reduce the thermal conductivity [70].

In other applications which require higher thermal conductivity such as in electronic packaging and encapsulations, satellite devices and in areas where good heat dissipation, low thermal expansion and light weight are needed, polymers reinforced with fillers, organic or inorganic, are becoming more and more common in producing

advanced polymer composites for these applications. One example is crystalline polymers, for which the structural and morphological features may be significantly changed with the speed of cooling. Careful consideration in designing polymer processing is vital to achieve desired properties [65].

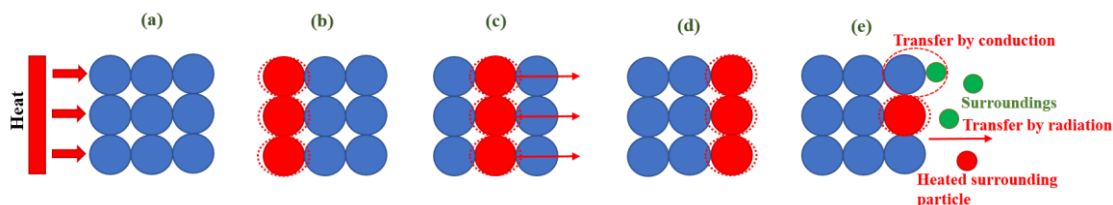


Figure 2.1 The schematic of thermal conduction in a crystalline material [70]

In case of polymer composites, the thermal conductivity of polymer composites is a function of the thermal conductivity of both polymers and fillers. However, the importance of the thermal conductivity of polymers is often neglected in the design of thermally conductive polymer composites because it is usually quite low compared to that of the filler. The thermal conductivity of various electrically insulating materials at different temperatures is shown in Table 2.1.

The thermal conductivity of polymers is particularly important at low filler loadings, as the thermally conductive fillers are separated by polymer matrix, which acts as a thermal barrier and becomes rate-limiting in the thermal conduction pathway. The addition of thermally conductive inorganic fillers is dispensable for achieving high thermal conductivity. The filler type, loading level, filler size and filler shape have a strong influence on the thermal conductivity of polymer composites. Many types of filler have non-spherical shapes (plate-like or needle-like). They can be oriented during processing, which leads to composites with anisotropic thermal conductivity. In some applications, an anisotropic thermal conductivity is not preferred or the orientation direction of the fillers is not in the desired direction. Novel techniques are being developed for obtaining the desired filler orientation. Often creating a continuous filler network is the key to obtaining high thermal conductivity in composite structures. Network formation, however, usually takes place at high filler loading levels. This can lead to poor processability, poor mechanical properties, and high cost. Studies are ongoing to develop composites with high thermal conductivity at a lower filler loading level by carefully controlling filler spatial arrangement. The interaction of filler with the polymer matrix is also important to the thermal conductivity. The poor interface between

filler and polymer could lead to high thermal interfacial resistance and reduce the thermal conductivity [8].

Table 2.1 Thermal conductivity of various electrically insulating materials at room temperatures [71]

Materials	Thermal conductivity (W / mK)
Polystyrene	0.04-0.14
Polypropylene	0.14
Polyvinyl chloride	0.12-0.17
Polymethyl methacrylate	0.15-0.25
Polycarbonate	0.19
Epoxy	0.17-0.21
Silicone elastomer	0.17-0.26
Polytetrafluoroethylene	0.25
Polyetheretherketone	0.25
Polybutylene terephthalate	0.25
Nylon 6,6	0.25
Polyethylene terephthalate	0.29
Low-density polyethylene	0.33
Nylon 11	0.36
High-density polyethylene	0.45-0.52
Fused SiO ₂	1.5-1.6
Crystalline silica	3
BaTiO ₃	6.2
Al ₂ O ₃	38-42
ZnO	60
SiC	85
Si ₃ N ₄	86-120
AlN	150-220
BN	29-300
BeO	300
Diamond	2000

In addition to engineering the morphology of polymer chains, another common method to enhance the thermal conductivity of polymers is to blend polymers with high thermally conductive fillers. The thermal conductivity is essentially determined by the filler matrix coupling, i.e, interfacial thermal resistance, the concentration, and the geometric shapes of fillers. In general, there are two types of polymer nanocomposites depending on whether nano-fillers form a network or not. When the filler concentration is low, no inter-filler networks could be formed. When the filler concentration is large enough, high conductivity fillers might form thermally conductive networks. Although

nanocomposites with filler network could possess a higher thermal conductivity than that without a network, their thermal conductivity could still be low due to the large inter-filler thermal contact resistance [68].

Several different models developed to predict the thermal conductivity of traditional polymer composites are reviewed elsewhere. Many theoretical and empirical models have been proposed to predict the effective thermal conductivity of two phases mixtures. There are some reviews that discussed in these models [72]. Two basic models representing the upper bound and the lower bound for thermal conductivity of composites are the rule of the mixture and the so-called series model, respectively. In the rule of mixture model, in case of the parallel model, each phase is assumed to contribute independently to the overall conductivity, proportionally to its volume fraction in Equation (2.4).

$$\lambda_c = \lambda_p \phi_p + \lambda_m \phi_m \quad (2.4)$$

Where λ_c , λ_p , λ_m are the thermal conductivity of the composite, particle, matrix, respectively, and ϕ_p , ϕ_m are volume fractions of particles and matrix, respectively. The parallel model maximizes the contribution of the conductive phase and implicitly assumes perfect contact between particles in a fully percolating network. This model has some relevance to the case of continuous fiber composites in the direction parallel to fibers, but generally results in very large overestimation for other types of composites. On the other hand, the basic series model assumes no contact between particles and thus the contribution of particles is confined to the region of matrix embedding the particle. The conductivity of composites accordingly with the series model is predicted by Equation (2.5).

$$\lambda_c = \frac{1}{(\phi_m + \lambda_m) + (\phi_p + \lambda_p)} \quad (2.5)$$

Thermally conductive but electrically insulating polymer composites have become increasingly important for the industry. Various kinds of fillers such as metal, metal oxide, carbon black, carbon fiber, carbon nanotube, ceramic, inorganic fillers, etc. have been studied extensively to prepare thermally conductive polymer composites.

2.2 Fundamental on polyurethanes

Prisacariu [73] has provided a detailed overview on the polyurethane polymerization. The most important information related to my work are given in this chapter. Polyurethanes (PU) are widely used in industry due to their properties such as

high impact strength, good elasticity, high elongation etc. Moreover, polyurethane is a special polymer that can consists of hard segment (HS) and soft segments (SS). The hard segments are formed by short diols (chain extender) and diisocyanates. For the soft segments are composed of long polyester-based polyols. The properties of PU can be easily improved by changing the molecular chain structure of the soft and hard segments [74]. Polyurethanes have two types, thermoplastic and thermoset polymers. It is a broad class of materials utilized in a wide variety of applications. Products in this family are chemically complex and may contain different types of bonds. The two phases of SS and HS provides the key to control the properties of the final product and gives the manufacturer versatility in tuning properties as desired by varying the composition or content. Polyurethane elastomers are one of the importance groups of polyurethanes [73] The structure of the urethane bond form polyurethanes is presented in Figure 2.2.

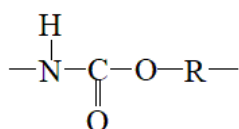


Figure 2.2 Basic urethane group

Polyurethane elastomers (PUR) are a class of materials displaying high reversible deformation. High chain flexibility and weak interaction results in low glass transition temperature (T_g).

Crosslinking will increase T_g by prevent the residual plastic deformation. The crosslinks can be of a chemical or physical nature. Physical crosslinking can be obtained through hydrogen bonding and hard domain formation. Chemical crosslinking is introduced with tri- or multifunctional constituents. It cannot be easily destroyed by thermal treatment as physical crosslinks, except in some special cases of labile chemical groups, producing an irreversible network. Physically crosslinked polyurethane elastomers are block copolymers, consisting of alternating rigid and flexible blocks. Due to the different polarity and chemical nature of both blocks they separate into two phases designated as "soft" and "hard". Hard blocks also associate into domains because of rigidity and hydrogen bonding. Hard segment are rigid phases. It includes the isocyanate group and short chain of a chain extender. The structure of the segmented urethane molecule and domain formation is schematically represented in Figure 2.3. Segmented polyurethanes are two phases polymer and their properties are strongly affected by the amount of phase separation. Furthermore, soft segments are obtained by reacting polyols having molecular weights between 400 and 6000 [6], these are long ethers or esters oligomer chains.

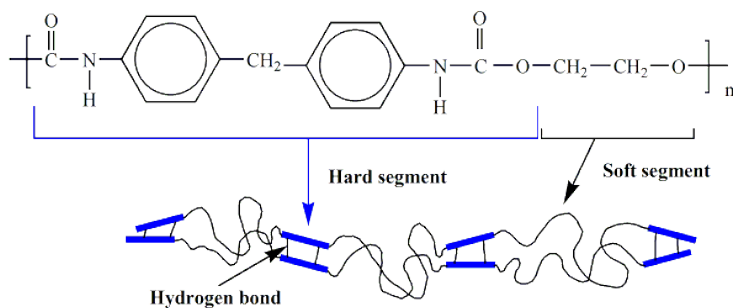


Figure 2.3 Polyurethane alternating hard- and soft segment structure

Since the soft segment usually has its glass transition below ambient temperature and the hard segment is frequently a relatively rigid aromatic molecule with the glass transition above ambient temperature. The hard segment is built from alternating diisocyanate and chain extender sequences while the soft segment originates from the polyol. Because of rigidity and hydrogen bonding, the hard segment (either glassy or crystalline) are associated with hard domains acting as physical crosslinks within the rubbery soft segment matrix [73]. The immiscibility between hard segment and soft segment leads to phase separation in finally produced polyurethane elastomers. The degree of phase separation and domain formation depends on many factors including, the hard segment and soft segment nature and sizes, the type of the diisocyanate and polyol employed to produce prepolymers, the type of the chain extender and the molecular weight of the soft segment. It is also influenced by the hydrogen bond formation between the urethane linkages, by the manufacturing process and reaction conditions.

PUR microstructure and mechanical behavior are strongly dependent on the synthesis method. The main difference between the materials prepared by the prepolymer and the one-step methods involves the chain build-up. The one-step route begins with the slightly favored reaction between glycol and diisocyanate which produces highly crystalline, mobile chain elements. These areas of crystallinity, acting as crosslinks, increase the tensile strength of the one-step PUR. In the one-step method, factors like the different reactivity of isocyanate groups and the different hydroxyl groups of a polyol and a chain extender may affect the distribution of HS in the chain or even produce a mixture (oligomer) of diisocyanate chain extender and diisocyanate macrodiol homopolymers. In case of two-step polymerization technique, the first step of the reaction a prepolymer is produced through the reaction of a SS oligomer with an excess of diisocyanate, followed by chain extension with a short diol (urethane or ester) or a diamine (urea, urethane urea, amide or ester-amide) to form the HS and also to increase the overall molecular weight of the polymer. PUR structures obtained by the two-step procedure tend to be more regular than the corresponding polymers obtained by the one-step route. The structural regularity may result in better mechanical properties since HS

aggregate much easier to form physical cross-linking points. The bonding of SS and HS microphases in the PUR copolymer structure is possible only by joining the isocyanic (NCO) rest of one of the softs or hard elements to the free hydroxyl (OH) group of another soft or hard element. The total number of isocyanic groups taken into reaction equals the total number of OH groups to ensure theoretically the formation of infinite macromolecule lengths [73].

As discussed, the polyurethane elastomer is made from four main ingredients such as polyols (polyether and polyester), diisocyanate (aromatic and aliphatic), chain extender (diamines, hydroxyl compounds and polyols) and other chemicals. Therefore, we have shown the fundamental of these main ingredients which influence the properties of PUR in the next topic.

2.2.1 Polyols

Elastomeric properties in the polyurethane is provided by the backbone or the soft segment. Polyols provide the soft segment of the polymer is capped with a hydroxyl group. Unless there are special requirements, the polyols are linear of molecular weight between 400 and 7000. The overall molecular weight of the soft segment controls the morphology of the polyurethane, since it influences the size and number of the hard segments and hence the hardness, resilience and stiffness of the final product. There are two main groups of polyols used to make castable polyurethanes consist of polyethers and polyesters [75]. Polyols are formed by base-catalyzed addition of propylene oxide (PO), ethylene oxide (EO) onto a hydroxyl or amine-containing initiator or by polyesterification of a diacid such as adipic acid, with glycols such as ethylene glycol or dipropylene glycol. Polyols extended with PO or EO are polyether polyols. Polyols formed by polyesterification are polyester polyols. Important characteristics of polyols are their molecular weight, percentage of primary hydroxyl groups, functionality and viscosity. In general, the mechanical strength of this class of polyurethane is lower than that of their polyester and polyether analogues with the advantage of giving polyurethane of very low glass transition temperatures and hence temperature flexibility. Polyester polyurethane is stiffer and have a higher strength than the polyether polyurethane with better resistance to high temperature, solvents and oxidation. Furthermore, polyether polyols give higher resilience with good hydrolysis resistance. Polyester polyols differ from the polyether polyols as they virtually have no unreactive end groups which contribute significantly to the increase of the strength of the material. Polyester polyurethane has good material properties but they are susceptible to hydrolytic cleavage

of the ester linkage while polyether-based urethanes have relatively high resistance to hydrolytic chain scission. Polyethylene oxide (PEO) based materials exhibit poor water resistance due to the hydrophilic nature of the ethylene oxide. Although the polyurethane mechanical properties obtained with polypropylene oxide (PPO) are not as good as those made from PTMO, PPO has also been widely used because of its low cost and reasonable hydrolytic stability [73].

2.2.1.1 Polyethers

Polyether diols form a very important segment of the diols used in the manufacture of polyurethanes. The normal route is by addition polymerization of the appropriate monomeric epoxide. The most important polyethers are polypropylene glycol and polytetramethylene glycol. The polyether glycols produce polyurethanes that are not as strong and tough as the polyester-based polyurethanes. The standard polyol in this group is polytetramethylene glycol (PTMEG) which gives compounds superior physical and mechanical properties to those produced with polypropylene glycol (PPG) based systems. Prepolymers based on polypropylene ether glycol (PEG) have excellent but not as good mechanical and wear properties as the PTMEG based materials. Improvements to the performance of the PPG material were made by the end capping of the propylene glycol chains with ethylene oxide. The modified PPG gave better processing and performance [73].

2.2.1.2 Polyesters

The chemical structure of the prepolymer influences its chemical resistance. As a result of their structure, polyesters have inherently better oil resistance but lower hydrolytic stability. The ether groups in the polyether urethanes provide better hydrolytic stability and are more flexible. Polyesters have three different types such as dibasic acid reacted with diol, polycaprolactone materials and polycarbonate-based materials. Dibasic acid type is a classically based polyester which made by the reaction of a dibasic acid diol with the formation of polyester and water. Polyesters produce strong, tough and oil-resistant materials. The basic polyesters are prepared by the reaction of a dibasic acid (usually adipic, sebacic or phthalic acid) with a diol such as ethylene glycol, 1,2-propylene glycol and diethylene glycol. Polyurethanes made from these ingredients suffer from relatively poor hydrolytic stability. Their main drawback is poor hydrolytic stability and susceptibility to fungal attack [73].

2.2.2 Diisocyanates

One essential component of polyurethane is the isocyanate. Molecules that contain two isocyanate groups are called diisocyanates. They are compounds containing the isocyanate group ($-NCO$). They react with compounds containing alcohol (hydroxyl) groups to produce polyurethane. The polyurethane hard segments can be either aromatic or aliphatic. The aromatic isocyanates are more reactive than the aliphatic diisocyanates, which can only be utilized if their reactivities match the specific polymer reaction and special properties desired in the final product. Furthermore, the reactivity of an isocyanate group may vary dramatically even within the same class of a diisocyanate. Two of the most important aromatic isocyanates are 2,4-tolylene diisocyanate (TDI) and 4,4-diphenylmethane diisocyanate (MDI). TDI consists of a mixture of the 2,4- and 2,6-toluene diisocyanate isomers. The polyurethane degree of phase separation or domain formation is also strongly influenced by the symmetry of the diisocyanate and by the selection of the chain extender, influencing the degree of interaction between the hard segments. A diisocyanate and a chain extender with a more symmetrical structure increase the crystal formation, leading to more complete phase segregation. The aromatic or aliphatic diisocyanates have profound effects on the polyurethane properties. The structural rigidity of aromatic hard segment generally produces elastomers with high tensile strength and modulus and enhanced thermal stability. However, these aromatic units are susceptible to attack by ultraviolet radiation, causing degradation and yellowing without the use of stabilizers [73].

2.2.3 Chain extender

The chain extenders play a very important role in PUR structure. Polyurethanes formed by directly reacting diisocyanate often do not exhibit microphase separation when reacting without the chain extender. The chain extender may increase the hard segment length to allow hard segment segregation which results in good mechanical properties such as high modulus and an increase in the hard segment glass transition temperature of the polymer [73]. Polyurethane chain extenders can be categorized into two classes such as aromatic diols and diamines and the corresponding aliphatic diols and diamines. Typical chain extenders are low molecular weight, it less than 400 difunctional intermediates designed to react with the isocyanate groups to become part of the HS. In general PU chain extended with an aliphatic diol produce a softer material than do their aromatic chain extended counterparts. Also, diamine chain extenders are much more reactive than diol chain extenders and give properties superior to those of similar

polymers prepared with the equivalent diol chain extenders. This is due to the HS (urea linkage) which has a higher density of hydrogen bonding, which results in a higher glass transition temperature and higher thermal stability. However, for the same reason, PU ureas made from diamine chain extenders tend to be less soluble in common solvents and therefore they are more difficult to melt. Examples of diol chain extenders include 1,6-hexanediol (HG), ethylene glycol (EG), 1,4-butanediol (BDO, BD or BG), and diethylene glycol (DEG). The chain extender structure strongly influences the PU mechanical performance [76], thermal [77] and electrical properties [78]. Modifying the ratio between the polyol and chain extender [69], PU may result in a change from hard, brittle material to a rubbery elastomer as a result of the variation of the HS concentration.

2.3 Inorganic fillers with high thermal conductivity

In this study, a new synthesis of polyurethane elastomers with different chain extender contents is presented. Then, the selected flexible and rigid PUR matrices will be loaded with both inorganic fillers and some metal filler. These fillers consist of silicon carbide, magnesium oxide, zinc oxide, and copper powder. Therefore, the fundamentals, advantages, and disadvantages of fillers were briefly presented.

2.3.1 Silicon carbide (SiC)

Silicon carbide is a compound of silicon and carbon with chemical formula SiC. It occurs in nature as the extremely rare mineral moissanite [80]. Silicon carbide is an important non-oxide ceramic which has diverse industrial applications. It has exclusive properties such as high hardness and strength, good chemical and thermal stability, high melting point, superior oxidation resistance, high erosion resistance, etc. All of these qualities make SiC a perfect candidate for high power, high-temperature electronic devices as well as abrasion and cutting applications. The simplest manufacturing process is to combine silica sand and carbon in a graphite electric resistance furnace at a high temperature between 1600 and 2500 °C [81]. SiC has been intensively studied by material scientists and engineers and has got plenty of applications in different fields. Besides, it has also been used as structural materials for its good mechanical strength and relatively low density [82]. It used in electric and electronic systems and devices, for example, lighting arresters. SiC has also high thermal conductivity. The value of thermal conductivity of pure single crystalline SiC can be as high as 3000 W / mK. However, commercially available SiC has thermal conductivity values in the range of several tens W / mK or even lower as the existence of impurities and defects which act as phonon

scattering sites [80]. Silicon carbide has been recognized as an important structural ceramic material because of its unique combination of properties, such as excellent oxidation resistance, strength retention to high temperatures, high wear resistance, and good thermal shock resistance [83].

2.3.2 Magnesium oxide (MgO)

Magnesium oxide known as magnesia is a beneficial material used in numerous fields such as catalysis, ceramics, and refractory as well as paint industry. The literatures have demonstrated that magnesium oxide can be elaborated by different techniques such as the dehydration of magnesium hydroxide, flame spray pyrolysis, sol-gel techniques, and so on [84]. MgO is produced by the calcination of magnesium carbonate or magnesium hydroxide. Calcining at different temperatures produces magnesium oxide of different reactivity. High temperatures of 1500-2000 °C diminish the available surface area and produces dead-burned (often called dead burnt) magnesia. Calcining temperatures of 1000-1500 °C produce hard-burned magnesia, which has limited reactivity and calcining at lower temperature (700-1000 °C) produces light-burned magnesia, a reactive form, also known as caustic calcined magnesia [85].

MgO has a high electrical resistivity of 1015 Ωcm at 600 K. In addition, it has high physical strength and stability and a melting point near 2852 °C. MgO is an effective insulation material for polymer materials at a sufficient level of addition. Therefore, it can be used to increase insulation properties [35]. MgO nanoparticles possess many interesting features including antimicrobial activity, thermal and electrical insulation, non-toxicity and good biocompatibility [36]. It is hygroscopic in nature and care must be taken to protect it from moisture. Moreover, MgO is an excellent insulator both electrically and electronically (with a band gap of 7.8 eV) [85]. The measured thermal conductivity ranges from 30 W / mK down to 8 W / mK. The electrical insulating power of magnesia is very high which makes for an excellent high-temperature electrical insulator. MgO has very limited solubility in water. In case of structural properties, the elastic modulus value of magnesium oxide is between 210-317 GPa, tensile strength is 95.8 GPa, shear modulus is between 75.8-131 GPa and compressive strength is between 0.83-1.44 GPa. There is a wide range of refractory and electrical applications where magnesia is firmly established. The properties of major interest are good refractoriness, good corrosion resistance, high thermal conductivity, low electrical conductivity and transparency to infrared [86].

2.3.3 Zinc oxide (ZnO)

Zinc oxide as a functional inorganic filler has been widely used in functional devices, catalysts, pigments, optical materials, cosmetics and ultraviolet absorbers. The ZnO micro-powders are successfully and widely used as one of the main components in manufacturing of various low cost and commercial thermal greases. ZnO is a largely inert, white compound which is used very widely as a bulking agent or filler and as a white pigment. The lack of center of symmetry in wurtzite, combined with large electromechanical coupling, results in strong piezoelectric and pyroelectric properties and the consequent use of ZnO in mechanical actuators and piezoelectric sensors. It is transparent to visible light and can be made highly conductive by doping. ZnO is a versatile functional material that has a diverse group of growth morphologies such as nanocombs, nanorings, nanohelices/nanosprings, nanobelts, nanowires and nanocages [87]. Moreover, it has unique physical and chemical properties, such as high chemical stability, high electrochemical coupling coefficient, broad range of radiation absorption and high photostability. It is an attractive filler due to its high thermal conductivity value, 60 W / mK, a low coefficient of expansion (2×10^{-6} 1/K) and low production cost [88].

Morphology of zinc oxide nanoparticles depends on the process of synthesis. They may be nanorods, nanoplates, nanospheres, nanoboxes, hexagonal, and so on [89]. The piezo- and pyroelectric properties of ZnO mean that it can be used as a sensor, converter, energy generator and photocatalyst in hydrogen production [90]. For last few years, among metal oxide nanoparticles, ZnO has been the subject of focused research due to their extraordinary electronic, optical, mechanical, magnetic and chemical properties that are significantly different from those of bulk counterpart [88]. Several studies have been conducted on the synthesis and the structure–property of ZnO nanoparticles. Semiconductor nanoparticles embedded in a polymer matrix have recently been considered as biosensors for the detection of species in biofluids. The synthesis, morphology, and optical properties of ZnO particle polymer thin films have also been reported more recently [91].

2.4 Metallic fillers with high thermal conductivity

Researches in the field of electroconductive polymer composites filled with metal powders have experienced great development in the last two decades. Adding metal filler polymer matrix allows the preservation of the mechanical properties of polymers while, at the same time, exploiting the electric conductive properties of metal [1]. In this study,

we focused on electrolytic copper powder due to high thermal conductivity around 390 W / mK [92]. Furthermore, it had good strength as well as good resistance to corrosion and fatigue.

2.4.1 Copper (Cu)

Copper and copper alloys are widely used in a variety of products that enable and enhance our everyday lives. They have excellent electrical and thermal conductivities, exhibit good strength and formability, have outstanding resistance to corrosion, and fatigue and generally nonmagnetic. Of all common metals, copper possesses the highest rating for both electrical and thermal conductivity. Copper in its pure, unalloyed state is soft, provides high electrical and thermal conductivity and has excellent corrosion resistance. All these make copper alloys unique conductors of electricity which can be used as connectors in electrical or electronic products. Miniaturization of electronic devices and components has benefited from the high strength and moderate to high conductivities offered by specialty copper alloys. Oxygen-free coppers are used specifically in applications requiring high conductivity and exceptional ductility. The density of copper is 0.321 lb/in³ (8.89 g/cm³), and its melting point is 1083 °C. Conductivity is the primary characteristic that distinguishes copper from other metals. [93]. Copper is an excellent electrical conductor. Most of its uses are based on this property or the fact that it is also a good thermal conductor. A good electrical conductivity is the same as a small electrical resistance. Copper is a good conductor of heat. This means that if you heat one end of a piece of copper, the other end will quickly reach the same temperature.

2.4.1.1 Electrolytic copper

Electrolytic copper powder is produced by following principles used in electroplating with the conditions changed to produce a loose powdery deposit rather than a smooth adherently solid layer. The formation of powder deposits that adhere loosely to the cathode is favored by low copper ion concentration in the electrolyte, high acid concentration and high cathode current density. The copper powder obtained by electrolysis is high purity material, averaging more than 99% copper. The powder is dendritic in shape. A wide range of powders having different apparent densities and high green strengths can be obtained by different method [92].

2.5 Polymer and high thermal conductive composites

Presently, the thermal conductivity of polymer is widely investigated. The effective thermal conductivity of polymer composite composed of particles of one material embedded in a polymer matrix. It is a function of the thermal conductivity of the constituents, the particle loading, the particle size and shape, the particle dispersion and the thermal interfacial resistance [30]. Many research works focused on adding various types of high thermal conductivity fillers to improve the thermal conductivity and mechanical properties of polymer composites. In this study, we have a focus on silicon carbide, magnesium oxide, zinc oxide, and copper fillers.

In case of SiC, there are several works which deal with incorporating SiC into epoxy matrix. Results show that thermal conductivity can reach 0.449 W / mK with adding 3 m/m% of silicon carbide nanowires (SiCNWs) in the epoxy matrix [30]. The modified 1D SiCNWs as thermal conductivity fillers to fabricated epoxy and orientated SiCNWs composites by coating method were investigated. The thermal conductivity of epoxy and SiCNWs composites was improved around 10 W / mK, at a comparatively low filler content of 5 m/m% [31]. It is a similar trend to loading 2.17 v/v% of SiCNW which can improve thermal conductivity of 406% per 1 v/v% loading [33]. Oxidized and silane treated micro SiC particles were also adding to epoxy. Thermal conductivity reached the maximum at around 20 times when adding 71.7 m/m% oxidized and silane treated micro-SiC [32]. Furthermore, polyurethane reinforced with SiC were synthesized by facile surface-initiated polymerization method, which can improve tensile strength and tensile modulus of nanocomposites with different loading. An increase of about 21.4 times and 2.2 times in tensile modulus and strength, respectively, was observed in the composites reinforced with 35 m/m% nanoparticles as compared with the pure polyurethane [94]. In contrast, tensile strength of the composites decreased when SiC was mixed with polyester matrix while compressive strength was raised with adding 40% SiC. Composite properties further improved by particulate size and shape, which enhances adhesion between reinforcement and matrix [95]. However, previous PU and SiC work did not focus on thermal conductive applications but only studied mechanical and thermal properties.

One kind of high thermal conductive filler is magnesium oxide (MgO). It has a low price and plentifully in industry. So, there were many research works used MgO to improve the properties of polymer composites. Mechanical properties of polystyrene were improved by adding MgO powder. Tensile strength, elongation at break and Shore

D hardness were increased with increasing MgO content until 10 m/m% [84]. The difference in the diameter of MgO fillers added in low-density polyethylene show a decreasing in the conductivity this decrease is observed only in the nanocomposites and not observed in the microcomposites [96]. Furthermore, MgO nanoparticle and poly(vinylidene fluoride-co-hexafluoropropylene) were prepared. The optimized material with 3 m/m% MgO offers a maximum electrical conductivity of $\sim 8 \times 10^{-3}$ S/cm at room temperature (~ 25 °C) with good thermal and electrochemical stabilities [97]. Thermal conductivity of MgO-ethylene glycol nanocomposites was also investigated. The obtained results show that the thermal conductivity increases with increasing fraction of MgO nanoparticles in suspensions [98].

For a long time, the ZnO micropowders are successfully and widely used as one of the main components at manufacturing of various low-cost, commercial thermal greases. In the meantime, the number of publications concerning the thermal conductivity of the nanostructured materials based on ZnO is limited. The thermal conductivity of the composite materials based on the zinc oxide powders with different average particle sizes dispersed in the polymethylsiloxane (silicone oil) was measured using the radial heat flow method. The thermal conductivity of ZnO and polymer composite with an average particle size of 50 μm was found to be 0.8 W / mK [15], while nano zinc oxide with high density polyethylene (HDPE) composites show a decrease in the elasticity modulus, yield strength, tensile strength, elongation, Izod impact strength and hardness of composites with increasing particle loading. This could be attributed to weak adhesion between fillers and the HDPE matrix and agglomeration of particles [16]. The incorporation of nano ZnO particles can improve crystallinity and thermal conductivity in polypropylene (PP) [17]. Moreover, tetrapod-shaped ZnO whiskers and epoxy composites were characterized. The thermal conductivity of ZnO and epoxy composites with 50 m/m% filler reaches 4.38 W / mK, approximately 1816% enhancement was obtained as compared to neat epoxy [18]. Thermal conductivities of silicone rubber filled with ZnO in a wide volume range were studied. With the increase of ZnO particles content in silicone rubber, the amount of formed conductive chains increases and the conductive chains trend linearly to increase the thermal conductivity of the composite. The tensile strength and elongation at break of silicone rubber increased initially with increasing volume content of ZnO in the range of 0–12 v/v% and then decreased. The reason is that the thermal conductive filler ZnO is also a kind of half reinforcing filler, which can improve the mechanical strength with low volume content. But when ZnO particles were

added with large volume content, the tensile strength and elongation at break decreased for the poor interfacial interaction between ZnO and silicone rubber matrix [19]. In case of thermoplastic elastomers, thermal conductivity and stability properties of the composites were also investigated. Results reveal that the addition of 10 m/m% ZnO concentration leads to increase in the thermal conductivity of composite to 1.7 W / mK compared to 0.3 W / mK for the neat polymer. At the same filler loading, ZnO nanoparticles exhibited a greater effect on thermal conductivity compared with submicron-sized particles [20]. Furthermore, ZnO nanorod and thermoplastic PU was prepared for shape memory performance. Tensile modulus enhancements were modest though, comparable to values observed for spherical nanofillers. Higher ZnO loadings (12 v/v%) exhibited clustering of ZnO nanorods into a mesh-like structure. Therefore, tensile modulus and shape recovery characteristics were improved [99].

Polymer composites filled with conductive metal particles are of interest to many fields of engineering. The interest in these composite materials arises from the fact that the thermal characteristics of such composites are close to the properties of metals, whereas the mechanical properties and the processing methods are typical for plastics [42]. Thermal conductivity but electrical insulating with polymer matrix composites was interested for electronic applications because the heat dissipation ability limit. Several studies have investigated the addition of metallic fillers to improve the physical properties of polymers [41-48, 47, 49]. In this study, copper powder was used as filler in polymer matrix because it has excellent electrical and thermal conductivities, good strength and formability, and so on [93]. Example for polymer and copper composites, thermal and electrical conductivity of unsaturated polyester resin with copper filler composite material are investigated. It is observed that the increase in the concentration causes the thermal and electrical conductivity of composite mixture to grow up. It has also been observed that both thermal and electrical conductivity increase with increasing filler particle size. The tensile strength values were found to increase with increasing Cu loading up to 16%. The maximum tensile strength value shows an improvement of about 129%. This increased tensile property can be attributed to the good dispersion of the filler in the polymer matrix. On the other hand, a gradual decrease in the elongation at break of the composites was observed with increasing Cu content. This is due to the metal particles dispersed in the matrix restrict the movement of the polymer chains [41]. Besides, copper powder filled polyamide composites are also investigated. Results have shown that thermal conductivity of copper filled polyamide composites depends on

several factors including the thermal conductivity of the filler particles, filler particle shape, size and the volume fraction and spatial arrangement of the filler particles in the polymer matrix [42]. The electrical and thermal conductivity of systems based on epoxy resin and poly(vinyl chloride) filled with copper powders have been studied [43]. Epoxy composites were fabricated by varying the copper/aluminium ratio and the results indicated that the thermal conductivity of the epoxy composite has been improved by adding metallic filler. The experimental results were correlated with the theoretical model. Thermal conductivity obtained from the series conduction model was shown better results compared to the experimental value [44]. The copper powder particle distributions were found to be relatively uniform at both low and high copper contents in low density polyethylene (LDPE) and linear low-density polyethylene (LLDPE). The thermal stability of the LDPE filled with Cu powder is better than that for the unfilled polymer. The LLDPE composites show better stability only at lower Cu contents. Generally, the composites show poorer mechanical properties (except tensile modulus) compared to the unfilled polymers. The thermal and electrical conductivities of the composites were higher than that of the pure polyethylene matrix for both the LDPE and LLDPE. The modulus slightly increases with increasing copper content. The size and distribution of filler particles also play a significant role, since the filler is much stiffer than the polymer matrix, and the stiffness increases with increasing filler content. The extent depends on the filler surface area, as indicated by an increase in tensile modulus, and a decrease in both elongation and stress at break [46]. The results of the properties of composite materials based on poly(methylmetacrylate) (PMMA) matrices filled with electrolytic copper powder, having very high dendritic structure. The results showed that the shape and morphology of the copper powder and fillers play a significant role in the phenomenon of electrical conductivity [45].

From the foregoing discussions, polymer composites with SiC, MgO, ZnO and Cu fillers can give evidence that there is no work had focused on improving thermal conductivity of thermosetting polyurethane elastomers with these filler types. Some works carried out using other polymer matrices was aiming to improve thermal conductivity while some works used these fillers to improved only mechanical properties of the thermoplastic polyurethane composites. Therefore, thermosetting polyurethane elastomer with high thermal conductive fillers is still an undeveloped filed of interest for electronic applications.

CHAPTER 3

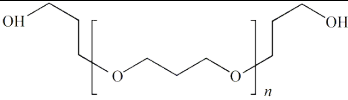
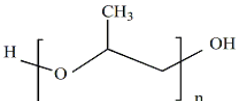
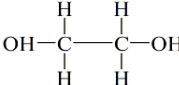
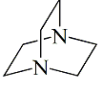
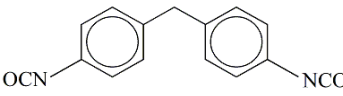
Experiment and Methodology

In this study, we intend to prepare high thermally conductive polyurethane elastomer composites. Both flexible and rigid polyurethane elastomer matrices were fabricated by varying the chain extender contents. After that, high thermal conductive fillers consist of silicon carbide (SiC), magnesium oxide (MgO), zinc oxide (ZnO), and copper (Cu) were loaded into both flexible and rigid polyurethane elastomers. The content of the high thermal conductive fillers was varied to determine the optimum fillers proportion in both polyurethane elastomer matrices. In this chapter, the used raw materials, preparation methods, and testing methods were explained.

3.1 Materials

The main raw materials were supplied by BorsodChem Zrt. (Hungary). However, the high thermally conductive fillers were purchased from other companies. All components are shown in Table 3.1.

Table 3.1 Components of polyurethane elastomer composites formula

Components	Trade Name	Formula	Amount (phr)
Polyether polyol	Caradol MC28-02		100
Polypropylene glycol (PPG-400)	ALCUPOL D411		5
Monoethylene glycol (chain extender)	mEG		7, 10, 22, 30, 34
Amine Catalyst	Dabco 33-LV		0.3 to 2.4
Moisture scavenger	Finmasorb 430 PR	N/A	5
4,4' diphenylmethane diisocyanate (MDI)	ONGRONAT XP 1117		22 to 52
Silicon carbide	Silicon Carbide	SiC (6.587 μm)	0 to 121 (0 to 14*)
Magnesium oxide	n.a.	MgO (3.505 μm)	0 to 100 (0 to 12*)
Zinc oxide	Zinc Oxide	ZnO (1.367 μm)	0 to 100 (0 to 8*)
Copper	n.a.	Cu (28.084 μm)	0 to 39 (0 to 2*)

* percent by volume

Caradol MC28-02 is the main polyol in this study. It is an activated propylene oxide/ethylene oxide-based polyether polyol. At 25 °C, viscosity and density are 1130 cP and 1021 g/cm³. It has a nominal molecular weight of 6000 g/mol and its typical hydroxyl value of 28 mgKOH/g. It was used as a polyol soft segment for preparing polyurethane elastomers. Its high molecular weight enhances the resilience and tensile properties of the foams whilst exhibiting excellent processing characteristics.

Diphenylmethane-4,4'-diisocyanate was used for isocyanates for polyurethane elastomer composites. ONGRONAT XP 1117 is a trading name of it. It is an acidified MDI blend based on ONGRONAT 2100, MI50, and pure 4,4' MDI. The average molecular weight is 266 g/mol and the equivalent weight is 127.33 g/mol. Its viscosity is 5-25 cP at 25 °C and NCO value is 31.5-33.5 m/m%.

Monoethylene glycol (mEG) is used as the chain extender. Its molecular weight is 62.07 g/mol. Ethylene glycol is produced from ethylene via the intermediate ethylene oxide. Ethylene oxide reacts with water to produce ethylene glycol. Monoethylene glycol can be used for applications that require chemical intermediates for resins, solvent couplers, freezing point depression, solvents, humectants, and chemical intermediates.

Polypropylene glycol (ALCUPOL D0411) is also polyol that used to prepare polyurethane elastomers matrix. It has molecular weight and hydroxyl point of 400 g/mol and 270 mgKOH/g, respectively. The viscosity is 86 cP at 25 °C.

Amine catalyst, Dabco 33-LV, was used for a catalyst to synthesis polyurethane elastomers and its composite. It is a mixture of 33% triethylene diamine and 67% dipropylene glycol. Its viscosity and specific gravity are 125 cP at 25 °C and 1.03 g/cm³ at 21 °C, respectively. It is a tertiary amine which has a strong influence on promoting the urethane reaction in a variety of flexible.

Finmasorb 430 PR is a moisture scavenger which prepared to use in this study. It is a molecular sieve pasted in castor oil at 50%, used for absorbing moisture in moisture sensitive systems. In polyurethane systems prevents foaming by CO₂ generated upon the reaction of the isocyanate with moisture that may contain raw materials used or present in the support where we will apply the product.

Silicon carbide (SiC) powder was purchased from Minerals Water, United Kingdom. The particle mean size is 6.587 µm. Scanning electron microscope (SEM) image shows SiC particle (Figure 3.1(a)). The result shown a flake-like shape particles and the biggest particle size is around 5 µm.

Magnesium oxide (MgO) powder was supplied by BorsodChem Zrt. The particle mean size is 3.505 μm . It was prepared by sieve shaking. Spherical-like shape and micro-sized were shown in Figure 3.1(b). It can be observed that aggregated particles have fragmented to particles smaller in size than SiC particles.

Zinc oxide (ZnO) was purchased from Subolab GmbH company, Germany. Its particle mean size is around 1.367 μm . SEM image revealed a cube-like or flake-like shape particle and both nano- and micro-sized. It can be clearly observed that it has more aggregate with smaller particles than SiC and as similar as MgO particles as present in Figure 3.1 (c).

Copper (Cu) was also supplied from BorsodChem Zrt. Its particle mean size is 28.084 μm and shown in Figure 3.1 (d). SEM image shows dendritic shape particles (electrolytic copper) with high thermal and electrical conductivity.

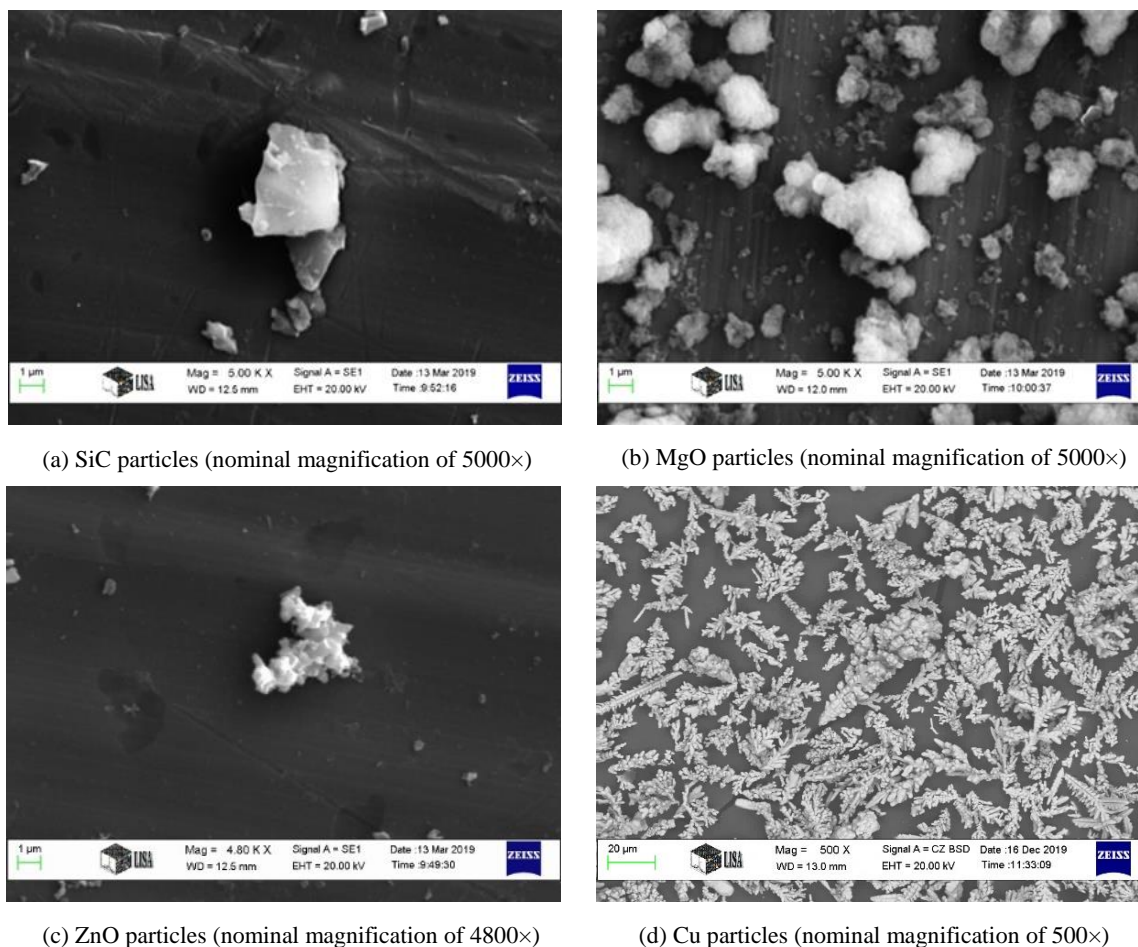


Figure 3.1 SEM images of high thermal conductive fillers

3.2 Preparation methods

To study the effect of the chain extender, a stoichiometric amount of polyether polyol (PEP), monoethylene glycol, polypropylene glycol (PPG 400), amine catalyst and

moisture scavengers were prepared and mixed by using sheared stirrer machine as shown in Figure 3.2. The chain extender content was varied from 7 to 34 phr while the other additives were kept at constant values to prepare flexible and rigid polyurethane elastomer matrices. All of the components were solution mixed, consist of polyether polyol, monoethylene glycol, polypropylene glycol, amine catalyst, and moisture scavengers by following Table 3.1. For example, synthesis polyurethane elastomers with the chain extender of 10 phr by weighting polyether polyol, monoethylene glycol, polypropylene glycol, amine catalyst and moisture scavengers of 100, 5, 10, 0.6 and 5 g, respectively, into a plastic bottle. After that, the mixture was homogenized by using a stirrer machine at around 1000 rpm for 10 mins. Then, the air bubbles were removed by using a vacuum pump machine for 60 mins before mixing with diisocyanate. The diisocyanate of 30.8 g was mixed with the pre-polyol blend by shear stirrer again for 8-15 secs at around 1000 rpm and suddenly poured into the pre-warm mould at 50 °C. Polyurethane elastomer sheet remains on the warm mould for 15-30 mins, solidification time of polyurethane sample depends on the chain extender and catalyst content. Then, it was removed off the mould. The dimension of polyurethane sheet is 1 mm and 4 mm in thickness, 150 mm in width and 220 mm in length. Polyurethane sheet was left at the room temperature at least 3 days before cut the specimen test by following the standard testing. All of polyurethane samples with different the chain extender content was prepared with the same method.

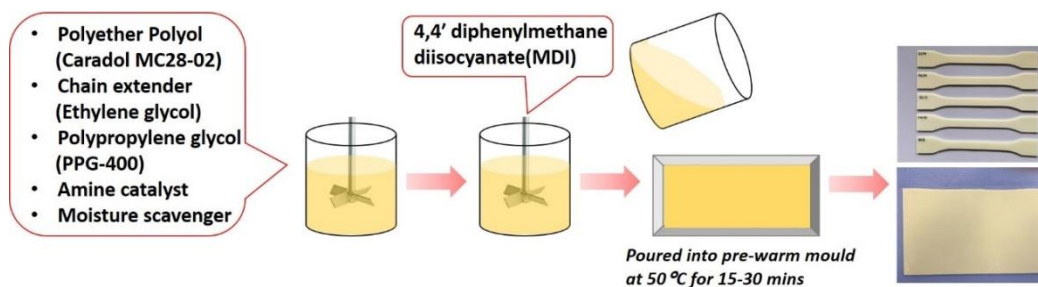


Figure 3.2 Preparation diagram of polyurethane elastomers sheet

In case of PUR composites, we had already selected two formulas from five to prepared PUR composites with high thermal conductive fillers. One formula was prepared for flexible PUR at the chain extender content of 10 phr and the others for rigid PUR at the chain extender content of 30 phr. The high thermally conductive fillers such as SiC, MgO, ZnO, and Cu were added and mixed in the pre-polyol blend step as shown in Figure 3.3. All of the fillers were dried at 90 °C for at least 3 days before adding into

the pre-polyol blend. For example, preparing flexible polyurethane elastomer composites with SiC fillers, polyether polyol, monoethylene glycol, polypropylene glycol, amine catalyst and moisture scavengers of 100, 5, 10, 0.3, and 5 g, respectively, were weighted and poured into a plastic bottle. After that, SiC powder at 21 g (3.79 v/v%) was added to the pre-polyol mixture. The mixture with SiC fillers was homogenized by using a stirrer machine at around 1000 rpm for at least 10 mins. Then, the air bubbles inside the mixture also were removed by using a vacuum pump machine for 60 mins. The MDI of 27.76 g was mixed with the mixture by shear stirrer again for 8-15 secs at around 1000 rpm and also suddenly poured into the pre-heated mould. Then, the specimen testing was prepared similar to PUR without fillers as represented in Figure 3.3. Both flexible and rigid polyurethane elastomers with different filler types and contents were prepared with the same method. All samples and variations of PUR and its composites are presented in appendix D.

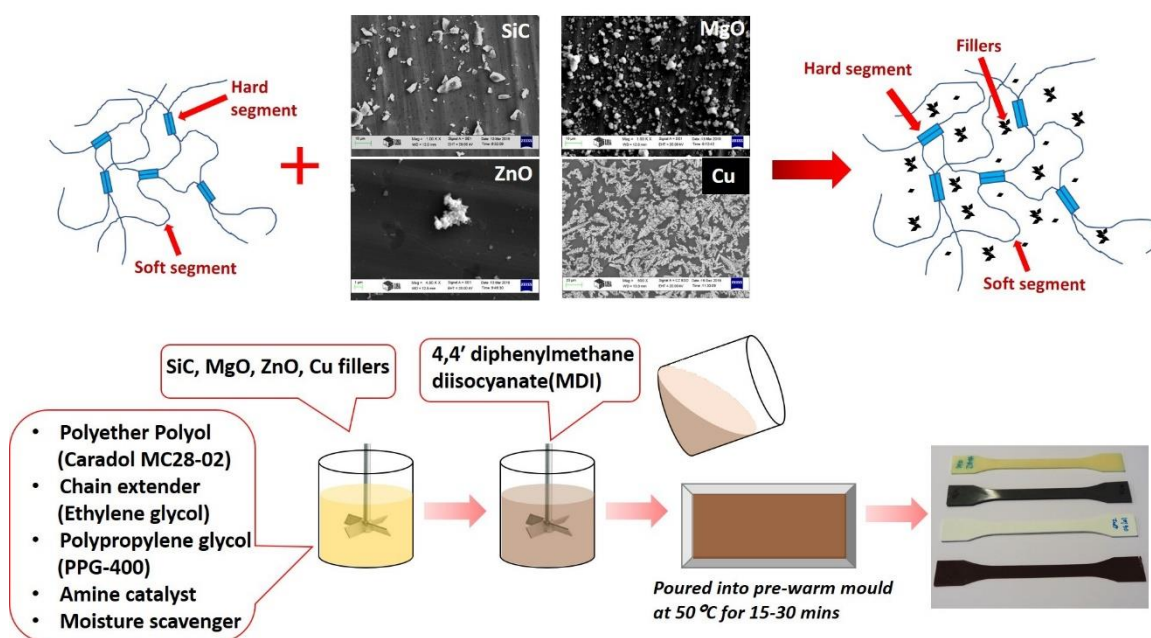


Figure 3.3 Preparation diagram of polyurethane elastomer composites sheet

The content of the high thermal conductive fillers was adjusted in both flexible and rigid PUR matrices as following Table 3.1. Therefore, homogenization and dispersion of fillers in the PUR matrix was investigated by scanning electron microscopy technique. For instance, Figure 3.4 reveals homogenization and evenly dispersion of SiC, MgO, ZnO, and Cu fillers in PUR matrix. Furthermore, the results confirmed that this solution mixing process can be homogenized and uniformed in both high thermally conductive fillers and PUR matrix.

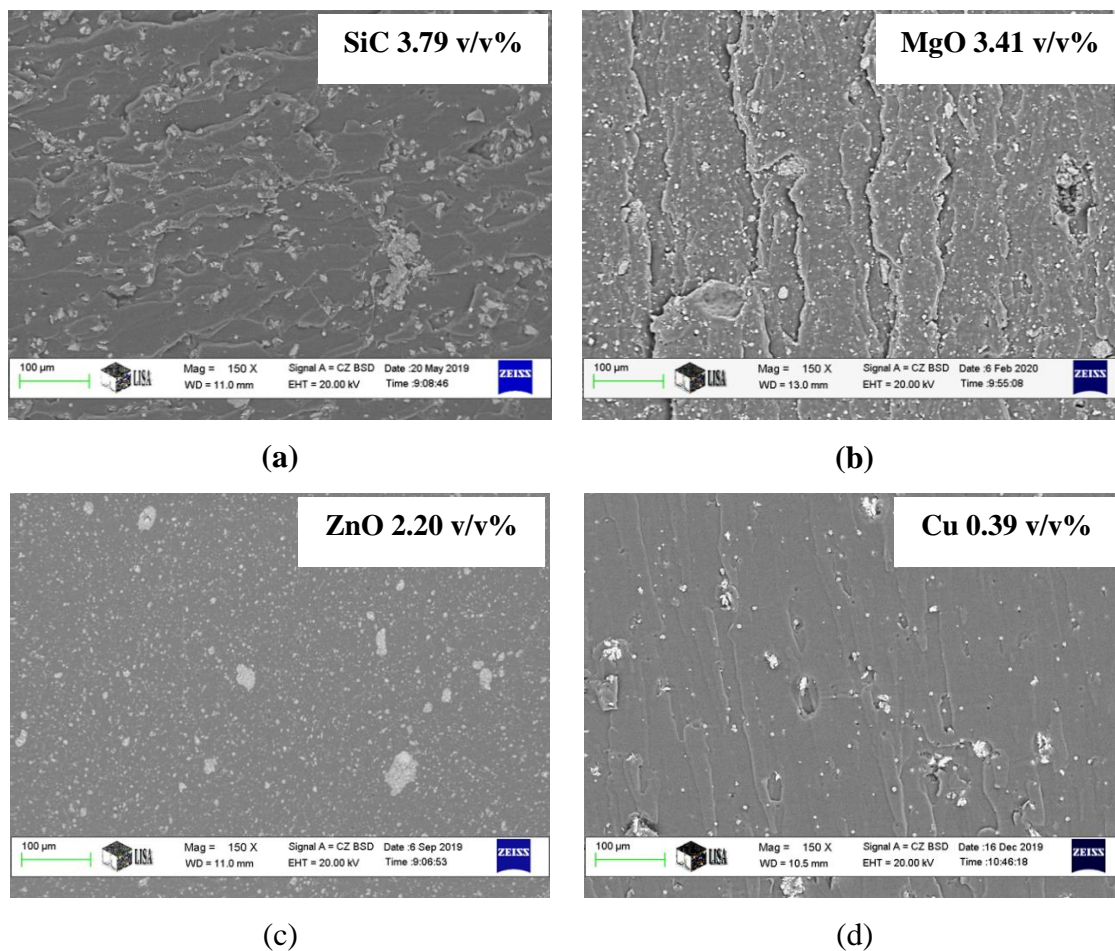


Figure 3.4 SEM images of SiC (a), MgO (b), ZnO (c) and Cu with flexible PUR composites (nominal magnification of 150 \times)

3.3 Testing methods

The properties of the new polyurethane elastomers with different chain extender amounts and high thermally conductive fillers were tested, characterized and analyzed. Thermal conductivity was measured by the C-THERM thermal conductivity analyzer (TCi) at the Institute of Ceramic and Polymer Engineering, University of Miskolc. The density was measured at the room temperature by the density tester at BorsodChem Company, Kazincbarcika, Hungary. The specimen test for thermal conductivity testing should be thicker than 5 mm. C-THERM TCi is based on the modified transient plan source technique. In case of density measuring following ISO 1183, density is the mass per unit volume of a material. Specific gravity is a measure of the ratio of the mass of at given volume of material at room temperature to the same volume of deionized water. The specimen is weighed in the air then weighed when immersed in distilled water at room temperature using a sinker and wire to hold the specimen completely submerged as

required. Density and Specific Gravity are calculated by following equations (3.1) and (3.2).

$$\text{Specific gravity} = a/[(a+w)-b] \quad (3.1)$$

$$\text{Density (kg/m}^3\text{)} = (\text{specific gravity}) \times (997.6) \quad (3.2)$$

Where a is mass of specimen in air, b is mass of specimen and sinker (if used) in water and w is mass of totally immersed sinker if used and partially immersed wire.

Mechanical properties were investigated by measuring of Shore A and Shore D hardness according to ISO 868 standard and operated at BorsodChem Company. Shore hardness is a measure of the resistance of a material to penetration of a spring-loaded needle-like indenter. The Shore A scale is used for testing soft elastomer (rubbers) and other soft polymers. On the other hand, hardness of hard elastomers and most other polymer materials such as thermoplastics and thermosets measured by the Shore D scale. The loading forces of Shore A are 822 g and Shore D is 4536 g. Shore hardness value may vary in the range from 0 to 100.

Tensile properties have been measured according to ISO 527 [100] and tensile specimens have been also prepared according to the same standard. Tensile specimens test was prepared by die cutting from 1 mm sheet both PUR without fillers and with fillers as shown in Figure 3.5. The samples were prepared of 5-10 specimens in every condition. The cross-head speed of the tensile test is 100 mm/min at room temperature measured by using Instron Universal Testing Machine. A tensile test is performed to determine the tensile properties of a material. The test samples are often prepared to a specified size according to the international testing standard. The amount of force (F) applied to the sample and the elongation (ΔL) of the sample are measured throughout the test. Material properties are often expressed in terms of stress (force per unit area, σ) and strain (percent change in length, ε). To obtain stress, the force measurements are divided by the sample cross-sectional area ($\sigma = F/A$). σ_b , σ_1 , and σ_2 are the stress at the specimen breaks, at specified value 1 and 2, respectively. Strain measurements are obtained by dividing the change in length by the initial length of the sample ($\varepsilon = \Delta L/L_0$). ε_b , ε_1 , and ε_2 are the strain at the specimen breaks, at specified value 1 and 2, respectively. To obtain tensile modulus (E), slope in the beginning of stress-strain curve is calculated ($E = (\sigma_2 - \sigma_1) / (\varepsilon_2 - \varepsilon_1)$). These values are then presented on a stress-strain curve as Figure 3.6.

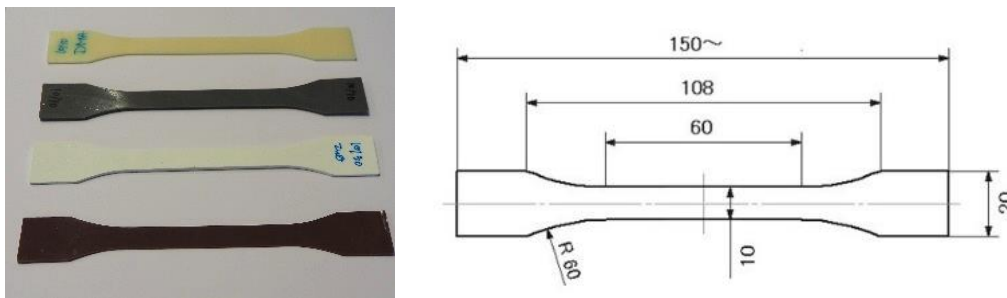


Figure 3.5 Show tensile specimens according to ISO 527 standard

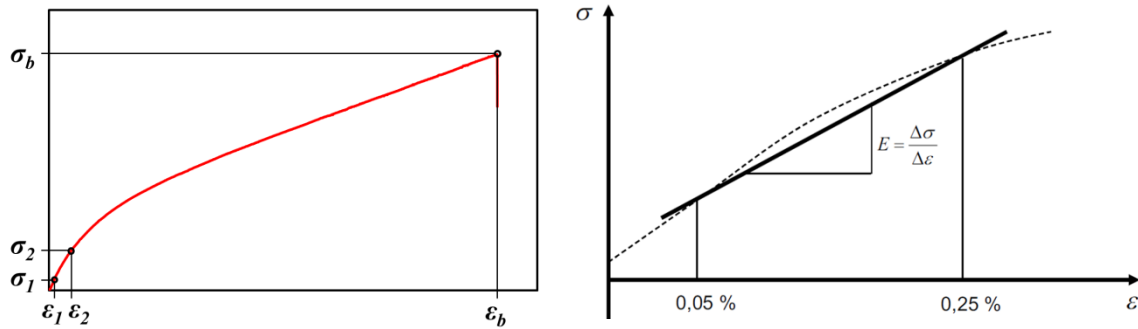


Figure 3.6 Show typical stress-strain curve and tensile modulus determination [100]

Thermal properties were characterized by differential scanning calorimetry (DSC) technique. DSC of pure PUR and its composites were performed on METTER TOLEDO model DSC823e with a heating rate of 10 °C/min from -100 to 250 °C. Melting points and glass transition temperatures (T_g) for most polymers are available from standard compilations and the method can show up possible polymer degradation by the lowering of the expected melting point, T_m . The percentage crystallinity of a polymer can also be found using the DSC technique. It can be obtained from the crystallization peak from the DSC curve since the heat of fusion can be calculated from the area under an absorption peak.

Viscoelastic properties were investigated by a dynamic mechanical thermal analyzer, DMA 8000 (PerkinElmer), at BorsodChem company. Storage modulus and $\tan\delta$ were analyzed from -80 to 150 °C with bending mode at 1 Hz and a heating rate of 2 °C/min. The modulus can express as an in-phase component (the storage modulus; E') and an out of phase component (the loss modulus, E'') when a sinusoidal force is applied. The storage modulus, either E' or G' , is the measure of the elastic behavior of the sample. The ratio of the loss to the storage is the $\tan\delta$ and is often called damping. Damping is the dissipation of energy in material under cyclic load. It tells us how good material will be at absorbing energy.

The infrared (IR) spectra of pure PUR and its composites were recorded on a Bruker Tensor 27 FTIR instrument at the Institute of Ceramic and Polymer Engineering, the University of Miskolc. The spectra were recorded in the range of 400 – 4000 cm^{-1} with a nominal resolution of 4 cm^{-1} .

Moreover, the swelling degree of pure flexible and rigid polyurethane was measured at room temperature using ten different solvents. The test samples are disks 1 cm in diameter and 1 mm in thickness, cut from the cast thin sheet. The samples were immersed in each solvent for 1 week. After that, these samples were removed from the solvent and weighted after removal of the excess solvent from the samples. The swelling degree was calculated using equation (3.3), where W and W_i are the sample weights after and before swelling.

$$\text{Swelling degree} = (W - W_i)/W_i \quad (3.3)$$

The swelling properties were measured for PUR without fillers both flexible and rigid PUR. In this theory, the rate of maximum swelling is the result of the equilibrium between two major adverse effects, the entropy of mixing and the entropy of polymer chain configuration [101].

Thermally stimulated discharge (TSD) technique was used to investigate the structure of both flexible and rigid PUR without fillers by thermally stimulated discharge machine, model TSC II. Sample disks of 26 mm diameter were cut by die-cutting. The polarizing field at 500 V/mm was operated in the temperature range of -120 to 10 $^{\circ}\text{C}$ while cooling and heating rates of 5 $^{\circ}\text{C}/\text{min}$ were used. TSD technique is ideal for the investigation of the structure of polymers, semi-crystalline polymers, and co-polymers because it is a more sensitive alternative than other thermal analysis techniques for detecting the transitions [102-104].

Besides, morphology and element of fillers and PUR composites were investigated by scanning electron microscopy technique (SEM; ZEISS EVO-MA10) and energy-dispersive X-ray spectroscopy (EDS) at the University of Miskolc. Every sample was coated by gold before the examination. SEM image of the composites are captured on fractured tensile sample surface. SEM is a type of electron microscope that produces images of a sample by scanning the surface with a focused beam of electrons with the intensity of the detected signal to produce an image of the specimen.

To obtain particle size distribution of the high thermal conductive fillers, all fillers used were measured using a laser scattering particle size distribution analyzer (HORIBA LA-950).

CHAPTER 4

Results and discussion

In this chapter, the results and discussion were demonstrated and concluded in each type of the high thermally conductive fillers such as silicon carbide (SiC), magnesium oxide (MgO), zinc oxide (ZnO) and copper (Cu) reinforced polyurethane elastomer (PUR) composites. However, the PUR matrix with different chain extender amounts was investigated to find the threshold limit content of the different high thermally conductive fillers in both flexible and rigid PUR matrices.

4.1 Polyurethane elastomers with different chain extender contents

From the literature overview, the chain extender is very important in the PUR structure. The chain extender influences the hard segment segregation in PUR structure and enhances the mechanical properties of PUR. Hence, the first step of this study is developing PUR formula by adjusting the chain extender content to produce flexible and rigid PUR matrices for different applications in electrical industry. The chain extender was varied from 7 to 34 phr to obtain a very soft to hard PUR matrices. After that, thermal conductivity, density, mechanical properties, thermal properties, dynamic mechanical properties, and chemical structure of the different PUR formulas were investigated and the optimal properties of the produced composite from flexible and rigid PUR matrices were determined, respectively.

4.1.1 Thermal conductivity and density

Thermal conductivity and density of PUR with different chain extender contents were measured. Results show that the thermal conductivity increases with increasing chain extender (mEG) as shown in Figure 4.1(a). The thermal conductivity was improved around 35% from 7 to 34 phr of the chain extender content as shown in Table 4.1. This result is due to increase the crystallinity level by increasing the hard segment when the chain extender content was increased. Increasing the chain extender content affects the hard segment length of PUR structure. The hard segment content also influences the physical properties of polyurethanes. In PUR structure, the hard segment is built from alternating diisocyanate and chain extender sequences while the soft segment originated from the polyol. The hard segment is associated into with hard domains acting as physical crosslinks and filler particles within the rubbery soft segment matrix [73].

Therefore, the physical crosslinks might increase with increasing the chain extender content and strongly affect their mechanical and thermal conductivity [76]. The thermal stability of polymer is connected to their chemical structure, the bond energy between individual atoms comprising the materials [105]. The increase in thermal conductivity value is correlated to the increase in the density as shown in Figure 4.1(b) and 4.1(c). Increasing of the density might be due to a high chain extender which has high reactivity with MDI and polyol that leads to high cross-linking structure, especially, the hard segment in PUR structure or urea linkage which has a higher density of hydrogen bonding [77].

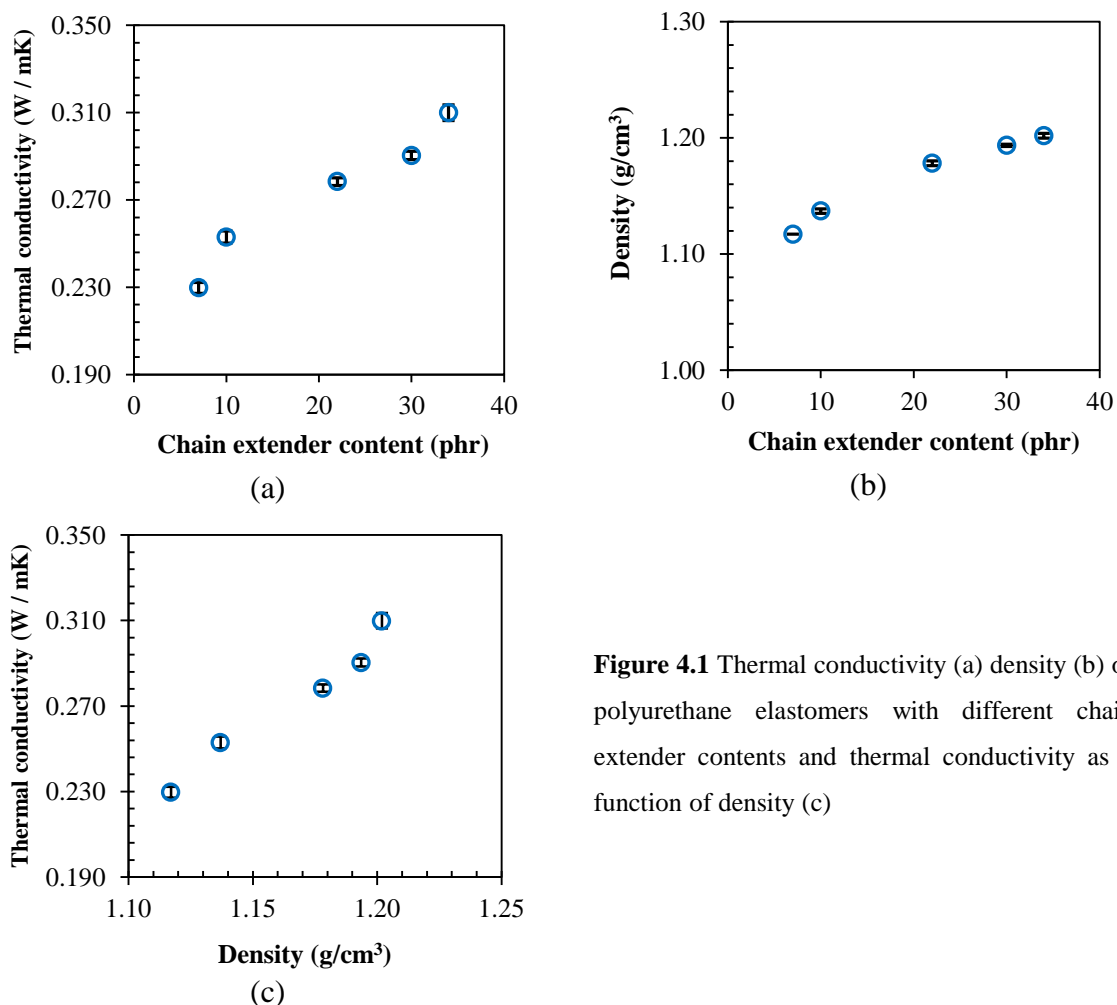


Figure 4.1 Thermal conductivity (a) density (b) of polyurethane elastomers with different chain extender contents and thermal conductivity as a function of density (c)

4.1.2 Mechanical properties

The mechanical properties were investigated to determine which formula suit for flexible PUR and rigid PUR matrices in this study. In this study, Shore A and D hardness and tensile testing were examined and presented.

Table 4.1 Thermal conductivity and density of polyurethane elastomers with different chain extender contents

Chain extender content (phr)	Thermal conductivity (W / mK)	Density (g/cm ³)
7	0.230 ± 0.003	1.117 ± 0.000
10	0.253 ± 0.003	1.137 ± 0.002
22	0.278 ± 0.002	1.178 ± 0.002
30	0.290 ± 0.002	1.194 ± 0.001
34	0.310 ± 0.004	1.202 ± 0.002

4.1.2.1 Hardness

The variations in Shore A and D hardness values of PUR with different chain extender contents between 7 and 34 phr are shown in Figure 4.2 (a) and (b) and Table 4.2. Results reveal that Shore A hardness rapidly increased with increasing the chain extender content from 7 up to 22 phr, around 1.4 times, while Shore D hardness also increased with increasing chain extender content, around 3.4 times. At high chain extender content, both Shore A and D hardness show almost constant value around 96 and 65, respectively. This constant value is due to Shore A hardness value was not sensitive enough for values over 90 therefore Shore D was also measured to confirm this result. Result can confirm that the chain extender at 30 phr is a threshold limit of Shore hardness value. Increasing the chain extender content tends to increase the hard segment and the hydrogen bonding index in PUR structure. If the hydrogen bonds are formed only within the hard segment, they may enhance crystallization and phase separation of PUR structure [106]. This result is clearly seen the correlation between thermal conductivity, density and Shore hardness. Increasing the chain extender content can raise cross-linking level of PUR structure which in turn increases the density and Shore hardness.

4.1.2.2 Tensile properties

Tensile strength, elongation at break, and tensile modulus were plotted as a function of the chain extender content as shown in Figure 4.3. As was expected, the tensile strength of polyurethane elastomers rapidly increased with increasing the chain extender content. Tensile strength was improved around 6 times when the chain extender content was increased from 7 to 30 phr. On the other hand, elongation at break rapidly decreased. It was decreased from 191 to 10%. However, tensile modulus also rapidly increased with increasing the chain extender content from 10 to 791 MPa as shown in Figure 4.3(b) and Table 4.3. It shows a huge enhancement by 79 times.

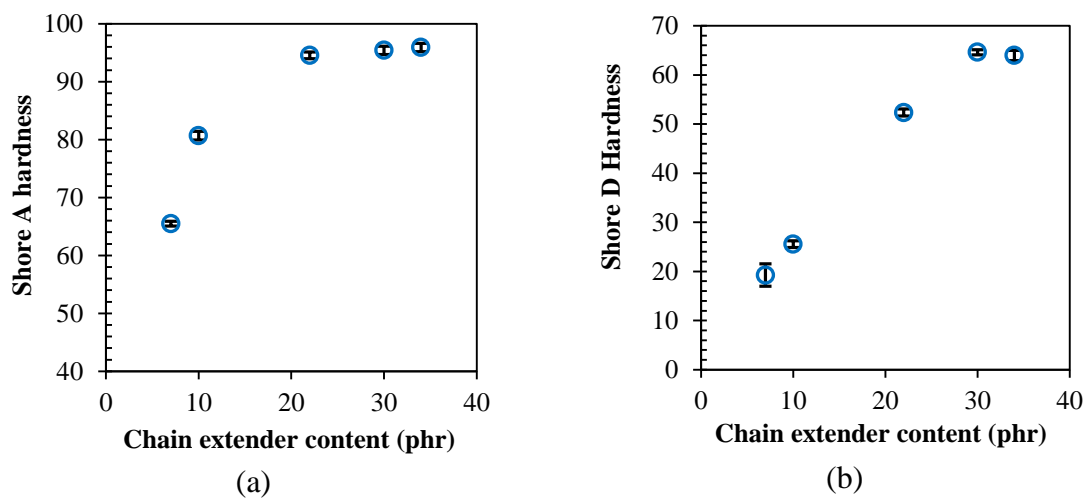


Figure 4.2 Shore A hardness (a) and Shore D hardness (b) of polyurethane elastomers with different chain extender contents

Table 4.2 Shore A and D hardness of polyurethane elastomers with different chain extender contents

Chain extender content (phr)	Hardness	
	Shore A	Shore D
7	66 ± 0.4	19 ± 2.3
10	81 ± 0.7	26 ± 0.7
22	95 ± 0.6	52 ± 0.7
30	95 ± 0.7	65 ± 0.5
34	96 ± 0.7	64 ± 1.1

It can be explained that increasing monoethylene glycol (mEG) which is a chain extender in polyurethane elastomers leads to the formation of phase-separated hard segments. It means that the hard segment concentration increases the tensile strength and modulus as well. This is in agreement with the widely accepted idea that the hard segment domains act as a reinforcing particle in the soft segment matrix.

Figures 4.1 and 4.2 show a very low standard deviation of the values for each sample series that means the repeatability of these mechanical tests are very good. However, the graphs show quite high scattering as present in the elongation at break result and tensile modulus (Figure 4.3). This is because there are several auxiliary effects. For instance, uncontrolled of little moisture during mixing and forming and uncontrolled of the mixing parameters (the real speed of rotation).

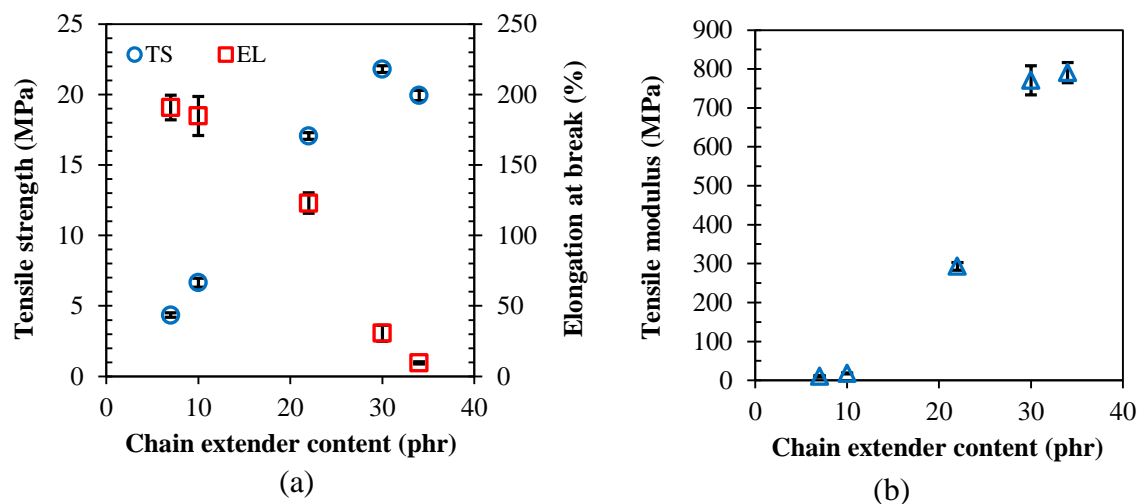


Figure 4.3 Tensile strength and elongation at break (a) and tensile modulus (b) of polyurethane elastomers with different chain extender contents

Table 4.3 Tensile strength, elongation at break and tensile modulus of polyurethane elastomers with different chain extender contents

Chain extender content (phr)	Tensile strength (MPa)	Elongation at break (%)	Tensile modulus (MPa)
7	4 ± 0.2	191 ± 9	10 ± 2
10	7 ± 0.3	185 ± 14	18 ± 1
22	17 ± 0.2	123 ± 7	293 ± 10
30	22 ± 0.2	31 ± 6	771 ± 38
34	20 ± 0.4	10 ± 1	791 ± 26

4.1.3 Thermal properties

Thermal properties of polyurethane elastomers with different formulas were characterized by differential scanning calorimetry (DSC). The first heating scans of polyurethane elastomers with different chain extender contents are shown in Figure 4.4. A small transition temperature at low temperature can be attributed to the glass transition temperature of the soft segment ($T_{g,SS}$) while at higher temperatures can be designated to the glass transition temperature of the hard segment ($T_{g,HS}$). The curve of all the PUR with different chain extender contents show $T_{g,SS}$ of PUR at the same temperature around $-60\text{ }^{\circ}\text{C}$ as shown in Table 4.4. However, $T_{g,SS}$ did not clearly observe at high chain extender contents, 30 and 34 phr. This result can be explained that increasing physical cross-linking of the hard segment with high chain extender content can obstruct the polyol segment motion which leads to having less soft segment ordered structures and the chain extender hinders the formation of hydrogen bonds [77].

Broader endotherms peak at low chain extender content can be ascribed to the small degree of ordering in hard segment domains and occur are partially the result of the wide distribution of hard segment lengths [107]. In case of the high chain extender content, endotherms peak show narrower and high intensity than the lower content that may be due to a high hard segment cross-linking. Furthermore, $T_{g,HS}$ of PUR with different chain extender content can be observed on DSC curves as well. $T_{g,HS}$ slightly increased with increasing the chain extender content. It is between 44 and 48 °C as shown in Table 4.4. This can be suggested that the chain extender content has no significantly influence on $T_{g,HS}$ as confirmed by DSC measuring because $T_{g,HS}$ is difficult evaluated by DSC technique. Endothermic temperature (T_{endo}) shows nearly the same value when the chain extender content was increased as shown in Table 4.4. This might be due to the chain extender content having no effect on the break up if the inter-urethane hydrogen bond [73]. DSC curve can evidence increasing of cross-linking level from narrower endotherm peak and it shows very small transition temperature of soft segment because phase separation at high chain extender content which correlated to high density, Shore hardness, tensile strength and modulus value.

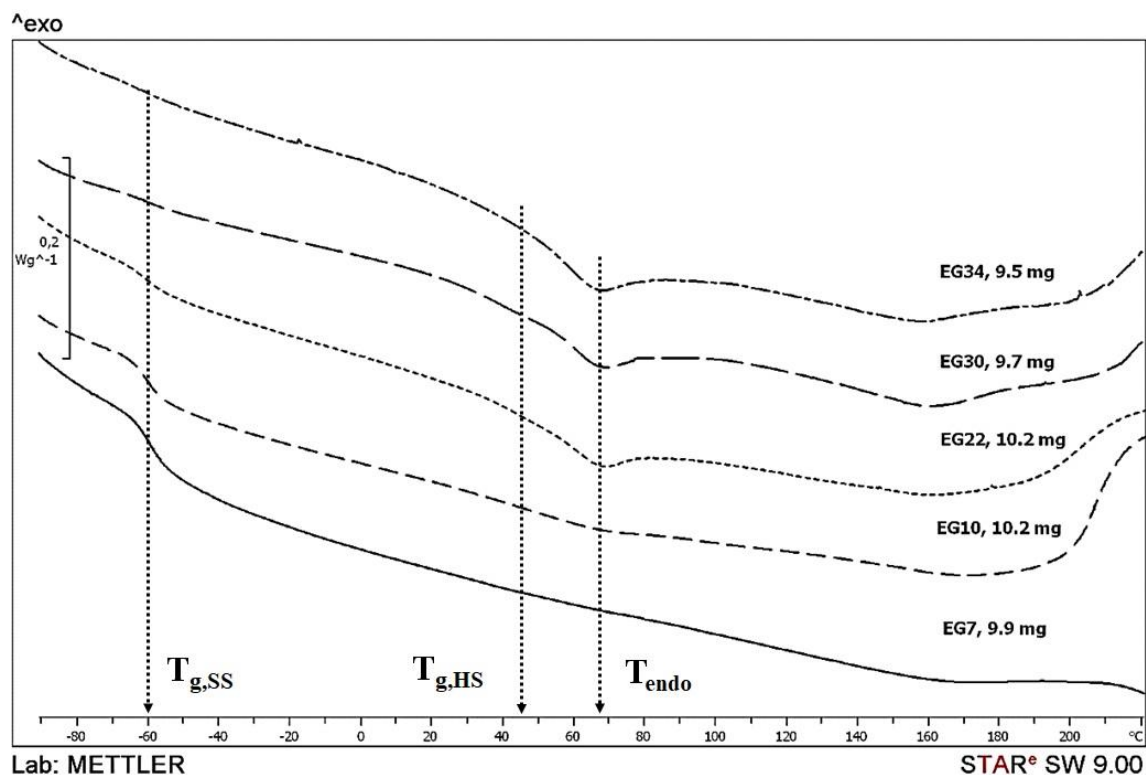


Figure 4.4 DSC curve of polyurethane elastomers with different chain extender contents

Table 4.4 Thermal properties of polyurethane elastomers with different chain extender contents

Chain extender content (phr)	T _{g,SS} (°C)	T _{g,HS} (°C)	T _{endo} (°C)
7	-60	N/A	N/A
10	-60	45	68
22	-60	46	68
30	-60	44	67
34	-60	48	66

4.1.4 Dynamic mechanical properties

The dynamic mechanical analysis (DMA) provides information on viscoelastic properties. The storage modulus (E') provides information regarding the stiffness of the material while the loss tangent ($\tan\delta$) measures the degree of molecular motion. The glass transition temperature of the soft segment is defined as the α transition in the $\tan\delta$ curve. The magnitude of $\tan\delta$ across the application temperature which is proportional to the ratio of energy absorbed as heat by sample to energy returns as the movement of the sample [73]. Therefore, the DMA technique was used to investigate the stiffness and the degree of molecular motion of PUR when the chain extender content was adjusted.

As in Figure 4.5, the E' and $\tan\delta$ of PUR with different chain extender contents in the temperature range from -80 to 150 °C are shown. The E' with various chain extender contents have high modulus at starting temperature and then it shows a decrease at around -60 °C. Furthermore, $\tan\delta$ shows a peak associated with the T_{g,SS} slightly decreased from -45 to -49 °C as shown in Table 4.5. In case of damping capacity, the intensity of the $\tan\delta$ peak of the soft segment decrease with increasing the chain extender content. This result proves that a low degree of polyol segment motion related to DSC curves hard to evaluate a small transition at high the chain extender content. At higher temperature, the mechanical loss factor exhibits the $\tan\delta$ peak shift in the curve to higher temperatures as shown in Figure 4.5. This result indicated that T_{g,HS} increases with increasing chain extender content as revealed in Table 4.5. This increase may be due to increase in the number of higher length hard segment chains in the hard segment domains that occur as the hard segment content of the polymer increased [108] and attributed to increasing hard segment crystallinity and phase separation which tend to reduce soft segment mobility. The increase in the hard segment resulted in larger hard microcrystalline domains that restricted the molecular motion of the soft segment [73]. Besides, the polymer chain with longer chain extender has longer hard segment. The

length of the hard segment has also an effect phase separation [77] and might increase $T_{g,HS}$ of PUR.

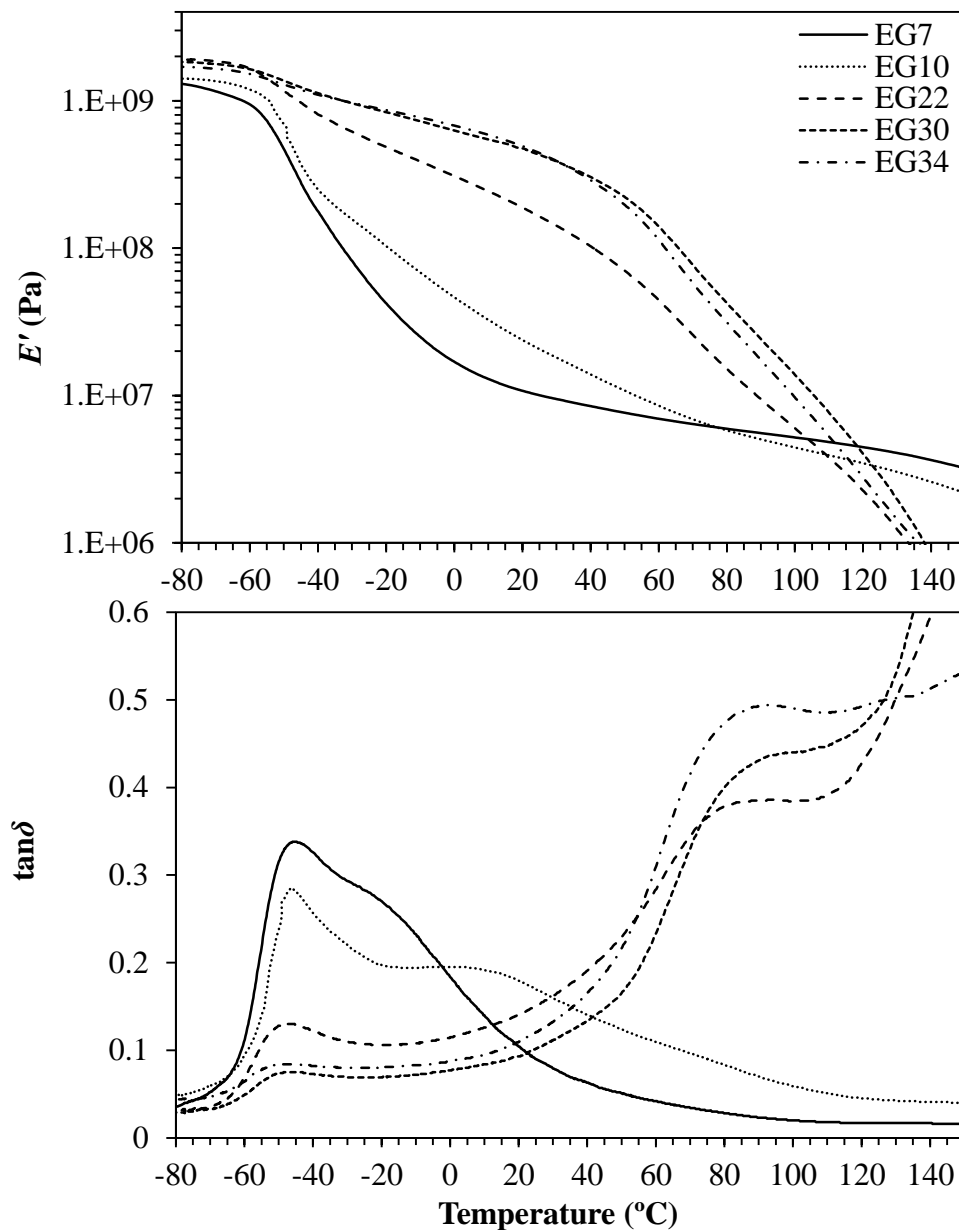


Figure 4.5 E' and $\tan\delta$ of polyurethane elastomers with different chain extender contents

For flexible PUR at the chain extender content of 7 and 10 phr, E' suddenly decreased at around -55°C . This reveals that the hard segments are not able to form a sufficient amount of physical cross-links. However, the chain extender content at 10 phr exhibits higher E' value than 7 phr and it has a similar pattern curve. This may be due to the high cross-linking of the hard segment in PUR structure which affects chain mobility of PUR molecular chain at the chain extender content of 10 phr. As a result of rigid PUR (at 22 phr, 30 phr, and 34 phr), the E' slightly decreases when the temperature increased

from -55 °C. After that, it decreases rapidly that can be assigned to the melting of the hard segment phases and may be due to the total destruction of the physical and chemical cross-linking sites between hard segments are totally destroyed at high temperature [77].

Table 4.5 The glass transition temperature of the soft and hard segment of polyurethane elastomers with different chain extender contents from DMA technique

Chain extender content (phr)	T _{g,SS} (°C)	T _{g,HS} (°C)
7	-45	-12
10	-46	11
22	-47	78
30	-48	83
34	-49	90

However, DSC and DMA result showed a significant difference in T_g. This result did not exactly confirm the earlier reasoning but it might be due the different mechanism to investigation. DSC technique operates by provide heat and characterizes from enthalpy change from specific heat change or chemical reactions while DMA technique operates by provide both of heat and force at the same time to investigate the mechanical behaviour of the material. Therefore, the complex structure of polyurethane elastomer had responded on two techniques in different manner.

4.1.5 Infrared spectroscopy (IR)

Infrared spectroscopy of PUR with different hard segment structures obtained by varying chain extender content is shown in Figure 4.6. The IR spectra of the elastomers exhibited the bands typical for PUR consist of -NH (free and bonded) at 3280 – 3340 cm⁻¹; CH₂ – at 2850 – 2970 cm⁻¹; C=O in bonded urethane group at 1710 – 1720 cm⁻¹; C=O free urethane group at 1706 cm⁻¹; 1540 cm⁻¹ (Amide I) and 1500 cm⁻¹ (Amide II). A few interactions among the polymeric chains are responsible for the shift of transmittance peak such as hydrogen bonding between -NH group and the carbonyl group of hard segments, dipole–dipole interaction between carbonyl groups of the hard segment and induced dipole–dipole interaction between aromatic rings of the hard segment. It suggests that hard segment gets more aggregated to form domains in the PUR block copolymer as hard segment content increases [109]. Figure 4.6 reveals clearly the effects of chain extender content on PUR structure. The hydrogen-bonded N-H stretches at 3305 cm⁻¹. The urethane C=O stretches near 1720 cm⁻¹ did not clearly reveal two peaks but it indicated the existence of both free and hydrogen-bonded types at 1720–1745 and

1698–1720 cm^{-1} , respectively [110]. Polyurethane block polymers investigated by hydrogen bond from IR spectra. However, the intensity peaks of all chemical band groups of PUR decrease with increasing the chain extender content. It can be explained that the chemical structure of PUR created more the hard segment aggregate to form domains in the PUR block copolymer as hard segment content was increased. For the N-H peak, the intensity decrease can imply bond disruption, the area should decrease as the number of free N-H groups increase [107]. This result correlated to $T_{g,ss}$ from DSC did not clearly see at high chain extender content. It may be due to increasing the chain extender increase the number free N-H groups.

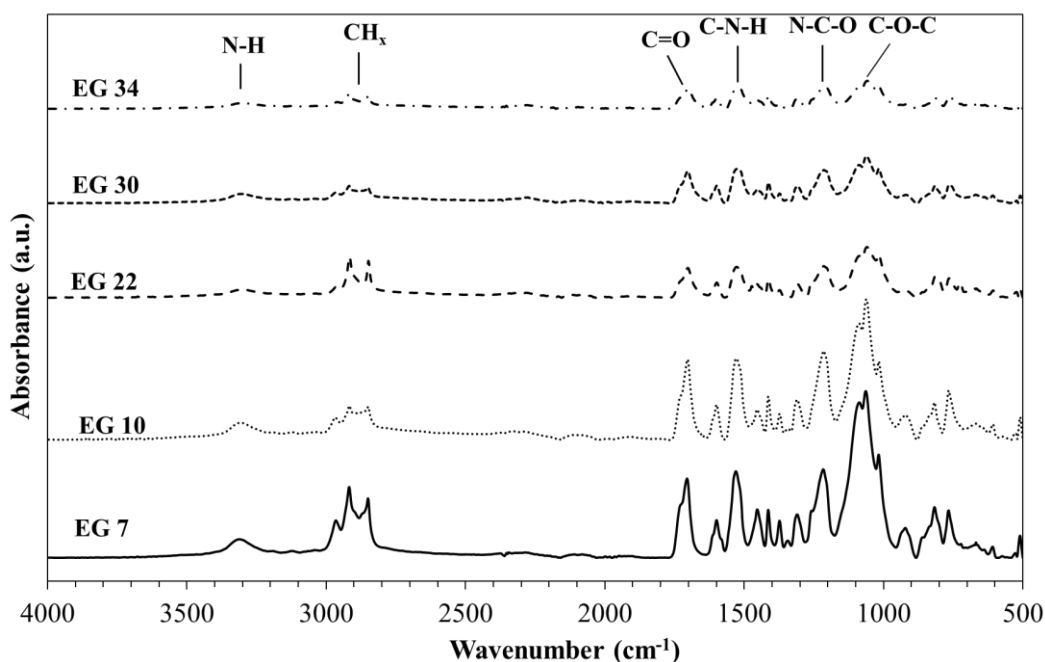


Figure 4.6 IR spectra of polyurethane elastomers with different chain extender contents

From the discussion above, we have chosen to fabricate two types of polyurethane elastomer matrix for preparing the high thermal conductive composites. The first one is a flexible PUR matrix at 10 phr and the other one is a rigid PUR matrix at 30 phr. It was chosen because it has higher thermal conductivity, Shore hardness, tensile strength and modulus than at 7 phr of the chain extender content, while the elongation at break still has high value as well. Furthermore, thermal properties, dynamic mechanical properties, and chemical structure of PUR with the chain extender content of 7 and 10 phr did not significantly change. In case of rigid PUR matrix, PUR with 30 phr of the chain extender content was chosen. This formula was selected due to it has higher properties than 22 phr and lower viscosity than at 34 phr (easily mixing).

4.1.6 Thermal stimulated discharge (TSD)

After selecting the proper PUR matrix, the molecular relaxations of both PUR matrices were investigated by using thermally stimulated discharge (TSD) technique. Most of the relaxation transitions could be observed with simple sample preparation in the thermal stimulated discharge measurement. Polyurethane elastomers can be considered as block copolymers with a long and soft aliphatic segment and the hard segment. The localized motions of the segments or the cooperative motion of the soft segment in association with the molecular backbone can be measured by the depolarization relaxation technique [111, 112]. This technique can confirm the glass transition temperature result. The TSD spectrum of polyurethane elastomers is shown in Figure 4.7. Each spectrum consists of two distinguishable peaks which can be designated as α and β peaks (The β does not mean the classical β relaxation here). Sample with both the chain extender content of 10 and 30 phr exhibited a similar pattern in TSD measurement. The observations of these α and β peaks as the real transitions. The peak occurs at a higher temperature for the hard segment of polyurethane that is based on MDI and at a lower temperature for the soft segment that is based on polyol. This β relaxation transition is associated with the molecular motion dominated by the soft segment [111].

As a result, the maximum temperature (ϑ_{\max}) of the β peak did not significantly change when the chain extender content was increased as shown in Table 4.6. This confirms that the chain extender content has no significant effect on $T_{g,SS}$. For $T_{g,HS}$, α peak the temperature rise from -3 to 25 °C with increasing the chain extender content. This also confirms that increasing the chain extender content increases the hard segment of the polyurethane molecular chain, therefore, affecting the relaxation of the polyurethane structure. The energy of activation estimated is of the same order of magnitude as predicted theoretically for the side group orientation in the polymer [113]. Furthermore, the apparent energy of activation (A_e) of the β and α peaks decreases with increasing the chain extender content from 73 to 64 kJ/mol and 82 to 48 kJ/mol, respectively. This is due to increasing of the hard segment influences the side group orientation of the polyol segment in PUR structure and it may be originated from the broader monomer distribution. The decrease in the value of the maximum peak current (I_{\max}) with increasing the chain extender content may be occurred due to the long hard segment that decreases the amount of free charge. The activation energy of rigid PUR shows lower value than flexible PUR in both soft and hard segment. This suggests that a flexible PUR has more mobility of soft and hard segments than rigid PUR. There is a

higher cross-linked structure (hard segment) in rigid PUR than flexible PUR and it affects the chain mobility and activation energy value.

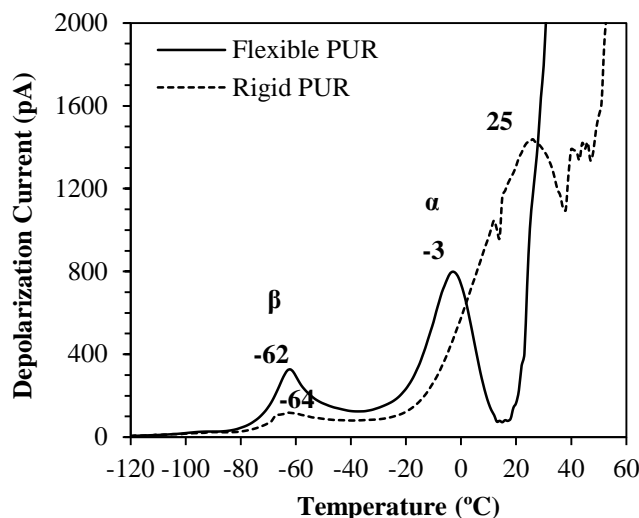


Figure 4.7 TSD spectra of pure polyurethane elastomers with different chain extender of 10 and 30 phr

Table 4.6 Maximum temperature, maximum current and energy of polyurethane elastomers with different chain extender contents from TDS measurement

Chain extender content (phr)	Soft segment			Hard segment		
	ϑ_{\max} (°C)	I_{\max} (pA)	A_e (kJ/mol)	ϑ_{\max} (°C)	I_{\max} (pA)	A_e (kJ/mol)
10	-62	312	73	-3	789	82
30	-64	98	64	25	1404	48

4.1.7 Swelling properties

Several characteristics in hydrogels such as permeability and mechanical, surface, and other properties are influenced by the swelling degree. The swelling degree is also modified by the chemical structure of the polymer network, the cross-linking density and the type of ionic groups in the polymers [114]. The degree of swelling is known to be dependent on the cross-linking density of polymer networks, the greater the cross-linking density, the less the degree of swelling [115]. Hence, a swelling degree was investigated in both flexible PUR and rigid PUR. In this study, various solvents were used for swelling testing with the solubility parameter range between 7.24 and 12.92 $\text{cal}^{1/2}\text{cm}^{-3/2}$ ($\text{cal}^{1/2}\text{cm}^{-3/2} = 2.04 \text{ MPa}^{-1/2}$). The result presented in Figure 4.8, it shows two peaks in both flexible and rigid PUR, which can indicate the swelling degree of the soft segment (at low solubility parameter) and the hard segment (at high solubility parameter). However, the flexible PUR has higher swelling degree than the rigid PUR. This might be

correlated to the low chain extender content of flexible PUR affect the low density of the cross-linking structure. Therefore, the ability of polymer chains of flexible PUR can absorb a solvent molecule increase and reveal higher swelling degree than the rigid PUR [116]. The swelling degree results exhibited the trend as similar to TSD result which both flexible and rigid PUR reveals two peaks that consist of the soft segment and the hard segment.

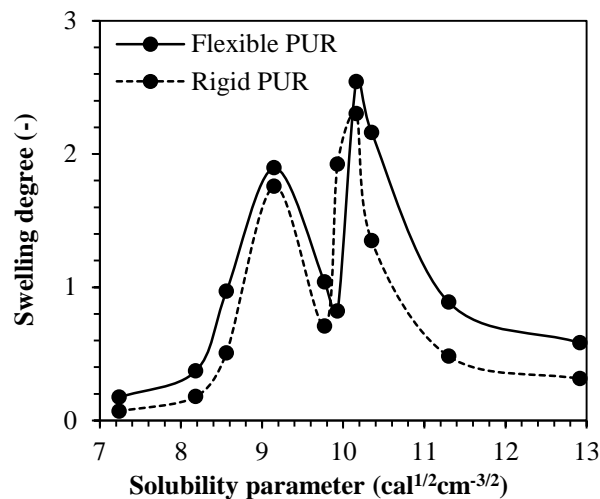


Figure 4.8 Swelling degree of pure polyurethane elastomers with different chain extender of 10 and 30 phr (Independent variable is the solubility parameter of the solvent)

4.2 Flexible and rigid polyurethane elastomer with silicon carbide composites

In this topic, one type of high thermal conductive fillers is silicon carbide (SiC). SiC was used to fabricate flexible and rigid polyurethane elastomer composites. SiC content was varied between 0 and 14 v/v% into both PUR matrices. As the same way as the previous topic, the properties were presented starting from thermal conductivity and density. Furthermore, a theoretical model to predict the thermal conductivity of polymer composites was discussed when PUR composites were prepared.

4.2.1 Thermal conductivity and density

In case of a theoretical model of thermal conductivity, various theoretical predictions of thermal conductivity reveal good agreement with the experimental results [117, 118]. However, some limitations of the theoretical models at high filler contents are still worth considering. Therefore, we have investigated and determined the thermal conductivity of layered composites on parallel and in series layers. We found out that the former model describes a constant temperature gradient and the latter a constant heat flow according to equations (4.1) and (4.2), respectively.

$$\lambda_u = \phi_1 \lambda_1 + \phi_2 \lambda_2 \quad (4.1)$$

$$\lambda_l = \left(\frac{\phi_1}{\lambda_1} + \frac{\phi_2}{\lambda_2} \right)^{-1} \quad (4.2)$$

Where λ_u , λ_l , λ_1 , λ_2 are the thermal conductivities of composite, the upper limit of thermal conductivity, the lower limit of thermal conductivity, thermal conductivity of components 1 and 2, respectively, while ϕ_1 and ϕ_2 are the volume fraction of components 1 and 2, respectively. Furthermore, the real dispersed of the two phases system also presented in Figure 4.9 (c). This applied model has estimated thermal conductivity in parallel and serial arrangement. The model of equal temperature gradient model results the upper limit of thermal conductivity as presented in Figure 4.9 (a) while the model of equal heat flow model results the lower limit as presented in Figure 4.9 (b). This is formally identical to the mechanical properties, namely the modulus of elasticity used by Coran and Patel [119] replacing the M modulus values by λ thermal conductivity in the following equations (4.3) and (4.4).

$$M_u = \phi_H M_H + \phi_S M_S \quad (4.3)$$

$$M_l = \left(\frac{\phi_H}{M_H} + \frac{\phi_S}{M_S} \right)^{-1} \quad (4.4)$$

Where M_u , M_l , M_H and M_S are the modulus of the upper limit of modulus, the lower limit of modulus, the modulus of the pure hard and soft phases, respectively. ϕ_H and ϕ_S are the volume fractions of the hard phase and the soft phase. For real, mixed systems the equation (4.5) is valid equation. Where M , is the modulus of the composite and n is the adjustable parameter since the upper and lower bound modulus.

$$M = M_l + \phi_H^n (n\phi_S + 1)(M_u - M_l) \quad (4.5)$$

Because of the similarity, it can be used for thermal conductivity as well as described in equation (4.6).

$$\lambda_c = \lambda_l + \phi_2^n (n\phi_1 + 1)(\lambda_u - \lambda_l) \quad (4.6)$$

Where λ_c , λ_u , λ_l are the thermal conductivity of composite, the upper limit of thermal conductivity and the lower limit of thermal conductivity, respectively, ϕ_1 and ϕ_2 are the volume fractions of components 1 and 2, respectively. Besides, n is the characteristic exponent. If $n = 0$ means that the heat conductivity of composite is at the upper limit and $n = 100$ means the lower limit [119]. For the calculations, a short computer program was compiled, $n = 100$ was used instead of ∞ because the error is less than 0.01%. From the applied model, we had expected that the thermal conductive value from the experiment can be predicted using the applied mechanical model which was not used before. Moreover, we expected that this applied model could be properly used to predicting the thermal conductivity of the composites at high filler content.

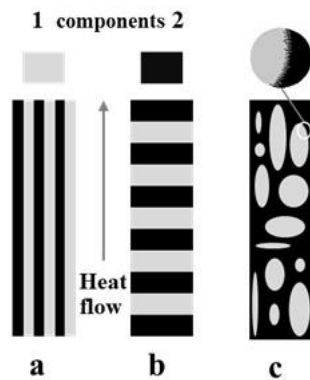


Figure 4.9 Schematic arrangement of equal temperature gradient (a), equal heat flow models (b) and represents a real dispersed two-phases system (c)

In this study, thermal conductivity from the experiment of both PUR matrices with different filler types were discussed and predicted by using the above mentioned mechanical model as a thermal conductivity model. Thermal conductivity of PUR and SiC composites were presented by varying SiC content in both flexible (0-13 v/v%) and rigid (0-14 v/v%) PUR matrices. Figure 4.10 shows that the thermal conductivity value tends to increase with increasing SiC content in both flexible and rigid PUR. As a result of flexible PUR, thermal conductivity increased from 0.253 to 0.521 W / mK, it was enhanced by 2 times when compared to pure flexible PUR as shown in Table 4.7. For rigid PUR composites, thermal conductivity increased from 0.290 to 0.542 W / mK, it was enhanced by 1.9 times. These results can be explained by the high thermal conductivity of SiC particles and because the evenly disperse of SiC particles in both flexible and rigid PUR matrices. When the filler concentration is high enough, high conductivity fillers might form thermally conductive networks [68]. The other reason for improving the thermal conductivity of the composites could be imply to the high phonons propagation by SiC particles through a boundary which separates one phase from another [120]. Uniform dispersion of SiC particles in the PUR matrix can form bridging between the particles, what the phonons can use to cross the polymer matrix faster. The phonons transport along the network of fillers. Therefore, the thermal conductivity of the composites with highly conductive fillers provides a good improvement [30, 33]. In this study, high contact resistance can form because of the gaps, and the small contact area between filler particles, it affects the composites, thus could not achieve high thermal conductivity.

Using Coran and Patel model, the thermal conductivity as a function of filler content was obtained to predict the thermal conductivity from the experiment. The result confirms that the experimental data was fairly good to the theoretical model line 2.5 as revealed in Figure 4.11 for both flexible and rigid PUR composites. This result indicated good dispersion of SiC particles in both PUR matrices even though high filler content was loaded. Unfortunately, higher SiC content (>14 v/v%) does not easily mix into PUR by solution mixing method to observe the thermal conductivity at higher SiC content. However, incompatibility between SiC and both PUR matrices has a strong effect on thermal conductivity (difficult to getting close the theoretical line 0). From the applied model, the results indicate that this applied mechanical model has a good fitting for the thermal conductivity of polyurethane composites. Moreover, this selected model might predict thermal conductivity to other polymers as well.

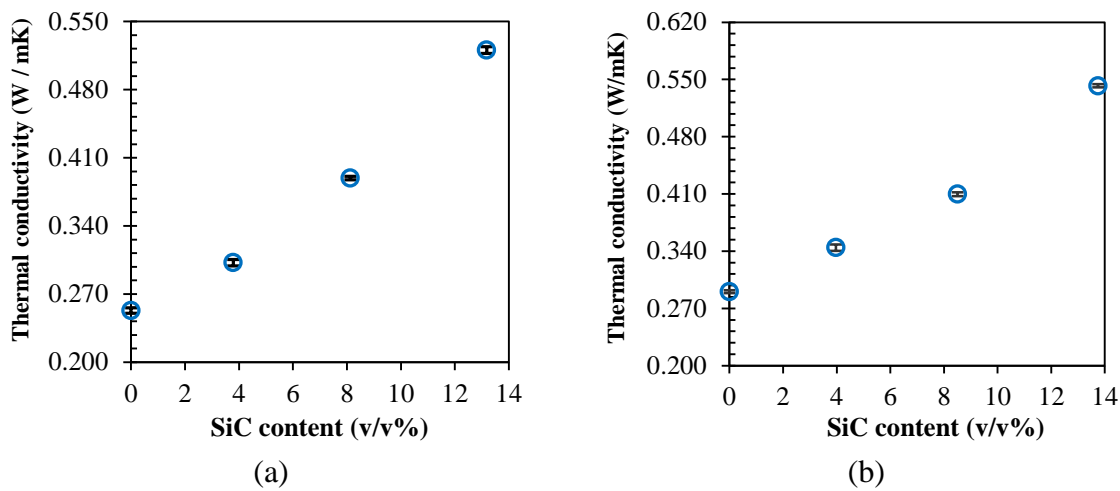


Figure 4.10 Thermal conductivity of flexible (a) and rigid (b) polyurethane elastomers with different SiC contents

Moreover, the density results can be correlated to the thermal conductivity of SiC and PUR composites. This correlation can indicate that increasing the density of the composites can raise their thermal conductive value [65]. The density was increased with increasing SiC content from 1.137 to 1.369 g/cm³ for flexible PUR matrix and from 1.194 to 1.441 g/cm³ for rigid PUR matrix as shown in Figure 4.12(a), (b) and Table 4.7.

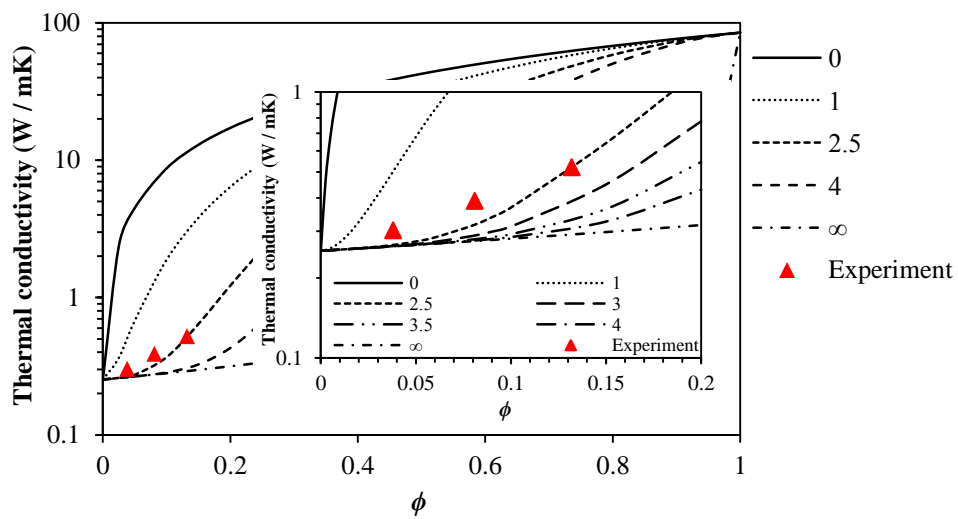
Table 4.7 Thermal conductivity and density of flexible and rigid polyurethane elastomers with different SiC contents

SiC content (v/v%)	Flexible PUR		SiC content (v/v%)	Rigid PUR	
	Thermal conductivity (W / mK)	Density (g/cm ³)		Thermal conductivity (W / mK)	Density (g/cm ³)
0.00	0.253±0.003	1.137±0.002	0.00	0.290±0.002	1.194±0.001
3.79	0.302±0.003	1.219±0.002	3.97	0.344±0.004	1.218±0.002
8.13	0.389±0.002	1.302±0.000	8.51	0.410±0.002	1.292±0.008
13.18	0.521±0.003	1.369±0.000	13.75	0.542±0.002	1.441±0.002

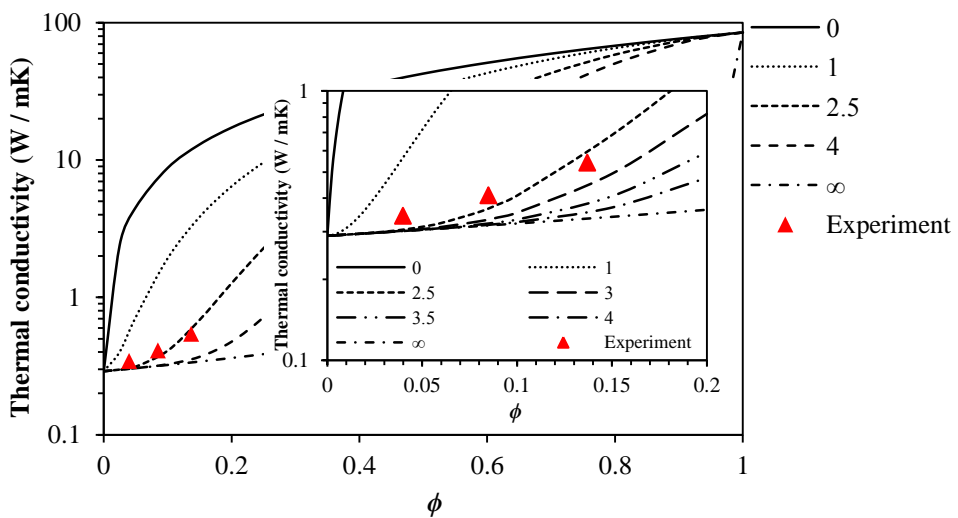
4.2.2 Mechanical properties

4.2.2.1 Hardness

Shore A and D hardness values of pure PUR and its composite with SiC have been shown in Figure 4.13(a) and (b). For flexible PUR composites, the result shows that both Shore A and D hardness rise with increasing SiC content. Shore A hardness increases from 81 to 88 while Shore D hardness increases from 26 to 37. This result reveals that SiC content and its dispersion influence the stiffness of flexible PUR composites. In case of rigid PUR composites, Shore A hardness did not significantly change when SiC content was increased while Shore D hardness slightly rises.

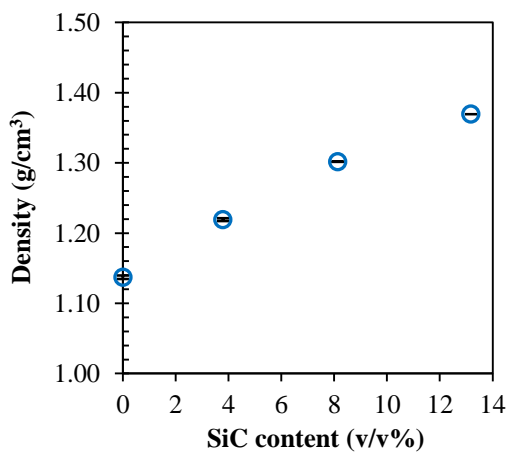


(a)

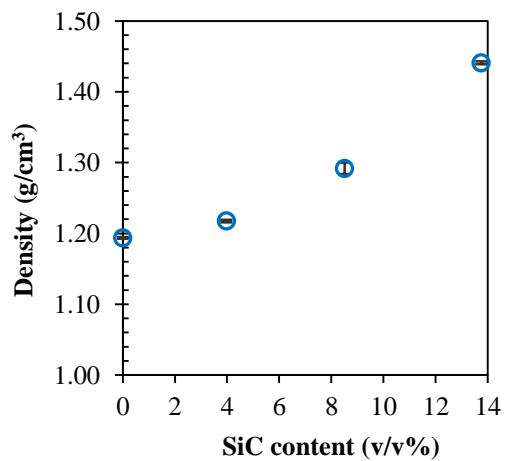


(b)

Figure 4.11 Thermal conductivity modelling of flexible (a) and rigid (b) polyurethane elastomers with different SiC contents



(a)



(b)

Figure 4.12 Density of flexible (a) and rigid (b) polyurethane elastomers with different SiC contents

This result proved that SiC particles are inactive filler for rigid PUR matrix. Increasing hardness can correlate to increasing the density of the composites due to increasing amounts of filler particles [121].

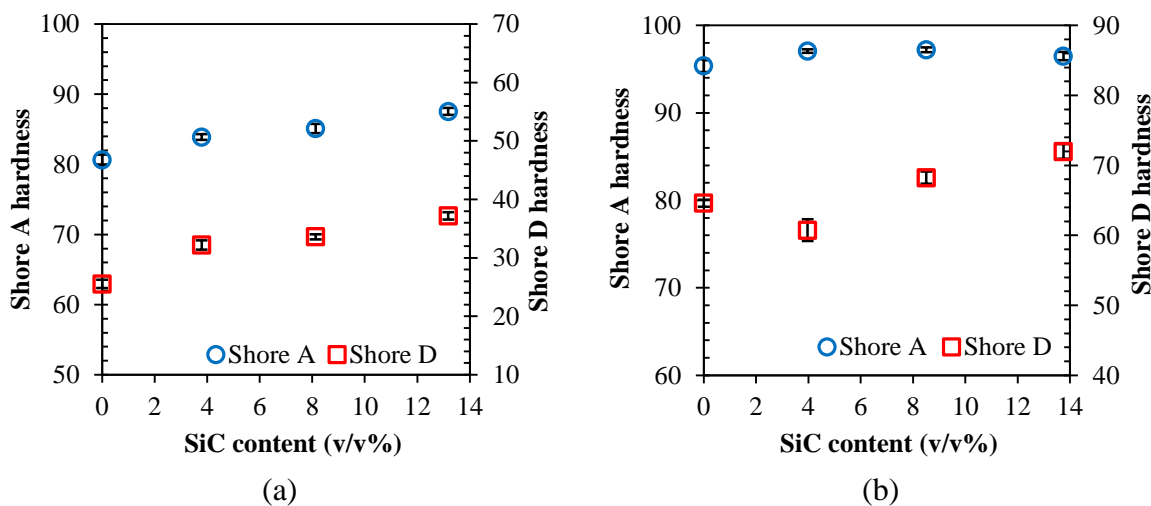


Figure 4.13 Shore A and D hardness of flexible (a) and rigid (b) polyurethane elastomers with different SiC contents

4.2.2.2 Tensile properties

The tensile property of PUR and SiC composites were tested by following the ISO 527 standard. Tensile strength, elongation at break, and modulus of flexible and rigid PUR with SiC composites were presented in Figure 4.14 and 4.15. As a result of the flexible PUR matrix, the tensile strength slightly increases from 7 to 9 MPa when SiC content was increased from 0 to 13.18 v/v%. The elongation at break value tends to decrease from 185 to 131% with increasing SiC content which decreasing as revealed in Table 4.8. For the rigid PUR matrix, the tensile strength did not significantly change when SiC content was increased. The elongation at break rapidly decreases from 31 to 11% with increasing SiC contents. This result occurs due to the poor adhesion between the fillers of both flexible and rigid PUR matrices and their inherent incompatibility [26]. Furthermore, the decreasing of elongation at break of PUR composites indicates hindrance by SiC to molecular mobility of PUR chain or deformability of composites which causes the matrix to lose its elastic deformation ability. Therefore, PUR and SiC composites were broken at a lower elastic deformation when compared to the pure PUR. The other reason is the bonding surface area between particles and matrix increases and hence bonding strength decreases [121]. On the other hand, tensile modulus was enhanced with increasing SiC contents. It can be enhanced by 1.7 times from 18 to 31 MPa for flexible PUR composites, while it was increased by 1.4 times from 771 to 1073

MPa for rigid PUR as shown in Table 4.8 and 4.9. This result can evidence the effect of dispersion of SiC particles and its content on the stiffness and elastic deformation of both flexible and rigid PUR matrices.

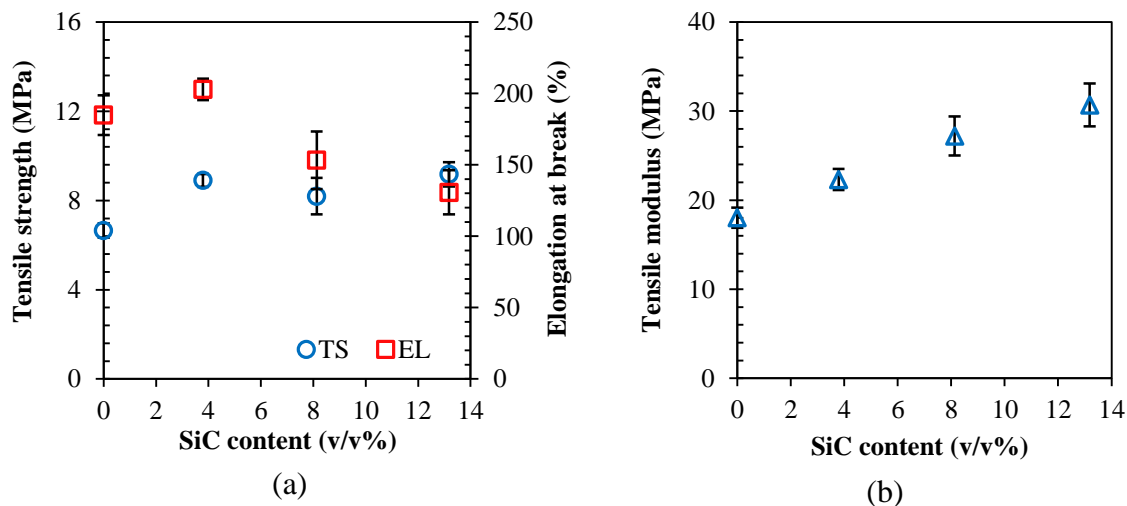


Figure 4.14 Tensile strength and elongation at break (a) and tensile modulus (b) of flexible polyurethane elastomers with different SiC contents

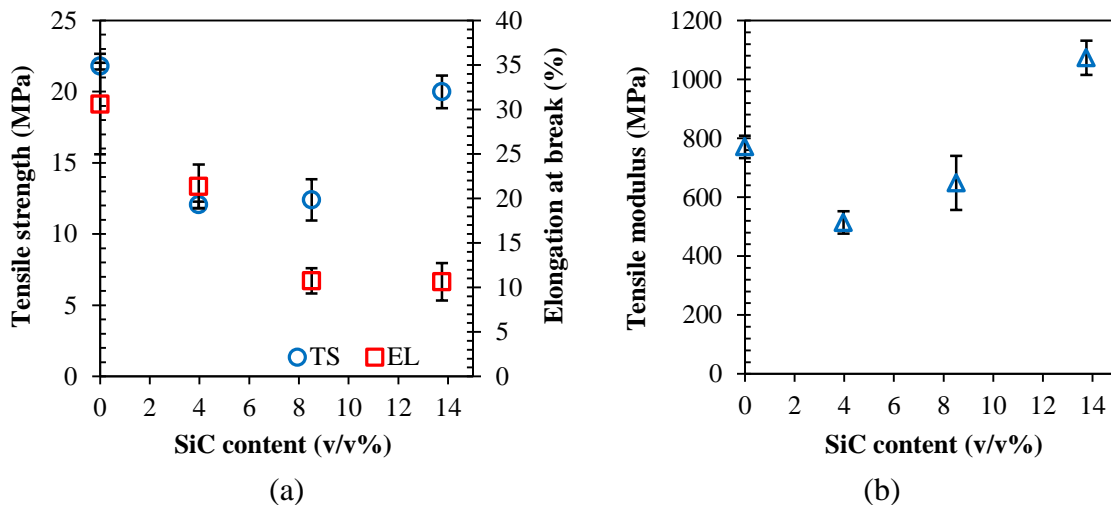


Figure 4.15 Tensile strength and elongation at break (a) and tensile modulus (b) of rigid polyurethane elastomers with different SiC contents

Table 4.8 Mechanical properties of flexible PUR with different SiC contents

SiC content (v/v%)	Shore A hardness	Shore D hardness	Tensile strength (MPa)	Elongation at break (%)	Tensile modulus (MPa)
0.00	81±0.7	26±0.7	7±0.3	185±14	18±1
3.79	84±0.4	32±0.8	9±0.3	203±7	22±1
8.13	85±0.7	34±0.5	8±0.8	153±20	27±2
13.18	88±0.5	37±0.6	9±0.5	131±16	31±2

Table 4.9 Mechanical properties of rigid PUR with different SiC contents

SiC content (v/v%)	Shore A hardness	Shore D hardness	Tensile strength (MPa)	Elongation at break (%)	Tensile modulus (MPa)
0.00	95±0.7	65±0.5	22±0.2	31±6	771±38
3.97	97±0.2	61±1.6	12±0.2	21±2	514±38
8.51	97±0.3	68±0.9	12±1.4	11±1	648±91
13.75	97±0.5	72±1.0	20±1.1	11±2	1073±58

4.2.3 Thermal properties

The thermal property of pure PUR and its composites with SiC were examined by DSC technique. The DSC curves of flexible and rigid PUR and its composites were shown in Figure 4.16 and 4.17. $T_{g,SS}$ observed at -60 °C for both flexible and rigid PUR matrices. Increasing SiC content has no significant effect on $T_{g,SS}$ of both flexible and rigid PUR as shown in Table 4.10. It can be explained that SiC particles do not influence on polypropylene glycol polyol segment motion in PUR structure. The incorporation of particles constrains the movement of the molecular chains, leading to increase the glass transition temperature. On the other hand, particles can also disturb the entanglement network of polymer chains and leading to a slight decrease in glass transition temperature as well [122]. However, $T_{g,SS}$ of rigid PUR and SiC composites are not clearly observed when SiC content is loaded from 3.97 to 13.75 v/v%. This may be attributed to SiC content does not influence the cross-linking and chain decomposing of rigid PUR. In case of rigid PUR composites, broader endotherms peak at high SiC content can be suggested to a small degree of ordering in hard segment domains. At low SiC content, endotherm peaks show narrower and high intensity than the higher content which indicates to a high of the hard segments cross-linking. It can be suggested that the high amount of SiC obstructed the molecular chain movement physically in the cross-linked structure. For the hard segment, the $T_{g,HS}$ of both flexible and rigid PUR were shown in Table 4.10. $T_{g,HS}$ present around 44 °C for flexible PUR composites. For rigid PUR composites, $T_{g,HS}$ slightly decreases from 44 °C to 39 °C. The enthalpy of melting tends to increase with increasing SiC content for flexible PUR composites. This reveals that the crystalline phase was increased with increasing SiC content and improved the hard segment phase separation in flexible PUR structure. On the other hand, the enthalpy of melting tends to decrease with increasing SiC content for rigid PUR composites which can be related to the broad endotherms peak. Adding high SiC content decreased the enthalpy of melting because of the incorporation of micro-fillers does not catalyze or enhances the

polymerization of rigid PUR matrix. This due to the effect attributed to the ceramics which increases the viscosity of thermoset materials resulting in an enhancement of the curing temperature [123]. Furthermore, endothermic temperature (T_{endo}) has no trend when SiC content was increased while it was decreased with loading SiC fillers as revealed in Table 4.10.

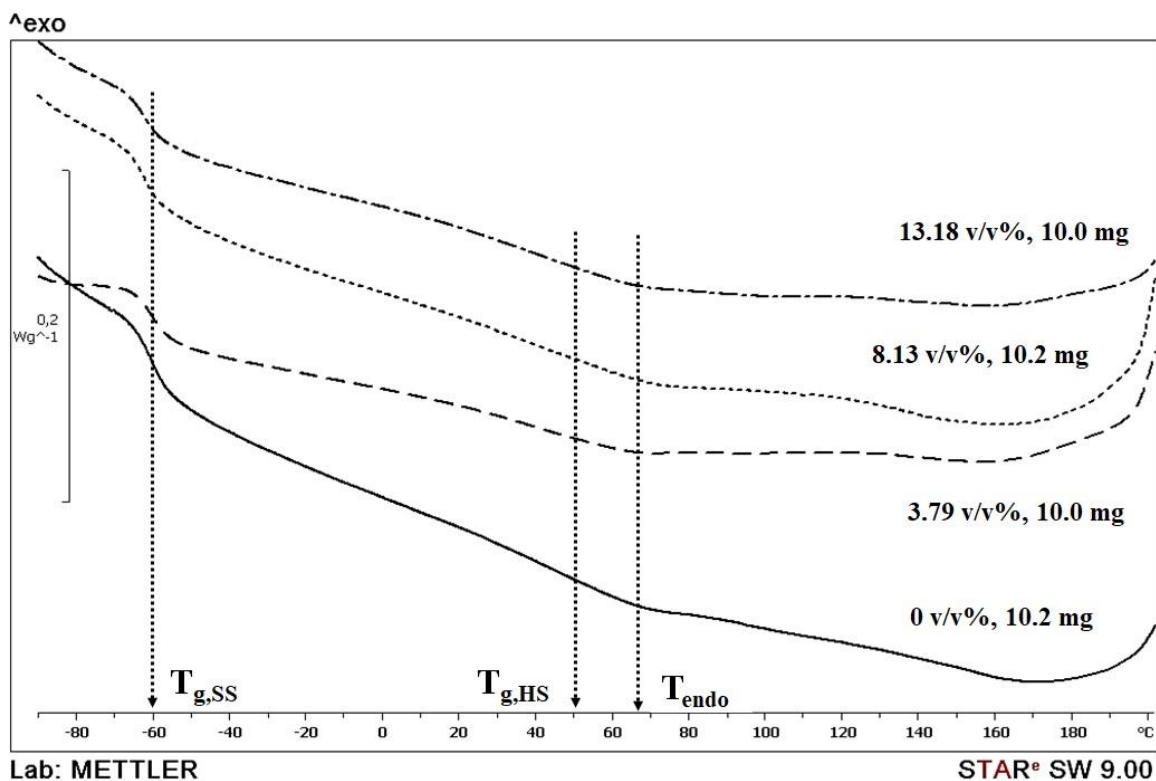


Figure 4.16 DSC curve of flexible polyurethane elastomers with different SiC contents

4.2.4 Dynamic mechanical properties

DMA provides information on viscoelastic properties of both flexible and rigid PUR with addition of SiC fillers. The dynamic mechanical behavior of polyurethanes is not quite easy to elucidate due to the complex phenomena that interfere during the scanning. The phase separation between the soft segment (SS) and the hard segment (HS) domains seems to be the dominating factor that controls the relaxation events [124]. DMA thermograms show that the addition of SiC had affected the mechanical behaviour of the flexible PUR. The storage modulus graph of flexible PUR with various SiC contents in the range of 0 and 13.18 v/v% exhibits a very high modulus at the starting temperature in the glassy state and tends to decrease with increasing SiC content, as shown in Figure 4.18. The storage modulus of the composites was raised when SiC content was increased. This can confirm the reinforcement effect of SiC content and

good the dispersion in flexible PUR matrix as revealed in other works [125]. Moreover, it might be due to SiC fillers affect chain mobility of PUR molecular chain as well.

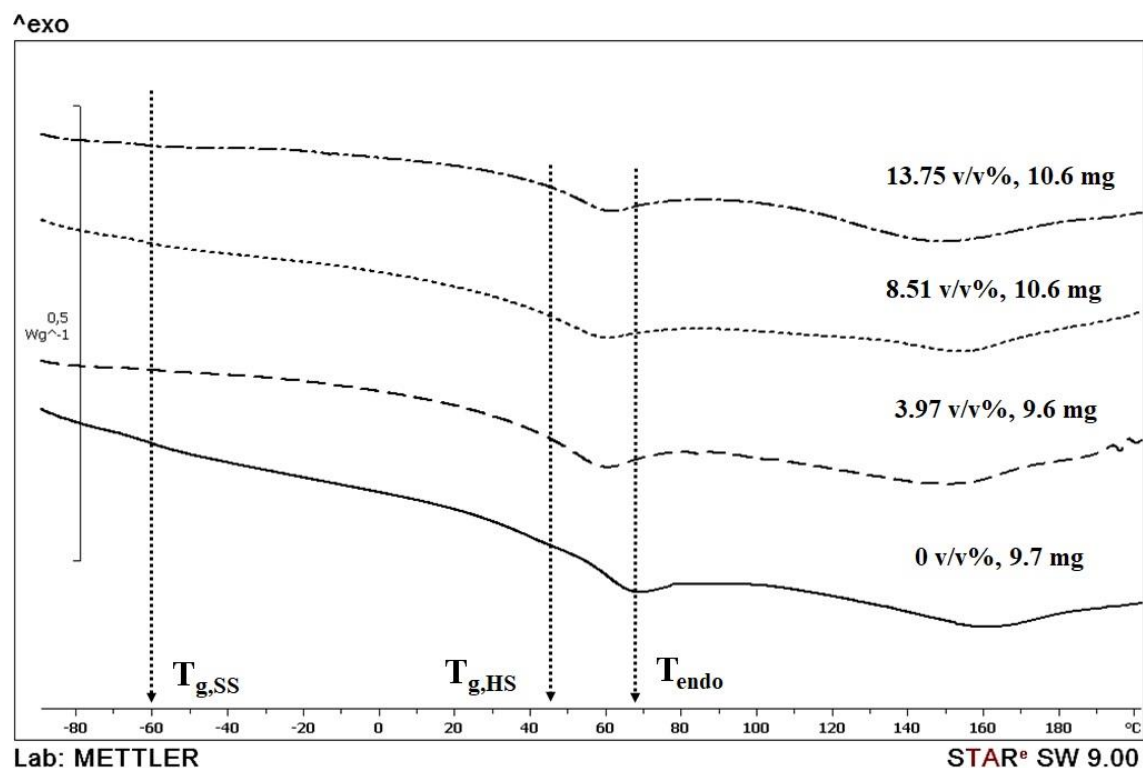


Figure 4.17 DSC curve of rigid polyurethane elastomers with different SiC contents

Table 4.10 Thermal properties of flexible and rigid polyurethane elastomers with different SiC contents

Flexible Polyurethane				Rigid Polyurethane			
SiC content (v/v%)	$T_{g,SS}$ ($^{\circ}C$)	$T_{g,HS}$ ($^{\circ}C$)	T_{endo} ($^{\circ}C$)	SiC content (v/v%)	$T_{g,SS}$ ($^{\circ}C$)	$T_{g,HS}$ ($^{\circ}C$)	T_{endo} ($^{\circ}C$)
0.00	-60	45	68	0.00	-60	44	67
3.79	-60	45	67	3.97	N/A	42	60
8.13	-61	43	70	8.51	N/A	42	58
13.18	-61	44	66	13.75	N/A	39	60

The $\tan\delta$ shows that the peak associated at lower temperature with $T_{g,SS}$ did not significantly change at -45 $^{\circ}C$ when SiC content was increased as shown in Figure 4.18. Moreover, the amplitude of $\tan\delta$ peak of soft segment tends to decrease with increasing SiC content. This may be due to SiC content and its dispersion influence the degree of polyol segment motion in both matrices. At high temperature, $\tan\delta$ peak shifts in the curve to lower temperature with increasing of SiC content. This can be attributed to the $T_{g,HS}$ was decreased. The shift of $T_{g,HS}$ can be indicated that SiC particle affect the decreasing level of cross-linking in flexible PUR [125]. The decrease in damping

capacity (amplitude of $\tan\delta$) implied the greatly restricted motion of polyurethane chains resulting from the cross-linking function of the filler for the isocyanate terminated polyurethane chains [126]. This decrease in melting point is may be due to the decrease in the number of higher length hard segment chains in the hard segment domains [108] and attributed to decreasing in the hard segment crystallinity and phase separation.

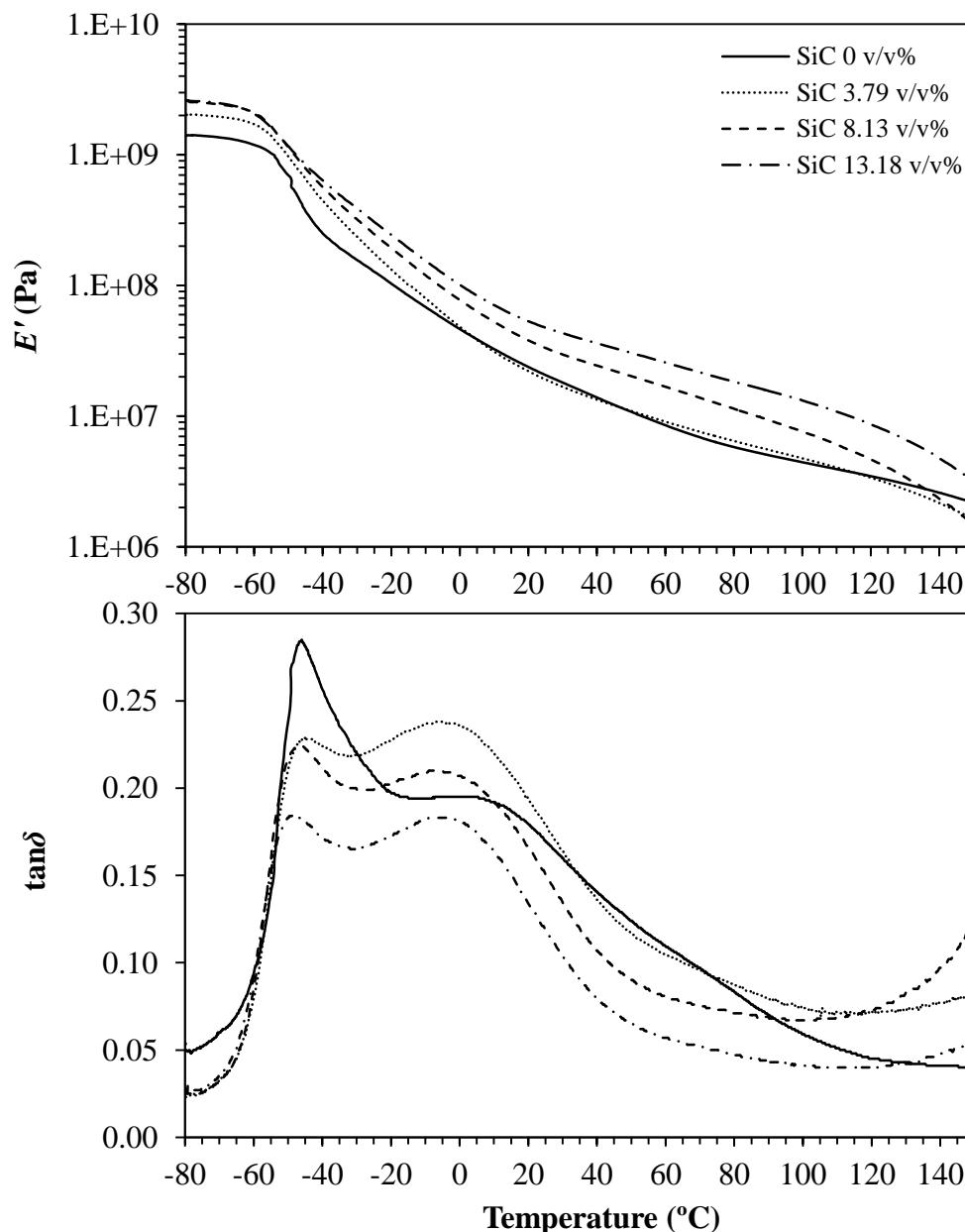


Figure 4.18 Storage modulus and mechanical loss factor from DMA of flexible PUR with different SiC contents

In case of rigid PUR matrix, the storage modulus of pure rigid PUR and its composites have also high value from starting temperature as shown in Figure 4.19. DMA thermograms show that E' of the composites decreases at high temperatures when SiC was added. It can reveal the effect of agglomeration of SiC particles and the particle

distribution in the rigid PUR matrix. $T_{g,SS}$ was found between -60 and -40 °C as shown in a small Figure and Table 4.11. At higher temperatures, $\tan\delta$ peak shifts in the curve to lower temperature with increasing SiC content similar to flexible PUR composites except at 13.75 v/v% of SiC content, which $\tan\delta$ peak reveals at a high temperature around 122 °C. This may be due to the effect of the high amount and agglomeration of SiC particles in a rigid PUR matrix. The shift of $T_{g,HS}$ is attributed to SiC particles affect which decrease the level of cross-linking in the rigid PUR matrix. In case of the high intensity of $\tan\delta$ peak at 13.75 v/v%, it because SiC particles dispersion influences the cross-linking segment motion in rigid PUR matrix.

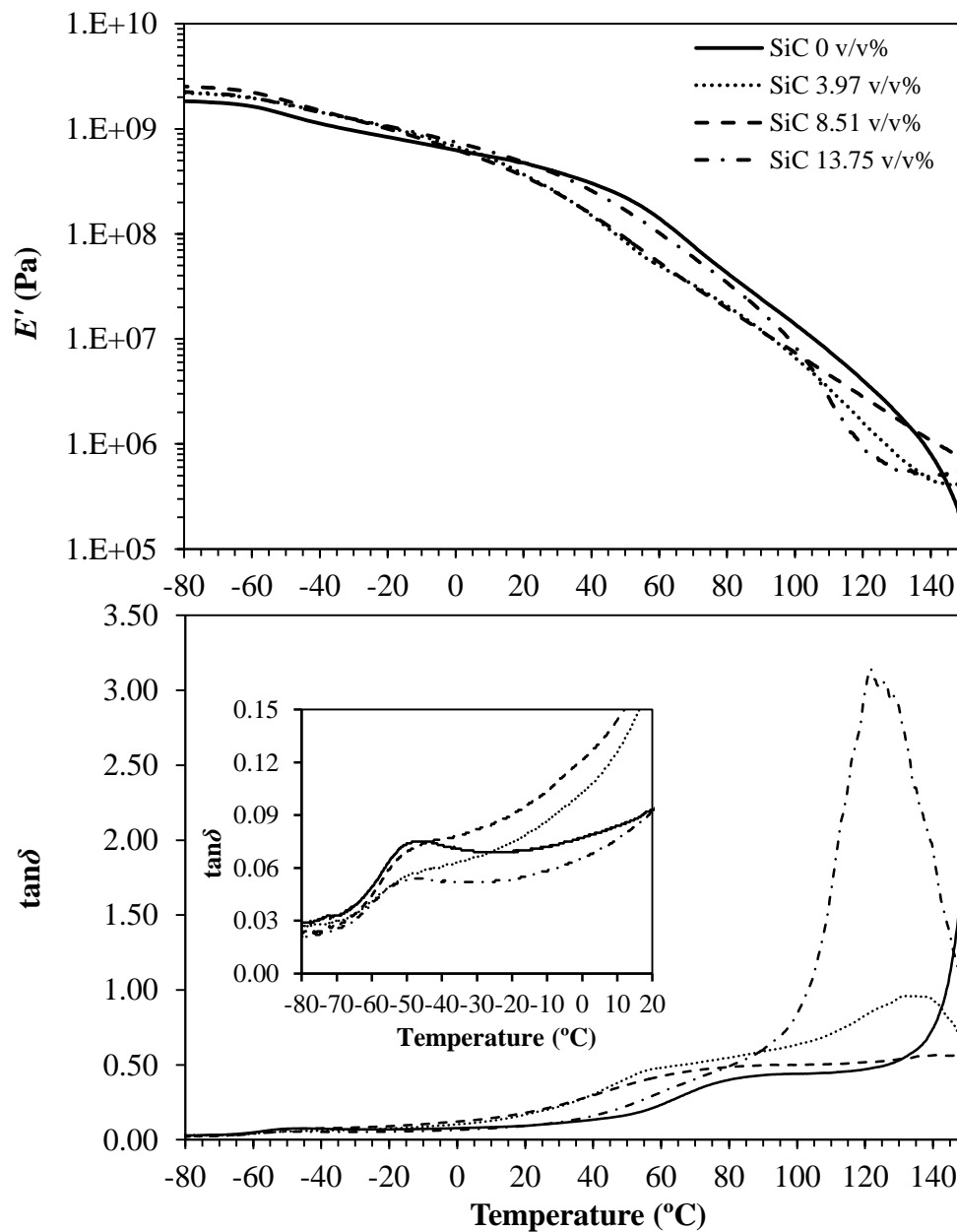


Figure 4.19 Storage modulus and mechanical loss factor from DMA of rigid PUR with different SiC contents

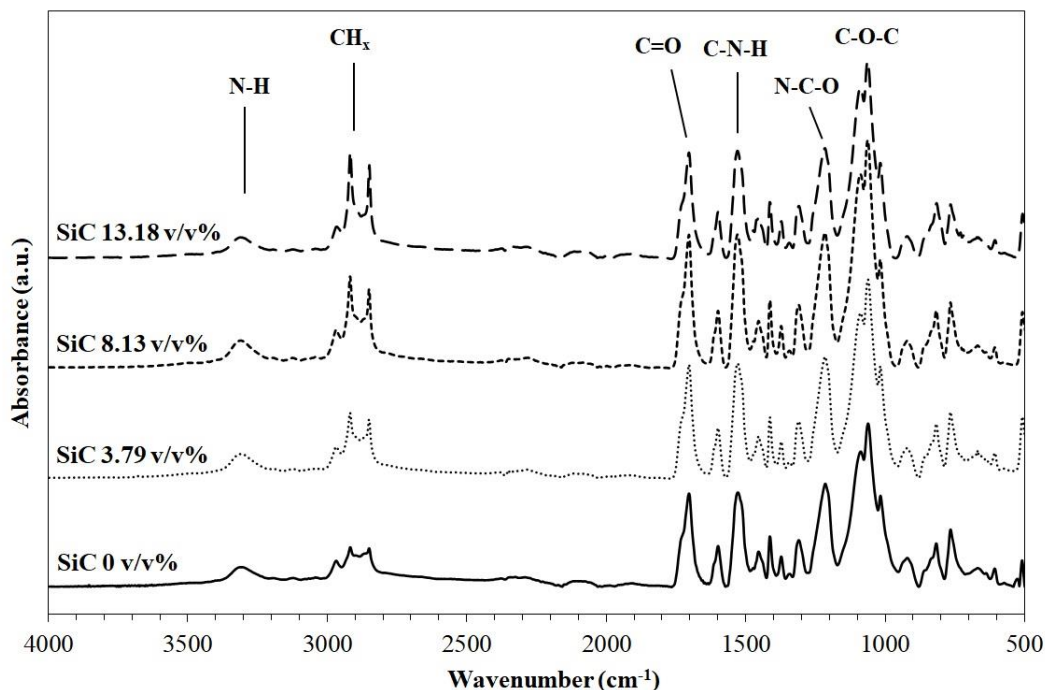
However, results show that although the T_g differs between the DSC and DMA measurements it is not affected by the filler in case of the rigid PUR matrix. A possible explanation is that the filler has no effect on the cross-linked structure of the rigid PUR. The difference between the results of different methods has to be caused by the relative rate of deformation of the sample experiencing during measurements. The DSC technique does not apply external force other than the relaxation of the polymer structure resulting in an almost 0 Hz cyclic frequency, while the DMA measurements were carried out using a 1 Hz frequency. The difference in deformation rates can explain the difference in the obtained T_g values.

4.2.5 Infrared spectroscopy

The effect of SiC fillers on the chemical structure of both flexible and rigid PUR matrices was characterized by IR technique as revealed in Figure 4.20 and 4.21. The IR spectra of the elastomers exhibited the bands typical for PUR. Moreover, a difference in both the free and hydrogen-bonded is exhibited as well as the differences in the peak related to $-NH$ group. The two $-NH$ groups are belonging to the urea in the hard segment show stronger hydrogen bonding than the one $-NH$ group from the urethane group. This may be affecting the peak corresponding to the wave number in the range of $3280 - 3340 \text{ cm}^{-1}$ [127]. IR spectra can confirm that SiC content did not significantly affect the main PUR structure in both flexible and rigid PUR. This might be due to the incompatibility between the filler and the matrix. In case of a flexible PUR matrix, the intensity peaks of CH_x group increase with increasing SiC content as shown in Figure 4.20. For rigid PUR matrix, all the intensities peaks of the spectra have no significant change when the SiC content was increased from 0 to 13.75 v/v% as shown in Figure 4.21. These may be due to SiC particles has no effect in the chemical groups of rigid PUR structures. On the other hand, adding SiC filler to any of the PUR matrices might increase their sensitivity to degradation. The assumed degradation tends to increase with increasing SiC content. This is can be implied from the increasing of the band's intensity [128].

Table 4.11 The glass transition temperature of the soft and hard segment of polyurethane elastomers with different SiC contents from DMA technique

SiC content (v/v%)	Flexible PUR		SiC content (v/v%)	Rigid PUR	
	T _{g,SS} (°C)	T _{g,HS} (°C)		T _{g,SS} (°C)	T _{g,HS} (°C)
0.00	-46	11	0.00	-48	83
3.79	-45	1	3.97	-48	55
8.13	-47	2	8.51	-48	72
13.18	-48	2	13.75	-49	122

**Figure 4.20** IR spectra of flexible polyurethane elastomers with different SiC contents

4.2.6 Morphology

Morphology of SiC particles and its composite both flexible and rigid PUR were investigated by scanning electron microscopy (SEM) technique. The morphology of the particles and the composites can be correlated to the properties of PUR composites. It might indicate the trend of properties of the composites. Therefore, the morphology results are important and have been discussed in this topic. All SEM micrograph of the examined PUR composites were collected from fracture surfaces of previously tested tensile specimens.

4.2.6.1 Particle size distribution and morphology of SiC particles

The particle size distribution of SiC particles was revealed in Figure 4.22. The particle median and mean sizes are 6.349 and 6.586 μm , respectively. The result can

demonstrate uni-model distribution of particles. Moreover, the flake-like shape particles were presented in Figure 4.23. It can be observed that coarse particles have fragmented to smaller particles. The particle size and shape implies the increasing of the thermal conductivity of the composites by supporting the phonon transportation.

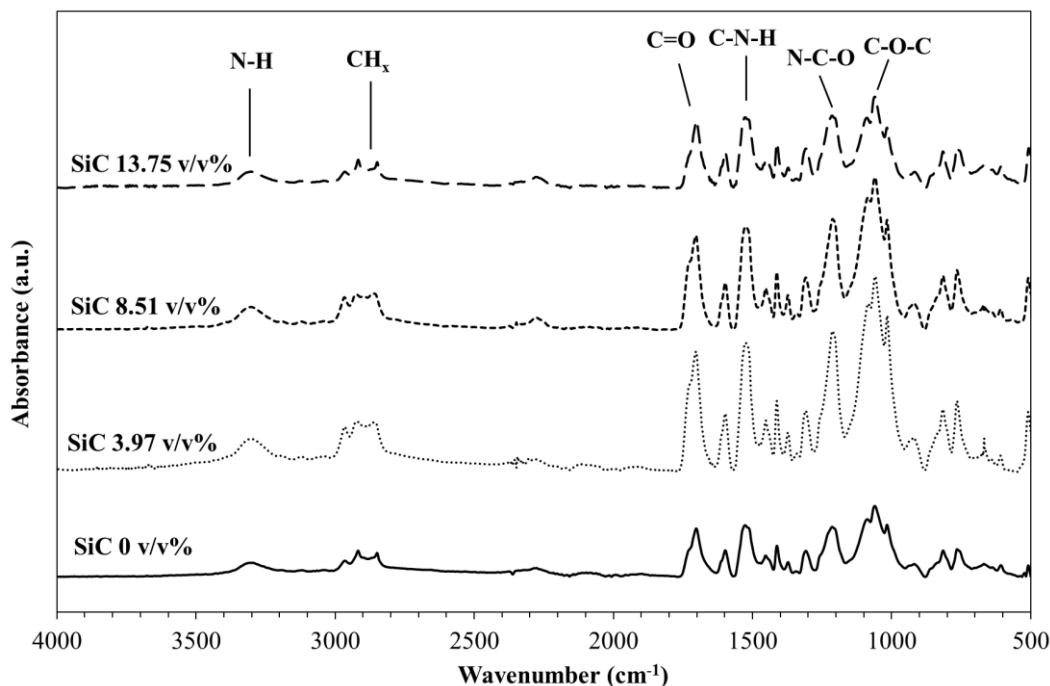


Figure 4.21 IR spectra of rigid polyurethane elastomers with different SiC contents

4.2.6.2 Morphology of flexible and rigid polyurethane elastomers with SiC fillers

SEM image shows the good mixing of the soft and hard segments for the PUR matrix. Flexible PUR matrix with SiC fillers has clearly revealed the presence of two phases of the matrix and SiC particles as shown in Figure 4.24 (b) and (c). SiC particles are evenly dispersed in the flexible PUR matrix. It can be seen that particles were embedded inside flexible PUR.

In case of rigid PUR matrix, the SEM image shows the agglomerated particles in a rigid PUR matrix at 3.97 v/v% as revealed in Figure 4.25 (b). It can show the effect of the high viscosity of rigid PUR matrix and the surfactant of SiC particles. However, SiC particles are evenly dispersed and embedded inside the rigid PUR matrix as shown in Figure 4.25 (c). SEM images can be seen that SiC particles were added and embedded inside both flexible and rigid PUR matrices, which also confirmed by EDS chart as shown in Figure 4.24 (d) and 4.25(d). EDS reveals that Si and C are the main elements of the particles which can be seen by SEM images. From SEM results, the morphology of both flexible and rigid PUR composites with SiC fillers tends to increase the thermal

conductivity value, density, Shore hardness, and tensile modulus for PUR composites. The lack of interaction between SiC particles and both PUR matrices lead to decrease the elongation at break and tensile strength in a rigid PUR matrix.

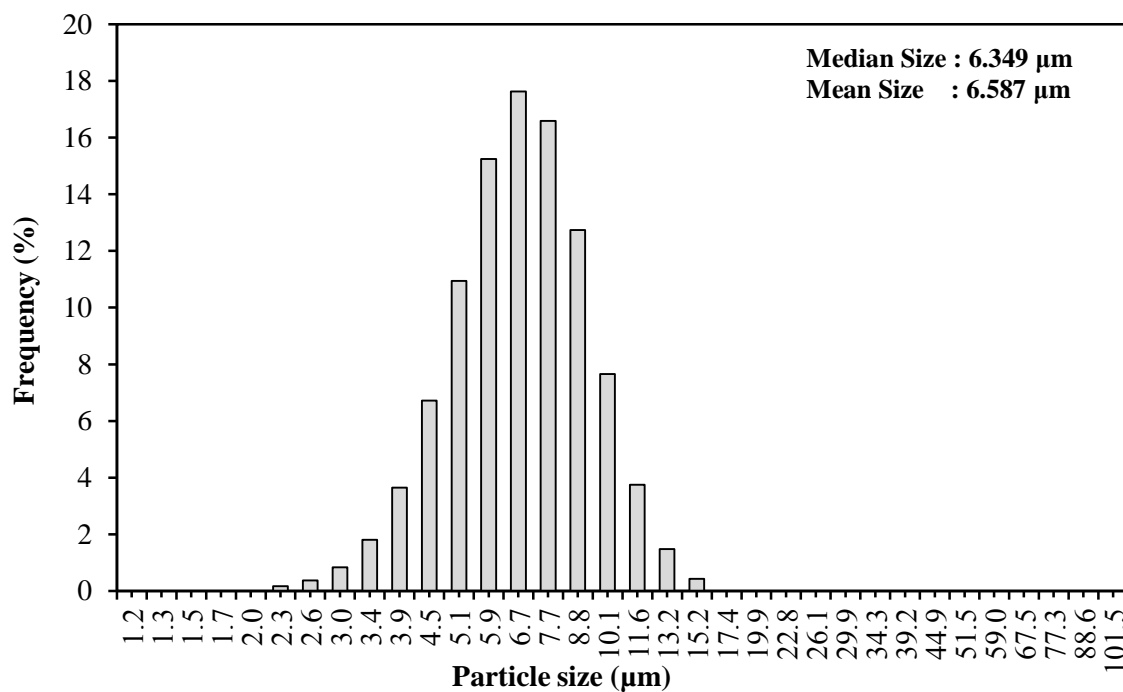


Figure 4.22 Particle size distribution of silicon carbide particles

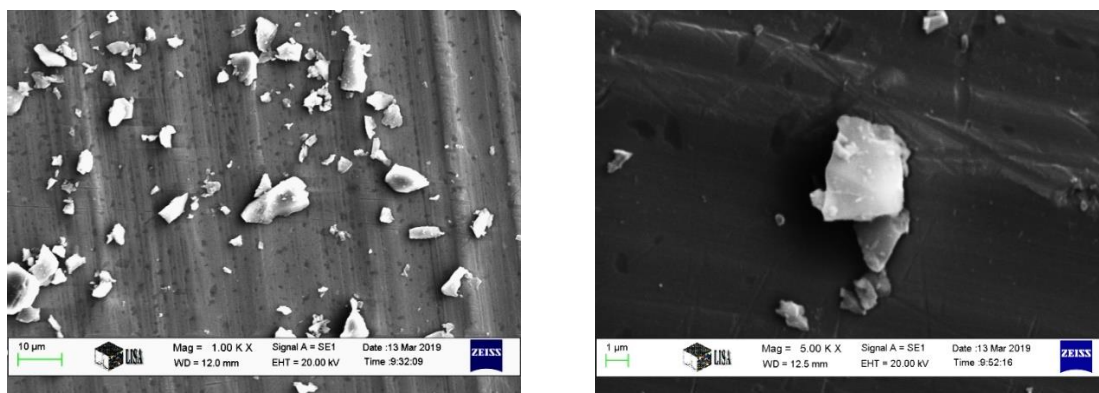
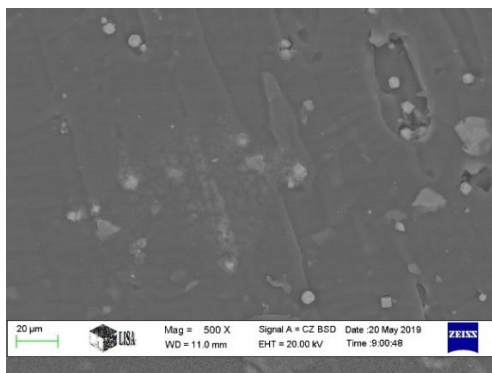
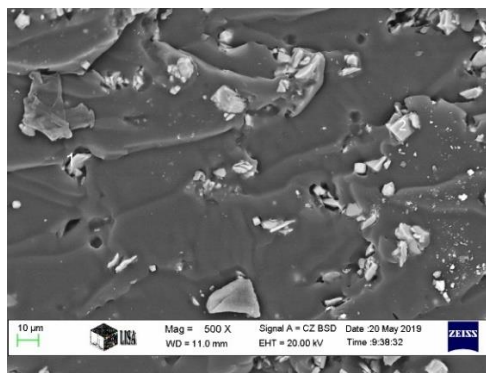


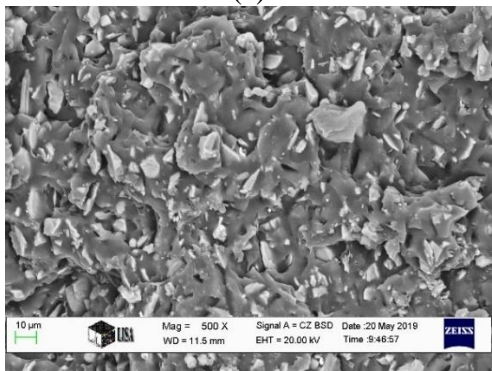
Figure 4.23 SEM image of silicon carbide particles (nominal magnification of 1000× and 5000×)



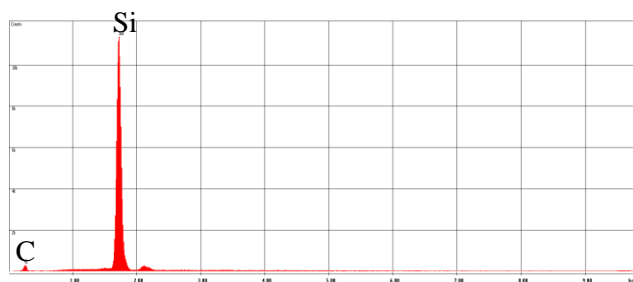
(a)



(b)

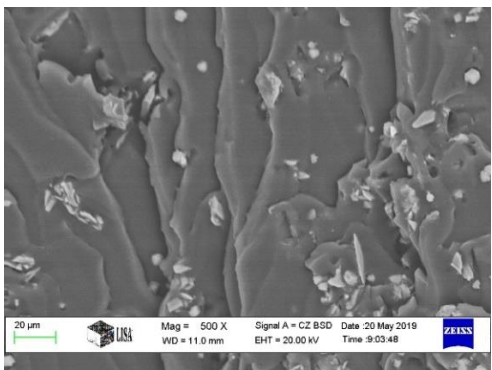


(c)

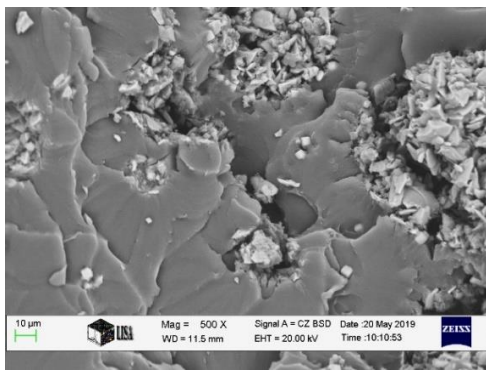


(d)

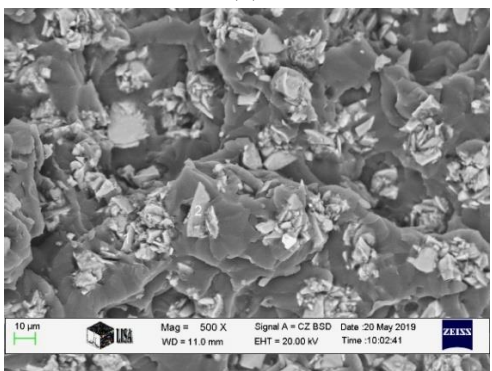
Figure 4.24 SEM image of flexible PUR with different SiC contents (a) SiC 0 v/v%, (b) SiC 3.79 v/v%, (c) SiC 13.18 v/v% (nominal magnification of 500×) and (d) EDS chart



(a)



(b)



(c)



(d)

Figure 4.25 SEM image of rigid PUR with different SiC contents (a) SiC 0 v/v%, (b) SiC 3.97 v/v%, (c) SiC 13.75 v/v% (nominal magnification of 500×) and (d) EDS chart

4.3 Flexible and rigid polyurethane elastomer with magnesium oxide composites

Magnesium oxide (MgO) is an inorganic material and it is one type of the high thermal conductivity filler. It has high thermal conductivity between 45 and 60 W / mK. In this topic, MgO content was varied from 0 to 12 v/v% into flexible while MgO content was varied from 0 to 11 v/v% for rigid PUR matrix because the limitation of mixing process during solution mixing and preparation of the sample.

4.3.1 Thermal conductivity and density

Thermal conductivity of pure flexible and rigid PUR and MgO composites with different MgO contents were revealed. As a result, the thermal conductivity tends to raises with increasing content of MgO from 0 to 11.98 v/v% for flexible PUR matrix. It was improved from 0.253 to 0.396 W / mK, by 1.6 times when compared to pure PUR, as shown in Figure 4.26(a) and appendix A. This result is due to the evenly dispersed MgO particles which can be promote the phonon propagation through the flexible PUR matrix as similar to loading SiC particles [120]. Uniform dispersion of the MgO fillers might be acting as filler network, where the phonon can easily cross the PUR matrix [30, 33]. For rigid PUR matrix, the thermal conductivity did not significantly change with raising MgO content from 0 to 10.49 v/v% as shown in Figure 4.26(b). The thermal conductivity value is found to be between 0.209 and 0.329 W / mK. At 3.57 v/v% of MgO content, which is higher than the other contents, it might be due to an optimum content of MgO particles in rigid PUR matrix. On the other hand, the thermal conductivity at higher content of MgO decrease and did not change as shown in Figure 4.26(b). This can be a clue that agglomerated particles of MgO at high content affect the phonon propagation through the rigid PUR matrix. Besides, it may be because of the MgO particles can easily create the air bubbles inside the rigid PUR matrix. Hence, it decreases the thermal conductivity because of the air bubbles inside the matrix obstructing the phonons transportation.

In case of prediction of the modeling, it is clearly seen that the experimental data shows a fairly good fitting in a flexible PUR matrix, which it is following to the theoretical model line 2.5 (Figure 4.27 (a)) as same as loading SiC fillers. This can confirm that increasing the content of MgO might create filler networks inside the flexible PUR matrix and supporting the phonon transportation. However, because of agglomeration of MgO particles and foam formation in rigid PUR matrix influence the thermal conductivity, from the experiment, the thermal conductivity tends to have a lower value than the theoretical model as shown in Figure 4.27 (b). Besides, the thermal

conductivity of the PUR and MgO composites have a lower value than the PUR and SiC composites. It is due to the lower thermal conductivity of MgO compared to the SiC particles.

As a result of density, results can be correlated to thermal conductivity in case of flexible PUR composites as shown in Figure 4.28. It tends to increase with increasing MgO content. On the contrary, the density decreases with adding MgO content in rigid PUR matrix as shown in appendix A. This can prove that there is air bubble creation during forming especially in rigid PUR matrix, then, the composites became slightly foam. Polymer foams are usually known as thermal insulating materials. Therefore, foam structure formation decreases the thermal conductivity of this composites. The reason of foam formation might be due to moisture during forming and high viscosity of rigid PUR matrix which is due to a high isocyanates fraction when preparing the rigid PUR mixture.

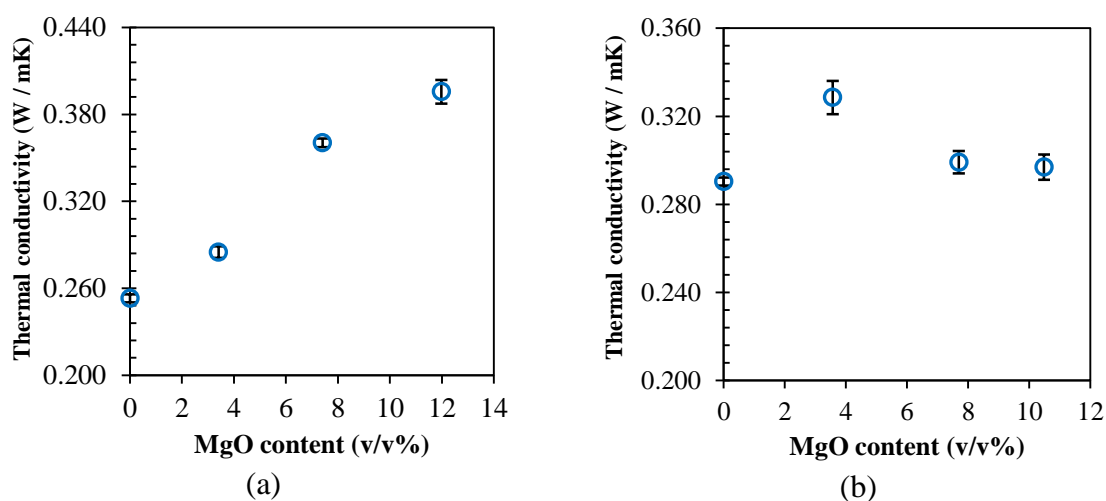


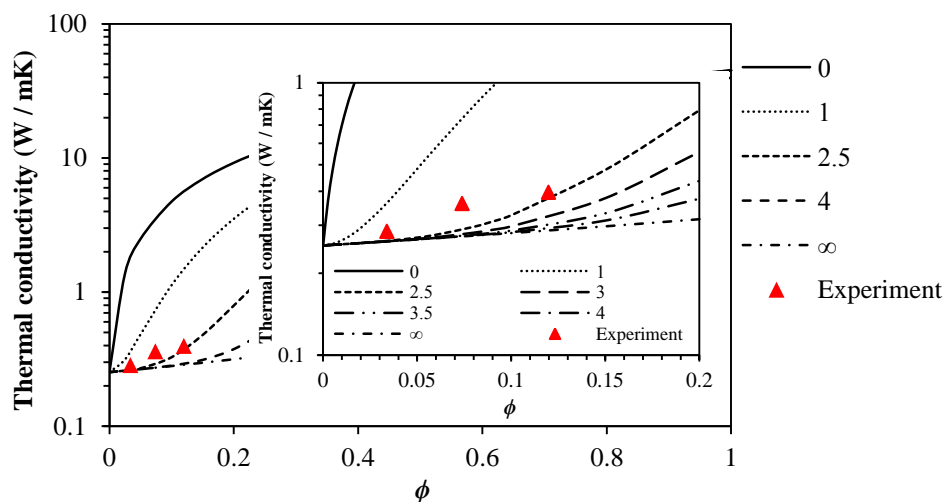
Figure 4.26 Thermal conductivity of flexible (a) and rigid (b) polyurethane elastomers with different MgO contents

4.3.2 Mechanical properties

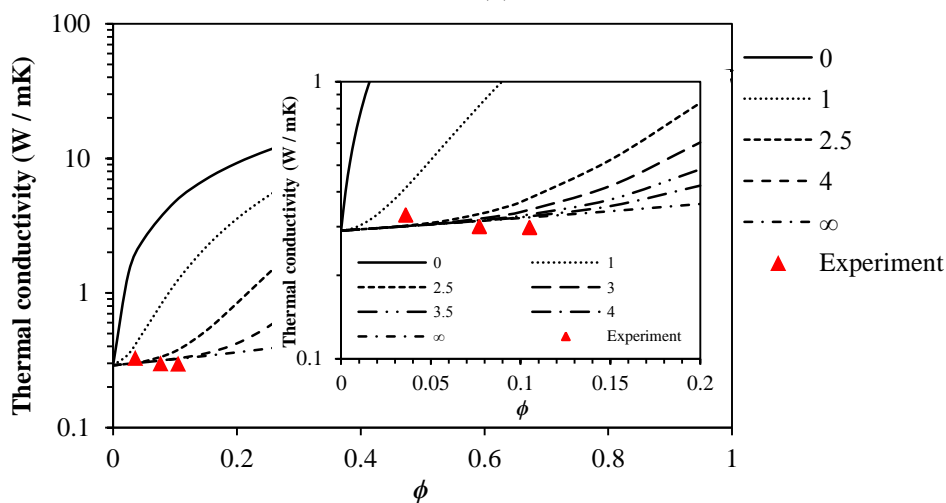
4.3.2.1 Hardness

Shore A and D hardness values of both flexible and rigid PUR and MgO composites are shown in Figure 4.29 (a) and (b). As was expected, the results show Shore A and D hardness slightly increase with increasing MgO content for a flexible PUR matrix. Shore A hardness raises from 81 to 87 while Shore D hardness raises from 26 to 35 as demonstrated in appendix A. This can be indicated that MgO content and the dispersion of MgO influence on the stiffness of flexible PUR composites. In contrast, both Shore A and D hardness did not significant change when MgO content was increased in the case of rigid PUR composites as shown in Figure 4.29 (b). This is

because the rigid PUR matrix was slightly foamed when adding MgO particles as discussed before.

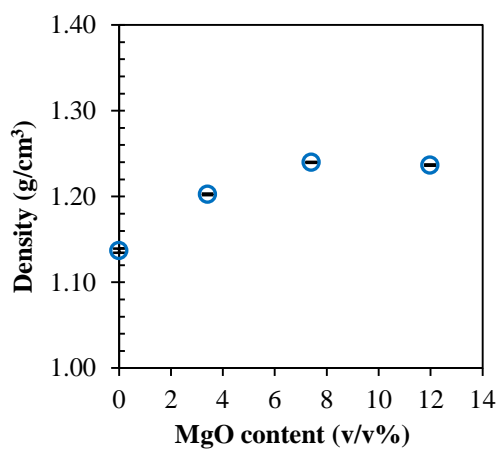


(a)

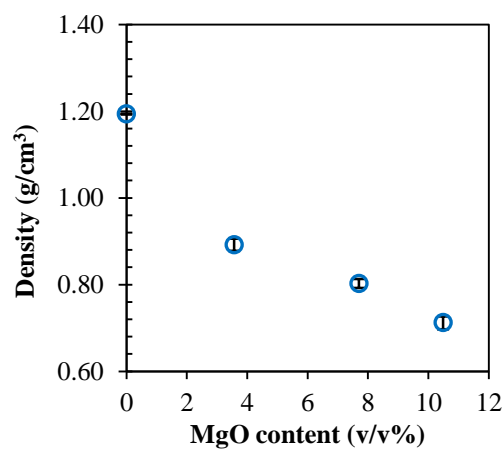


(b)

Figure 4.27 Thermal conductivity modelling of flexible (a) and rigid (b) polyurethane elastomers with different MgO contents



(a)



(b)

Figure 4.28 Density of flexible (a) and rigid (b) polyurethane elastomers with different MgO contents

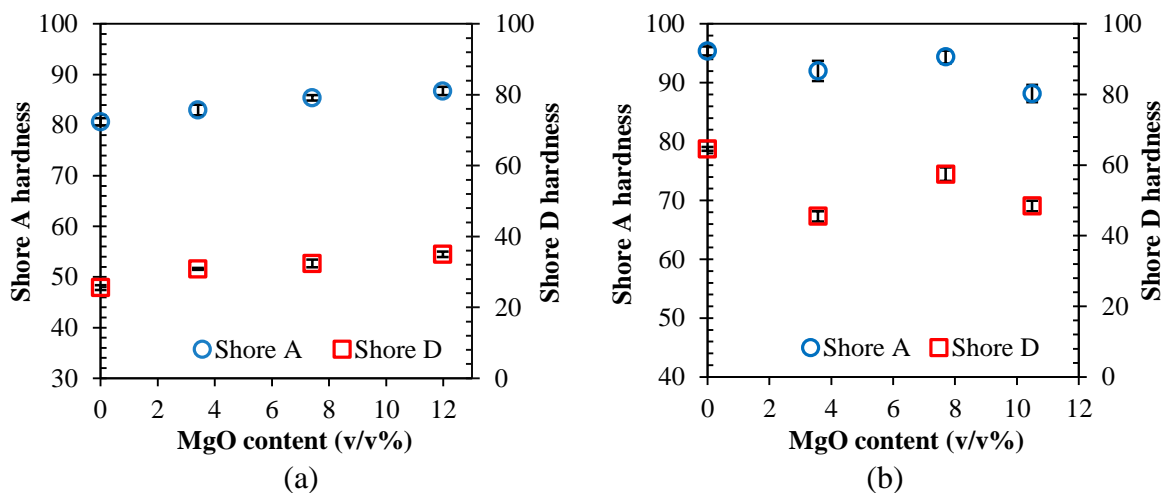


Figure 4.29 Shore A and D hardness of flexible (a) and rigid (b) polyurethane elastomers with different MgO contents

4.3.2.2 Tensile properties

Tensile strength, elongation at break, and tensile modulus of flexible PUR with different MgO contents were shown in Figure 4.30. The results show that the tensile strength did not significantly change while elongation at break value tends to decrease with increasing MgO content. Tensile strength shows at around 7 MPa while elongation at break decreased from 185% to 111%, these values were shown in appendix A. Besides, tensile modulus was enhanced when MgO content was increased for flexible PUR composites by 1.7 times from 18 to 31 MPa. The dispersion and content of MgO also had an effect on the elastic deformation of flexible PUR as similar to loading SiC fillers. In case of rigid PUR composites, tensile strength, elongation at break and tensile modulus have no trend with increasing MgO content as shown in Figure 4.31. This is due to their inherent incompatibility between MgO particle and rigid PUR matrix, agglomeration of MgO particles and foamed structure of this composite. Unexpectedly large scattering of tensile modulus might be due to the hindrance by poor adhesion of the filler and the formation of foam structure to deformability of composites which causes the matrix to lose its elastic deformation ability [26, 121]. Tensile result of rigid PUR matrix correlates to the thermal conductivity, density and Shore hardness.

4.3.3 Thermal properties

The DSC curves of both flexible and rigid PUR with MgO composites were shown in appendix A. For flexible PUR composites, the $T_{g,SS}$ is revealed at around -60 °C. Raising MgO content did not significantly affect the $T_{g,SS}$. This indicates that the MgO particle did not influence on polyol segment as same as adding SiC fillers. Besides, MgO

content did not have a significant effect on $T_{g,HS}$ in the DSC measuring as well. Broaden endotherms peak when increasing MgO content can be suggested to a small degree of ordering in hard segment in both flexible and rigid PUR matrices. $T_{g,HS}$ shows between 39 and 44 °C for a rigid PUR matrix. T_{endo} has no trend when MgO content was increased in both flexible and rigid PUR matrices. In this study, $T_{g,SS}$ of rigid PUR and MgO composites are not clearly observed when loading MgO content between 3.57 and 10.49 v/v%. This can be attributed to the fact that the MgO particles obscure the polyol segment's motion which leads to having less soft segments with ordered structures or crystals [77]. Furthermore, $T_{g,HS}$ is also slightly decreases with the raising of the MgO content as similar to loading SiC filler, 44 to 41 °C.

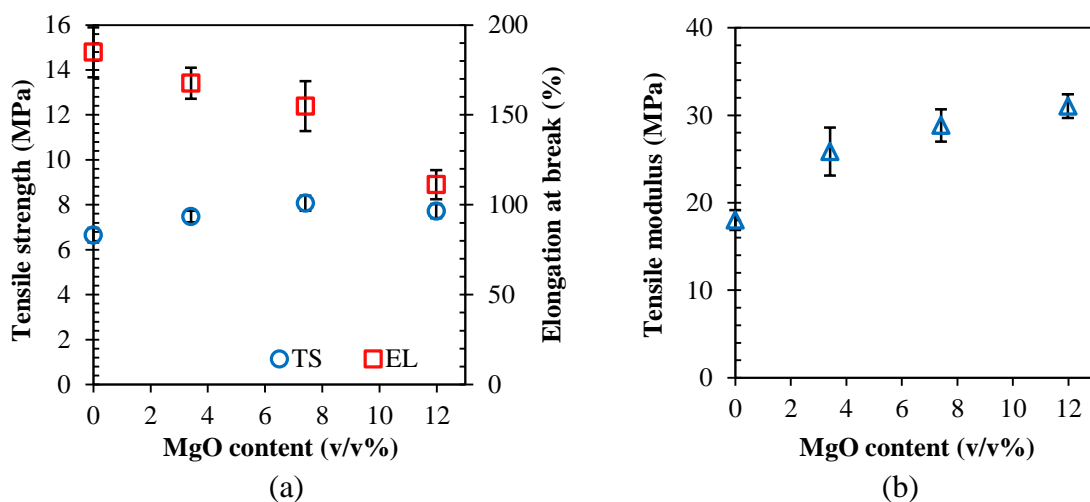


Figure 4.30 Tensile strength, elongation at break (a) and tensile modulus (b) of flexible polyurethane elastomers with different MgO contents

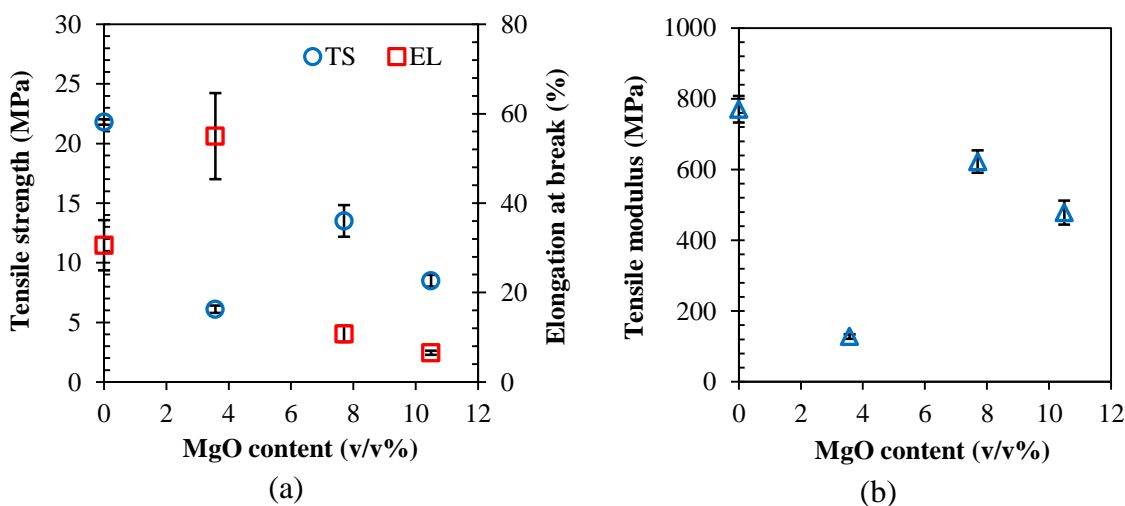


Figure 4.31 Tensile strength, elongation at break (a) and tensile modulus (b) of rigid polyurethane elastomers with different MgO contents

4.3.4 Dynamic mechanical properties

Dynamic mechanical analysis reveals the addition of MgO has a great effect on the mechanical behaviour of the flexible PUR matrix. The E' of the composites increases when MgO content was increased as shown in Figure 4.32. This can confirm the reinforcement of MgO fillers and good dispersion in the flexible PUR matrix. The amplitude of the $\tan\delta$ peak of the soft segment tends to decrease with increasing MgO content. This result is due to the addition of the MgO and its dispersion influence the polyol segment motion. The decreasing in the amplitude of $\tan\delta$ indicates the greatly restricted motion of the polyurethane chains [126]. At high temperatures, the $\tan\delta$ peak shift to the lower temperatures by adding MgO content. This can be evidence of the decrease in the $T_{g,HS}$. The decreasing level of cross-linking in flexible PUR affect the shift of $T_{g,HS}$ [125]. This result can imply that adding MgO filler might negatively affect the physical cross-linking level in PUR matrix.

In case of rigid PUR matrix reinforced MgO composites, E' decreases when MgO was loaded, especially at 3.57 v/v% as revealed in Figure 4.33. This is due to the composites became slightly foamed. Besides, the decrease of the storage modulus also correlates to the poor tensile result. The $\tan\delta$ shows a very small peak associated at a lower temperature which did not change with increasing MgO content as shown in appendix A. This can be confirmed that MgO does not influence the $T_{g,SS}$ of the rigid PUR matrix while the $\tan\delta$ peak slightly shifts the lower temperatures with increasing MgO fillers at a higher temperature. Furthermore, the amplitude of the $\tan\delta$ peak of the hard segment tends to decrease with increasing MgO content. This might be because of the restricted motion of polyurethane chains resulting from the increase of cross-linking function of high MgO content for the isocyanate terminated polyurethane chains are presented.

As discussed at earlier of DSC and DMA results, $T_{g,SS}$ and $T_{g,HS}$ from both DSC and DMA technique show similar trend in both PUR matrix. This correlation can be clued that MgO decrease the level of cross-linking in the PUR matrix.

4.3.5 Infrared spectroscopy

The effect of MgO on the PUR matrix chemical structure was characterized by the IR technique. IR spectra exhibited the same bands typical for PUR which consist of $-\text{NH}$, CH_x , and $\text{C}=\text{O}$ group. MgO content has no significant effect to change the chemical group on the main PUR structure. This might be due to their incompatibility between MgO particles and PUR matrix. The spectra of MgO can be revealed in the low-

frequency region due to the metal-oxygen stretching but it did not observe clearly in this examination. A difference in both the free and hydrogen-bonded is exhibited as well as differences in the peak related to $-NH$ group when increasing the MgO content. This can be indicated that MgO has a small effect on the amine group both flexible and rigid PUR matrices. Furthermore, adding MgO into both PUR matrices clearly show degradation effect. The rate of degradation might increase with increasing the MgO content as shown by the increasing every band's intensity [128] as shown in appendix A.

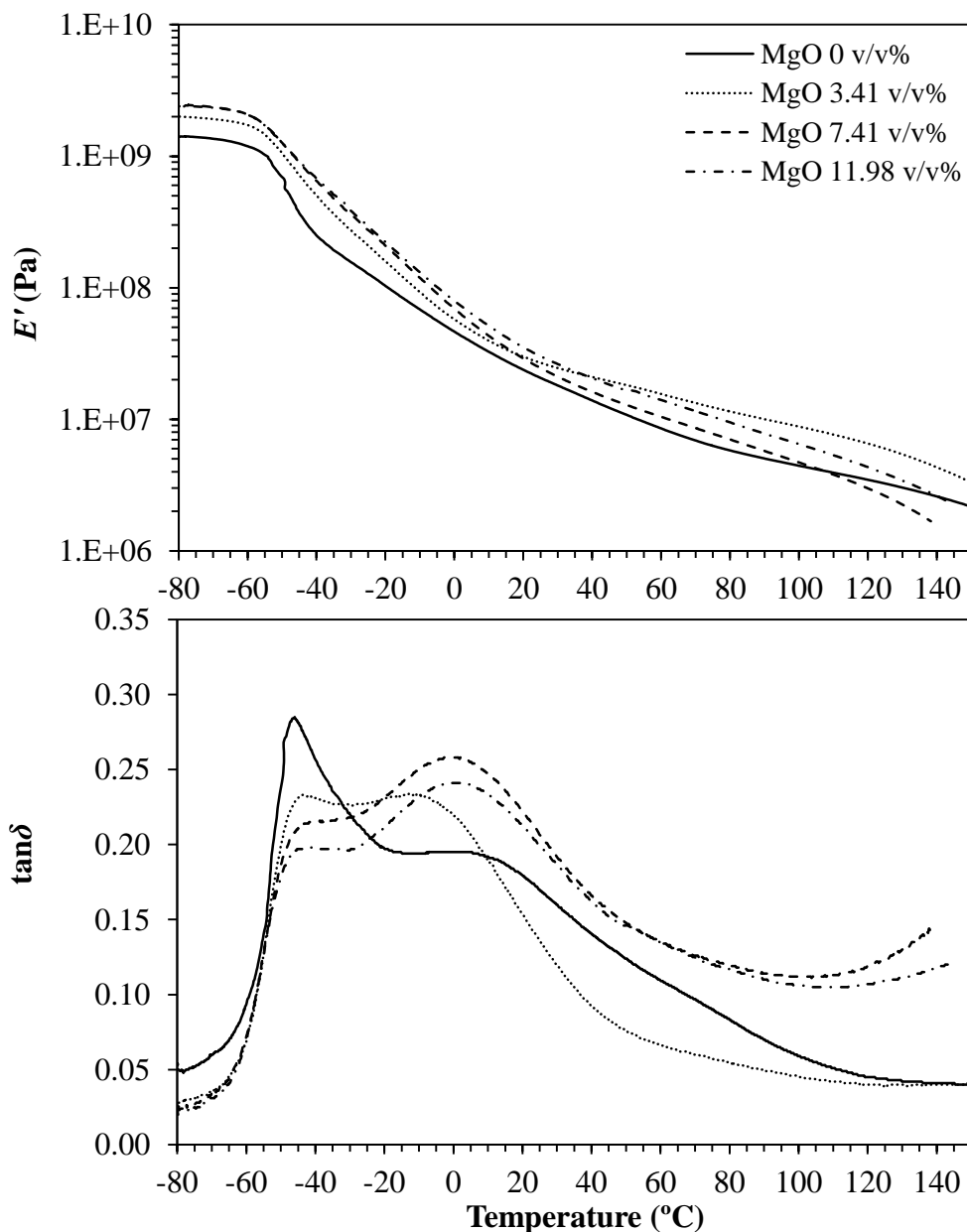


Figure 4.32 Storage modulus and mechanical loss factor from DMA of flexible PUR with different MgO contents

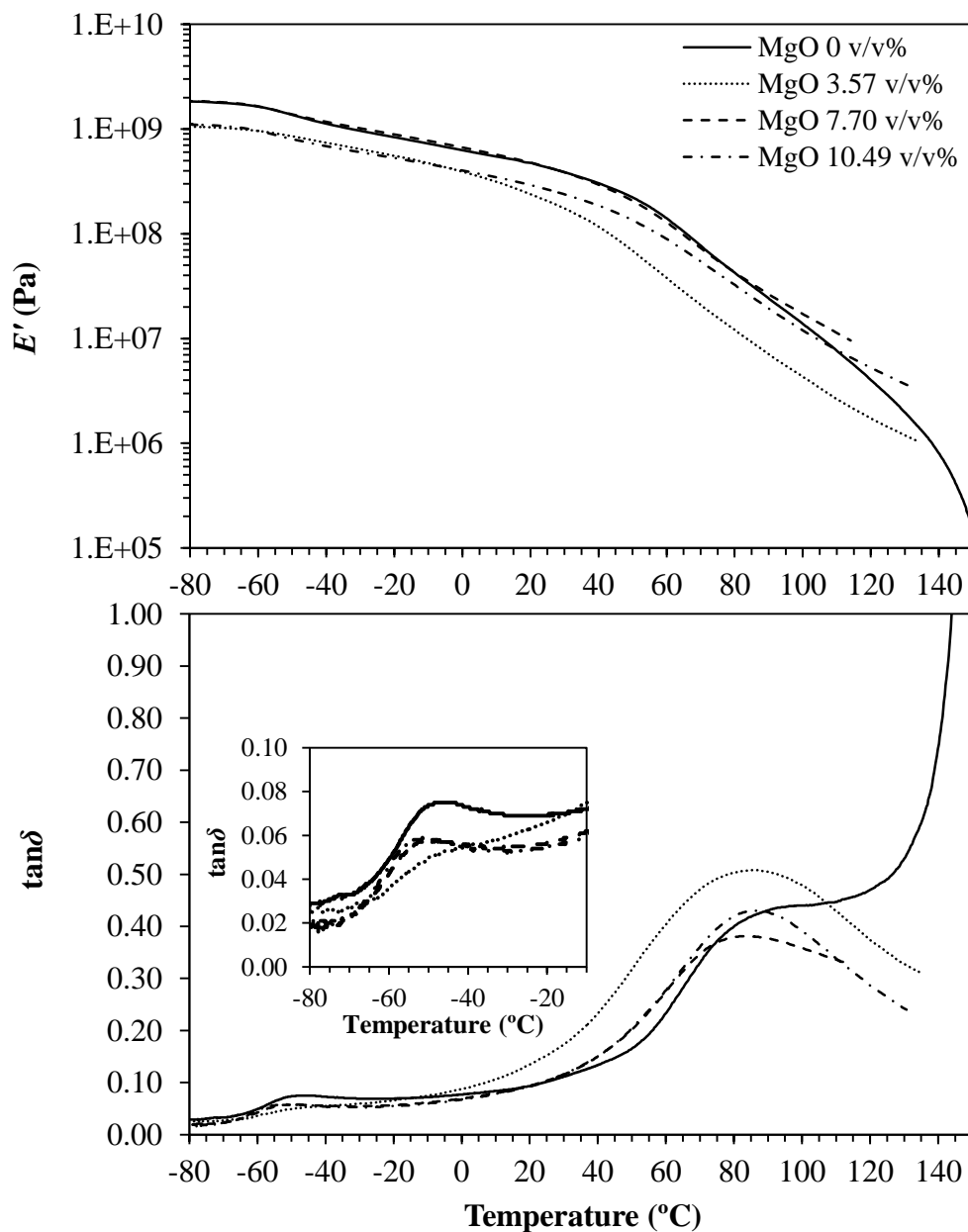


Figure 4.33 Storage modulus and mechanical loss factor from DMA of rigid PUR with different MgO contents

4.3.6 Morphology

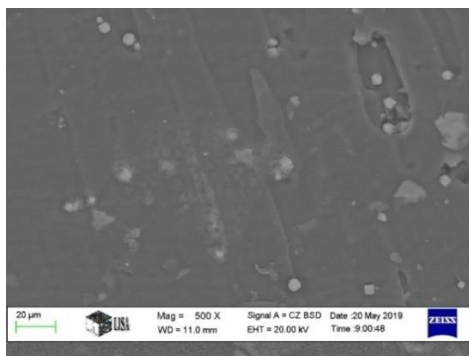
4.3.6.1 Particle size distribution and morphology of MgO particles

From particle size distribution results, the particle median and mean size of MgO are 3.376 and 3.505 μm , respectively. The result revealed a uni-modal distribution of particles similar to SiC particle size distribution. Furthermore, spherical-like shape was shown in appendix A. SEM images show more aggregated small particles than SiC particles. The particles size and shape of MgO fillers can correlate to lower thermal

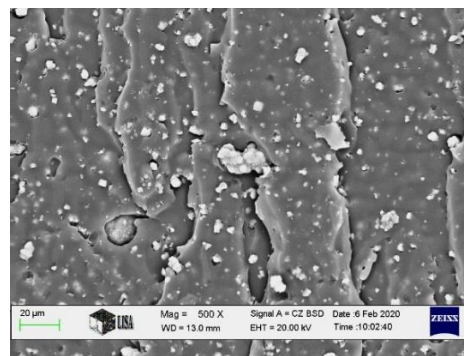
conductivity and some mechanical properties compared to adding SiC filler into the observed PUR matrix.

4.3.6.2 Morphology of flexible and rigid polyurethane elastomers with MgO fillers

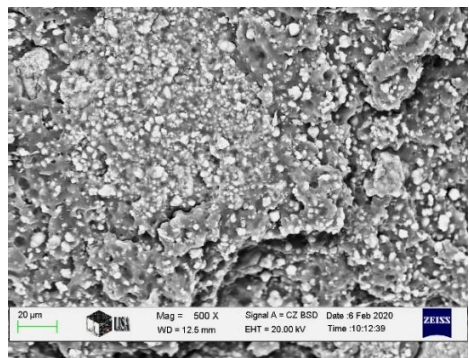
Morphology of both flexible and rigid PUR matrices with adding MgO fillers was shown in Figure 4.34 and Figure 4.35. SEM images revealed that MgO particles are evenly dispersed in both PUR matrices except at 3.57 v/v% in rigid PUR matrix. It can be seen that particles were buried inside both PUR matrices also. At 3.57 v/v% MgO content in rigid PUR, SEM image reveals high agglomerated particles and clearly seen two phases separation as shown in Figure 4.35 (b). This might be due to a high viscosity of rigid PUR resin (high amount of MDI fraction) and poor adhesion between MgO particles and matrix. This result can confirm that the foam formation effect decreases density, Shore hardness, tensile strength and modulus of rigid PUR composites. From SEM results, the elemental analysis of the composites was characterized by EDS analysis as revealed in Figure 4.34 (d) and Figure 4.35 (d). EDS chart shows the main elements of the composites consist of Mg, C, and O both of flexible and rigid PUR composites which can imply the existence of MgO particles inside both PUR matrices.



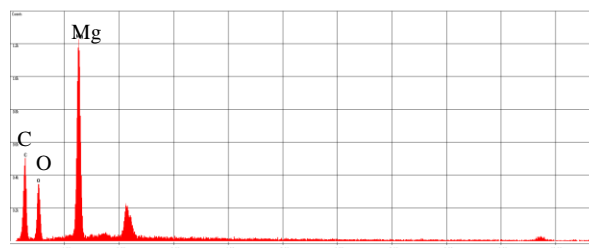
(a)



(b)

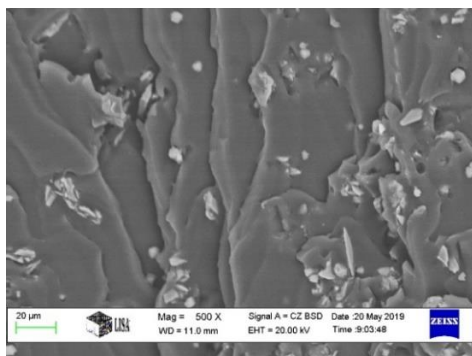


(c)

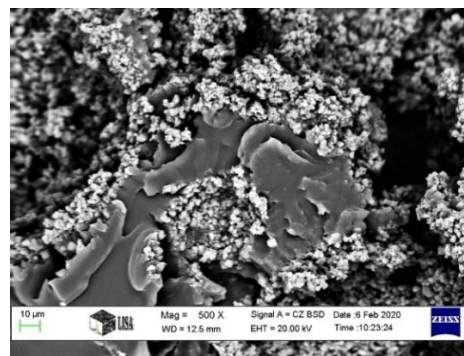


(d)

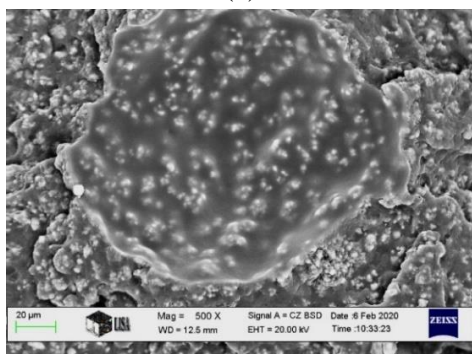
Figure 4.34 SEM image of flexible PUR with different MgO contents (a) MgO 0 v/v%, (b) MgO 3.41 v/v%, (c) MgO 11.98 v/v% (nominal magnification of 500×) and (d) EDS chart



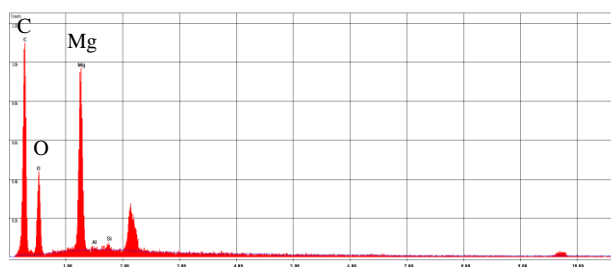
(a)



(b)



(c)



(d)

Figure 4.35 SEM image of rigid PUR with different MgO contents (a) MgO 0 v/v%, (b) MgO 3.57 v/v%, (c) MgO 10.49 v/v% (nominal magnification of 500×) and (d) EDS chart

4.4 Flexible and rigid polyurethane elastomer with zinc oxide composites

Zinc oxide (ZnO) is an inorganic compound with the formula ZnO. It is used as an additive in numerous materials and products including rubbers, plastics, ceramics, and so on. Furthermore, ZnO has a high thermal conductivity value at around 60 W / mK. Therefore, it was chosen for preparation of PUR and high thermally conductive composites.

4.4.1 Thermal conductivity and density

Figure 4.36 shows the thermal conductivity value of flexible and rigid PUR with ZnO composites. For flexible PUR composites, thermal conductivity tends to raise with increasing the content of ZnO from 0 to 7.99 v/v%. Thermal conductivity increased from 0.253 to 0.372 W / mK, it was enhanced by 47 % when compared to pure PUR. Good dispersion of ZnO fillers improves the thermal conductivity. This might be due to evenly dispersion of ZnO acting as network fillers which the phonons can cross the PUR matrix in the short time. In case of rigid PUR composites, thermal conductivity does not significantly change with increasing ZnO content from 0 to 6.96 v/v% as shown in Figure 4.36 (b). Thermal conductivity was improved from 0.290 to 0.357 W / mK with raising ZnO content from 0 until 5.05 v/v%. Then, it decreased to 0.249 W / mK. This may be due to the high amount of ZnO in rigid PUR lead to slightly increase the foam formation and it causes the decreasing of thermal conductivity value. This because of the phonon is obstructed in its transfer by the air bubbles similarly to addition of the MgO fillers.

As modeling results of ZnO and PUR composites, result reveal the same trend to loading MgO in both PUR matrices as shown in Figure 4.37. For the flexible PUR matrix, the thermal conductivity from the experimental data also following the theoretical modeling line 2.5 which means it has a good trend and fit for the theoretical model in the flexible PUR matrix. Moreover, from the experimental data it can be clearly seen that the thermal conductivity has a higher value than the theoretical model predicts (line 2.5). This might be attributed to ZnO having a little better dispersion inside the flexible PUR matrix than the SiC and the MgO particles. The other reason maybe the different particles size of these three fillers. The smaller particle size of ZnO than SiC and MgO can create more network within the filler that will result in a faster phonon transportation. However, improvement of thermal conductivity with adding ZnO result shows lower value than adding the other fillers. This might be due to smaller amounts of ZnO being loaded (limitation of ZnO fillers loading in this study). Unfortunately, foam formation and particle agglomerations have a strong influence on decreasing the thermal conductivity in

rigid PUR matrix which can be revealed that it has lower value than the lower line of theoretical modeling as shown in Figure 4.37 (b). For rigid PUR matrix result, the disorder of thermal conductivity from experimental data is due to foam structure which causes by moisture and effect of the incompatibility between ZnO particles and rigid PUR matrix. The reason of foam formation might be due to moisture during mixing and high viscosity of rigid PUR matrix as similar to loading MgO fillers.

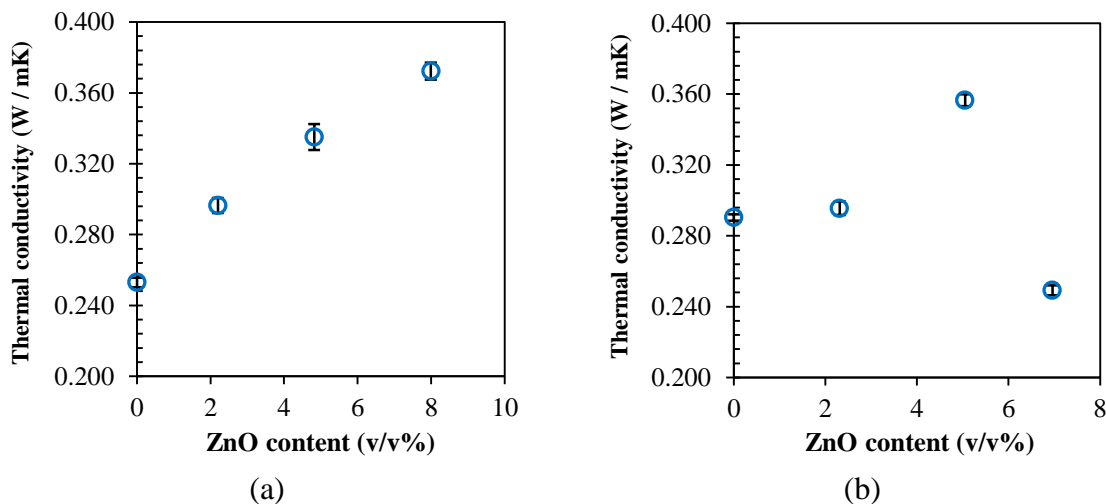


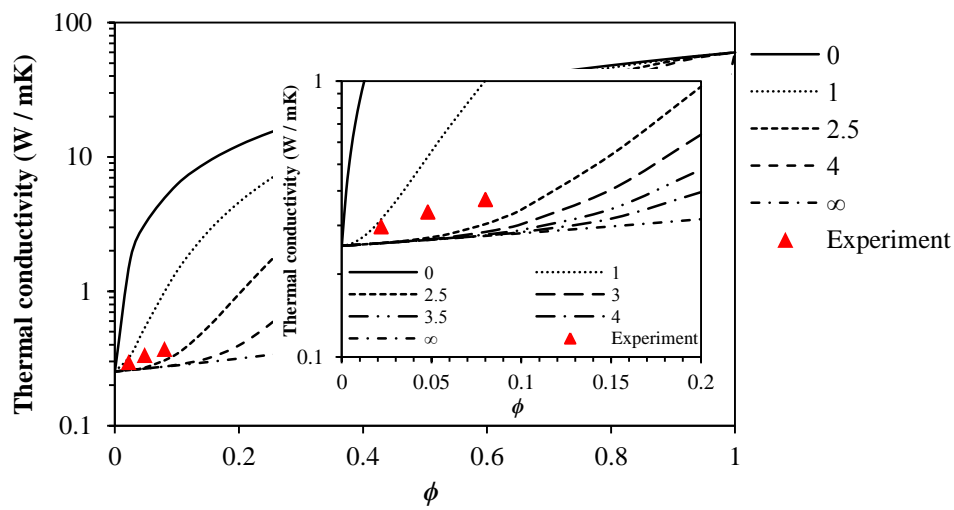
Figure 4.36 Thermal conductivity of flexible (a) and rigid (b) polyurethane elastomers with different ZnO contents

The density results tend to raises with increasing ZnO content which related to the thermal conductivity in flexible PUR composites as shown in Figure 4.38 (a). On the contrary, the density has no trend with increasing ZnO content in a rigid PUR matrix (Figure 4.38 (b)). This can be clued the foam formation of these composites as discussed above. Foam structure of this composite has caused an unexpectedly large scattering of the thermal conductivity. It almost looks like the composites became to thermal insulating polymers.

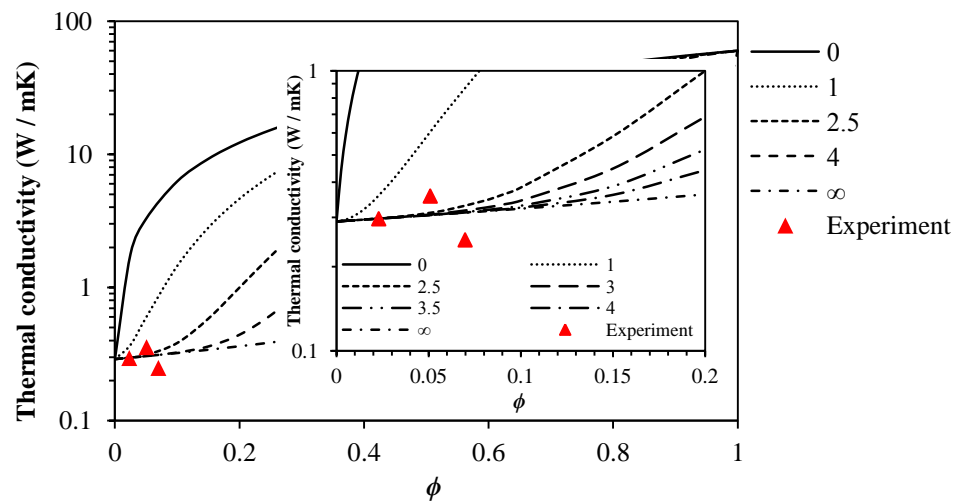
4.4.2 Mechanical properties

4.4.2.1 Hardness

Shore A and D hardness values of both flexible and rigid PUR with ZnO composites were measured and shown in Figure 4.39 (a) and (b). For both flexible and rigid PUR composites, the results show Shore A and D hardness did not significantly change with adding ZnO particles between 0 and 8 v/v%. For flexible PUR matrix, Shore A hardness presented at around 81 while Shore D hardness shows between 26 to 31, it did not show a trend. In case of rigid PUR matrix, Shore A hardness is around 93 while Shore D is between 40 to 65.

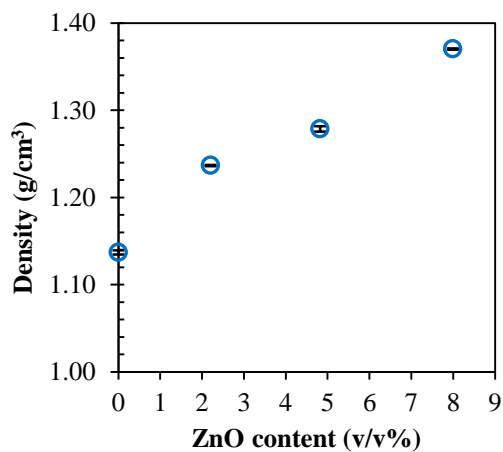


(a)

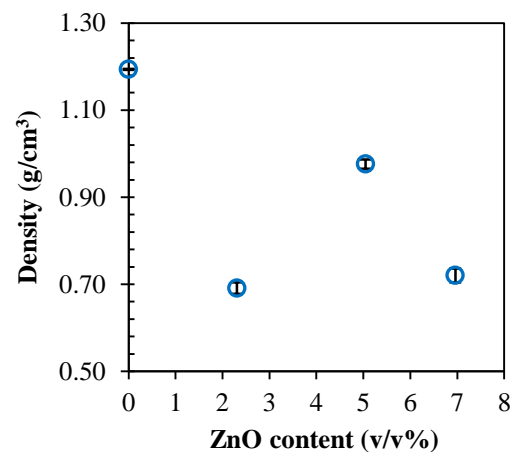


(b)

Figure 4.37 Thermal conductivity modelling of flexible (a) and rigid (b) polyurethane elastomers with different ZnO contents



(a)



(b)

Figure 4.38 Density of flexible (a) and rigid (b) polyurethane elastomers with different ZnO contents

Moreover, adding ZnO fillers in both flexible and rigid PUR matrices exhibited the same trend as adding MgO fillers. These results can be suggested that ZnO particles are inactive filler in both flexible and rigid PUR matrices.

4.4.2.2 Tensile properties

Tensile strength, tensile modulus and elongation at break of flexible PUR as a function of ZnO content are shown in Figure 4.40. Results exhibited that tensile strength and elongation at break tend to decrease with increasing ZnO content. Tensile strength was decreased from 7 to 4 MPa while elongation at break decreased from 185 to 104%. Besides, tensile modulus did not change with raising ZnO content. This result cause ZnO filler is not reinforcement fillers in flexible PUR matrix and may be due to effect of agglomerated fillers at high content (7.99 v/v%). However, tensile modulus slightly raises when ZnO content was increased from 0 to 4.82 v/v%. This might indicate a good dispersion of ZnO particles inside flexible PUR matrix until the filler content reach 4.82 v/v%.

In case of rigid PUR composites, tensile strength, elongation at break and tensile modulus also decreased with raising ZnO content between 0 and 6.96 v/v% as shown in Figure 4.41. It can be explained by their inherent incompatibility between ZnO particles and rigid PUR matrix as similar as adding MgO particles. The agglomeration of the particles at high content fillers also has influenced the decreasing of tensile properties [16]. Tensile result of ZnO and rigid PUR matrix is in correlation with the decrease of thermal conductivity, density and Shore hardness result similarly to when adding MgO fillers.

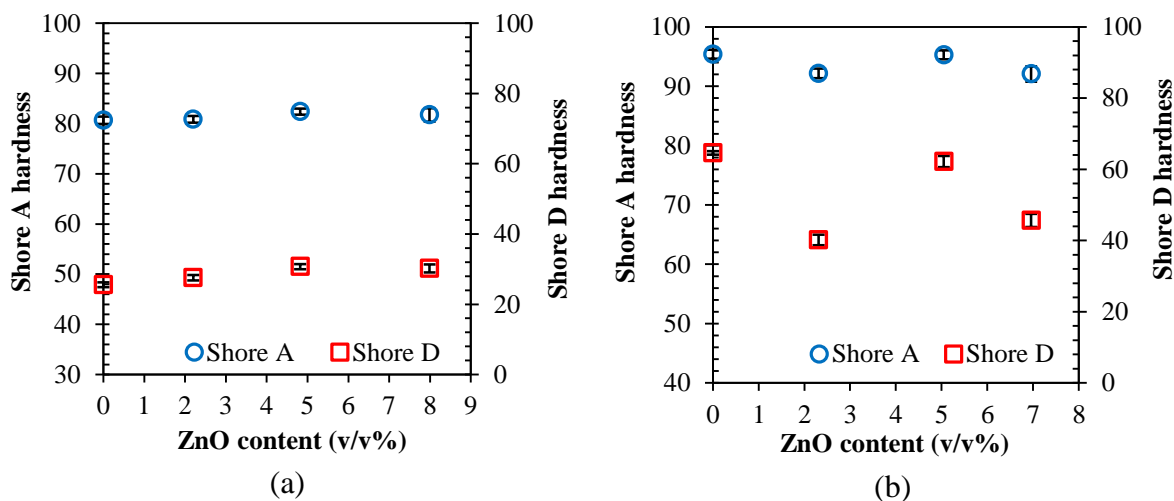


Figure 4.39 Shore A and D hardness of flexible (a) and rigid (b) polyurethane elastomers with different ZnO contents

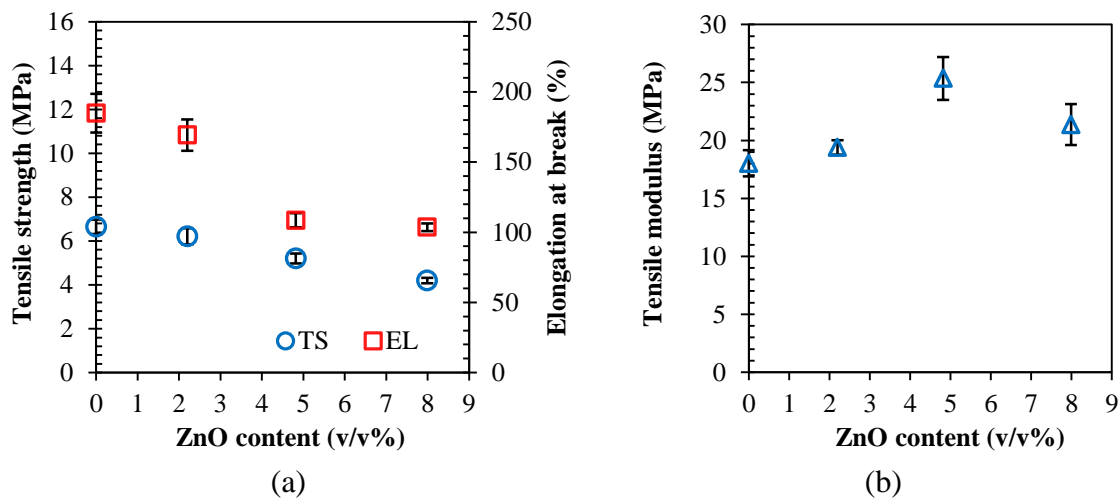


Figure 4.40 Tensile strength, elongation at break (a) and tensile modulus (b) of flexible polyurethane elastomers with different ZnO contents

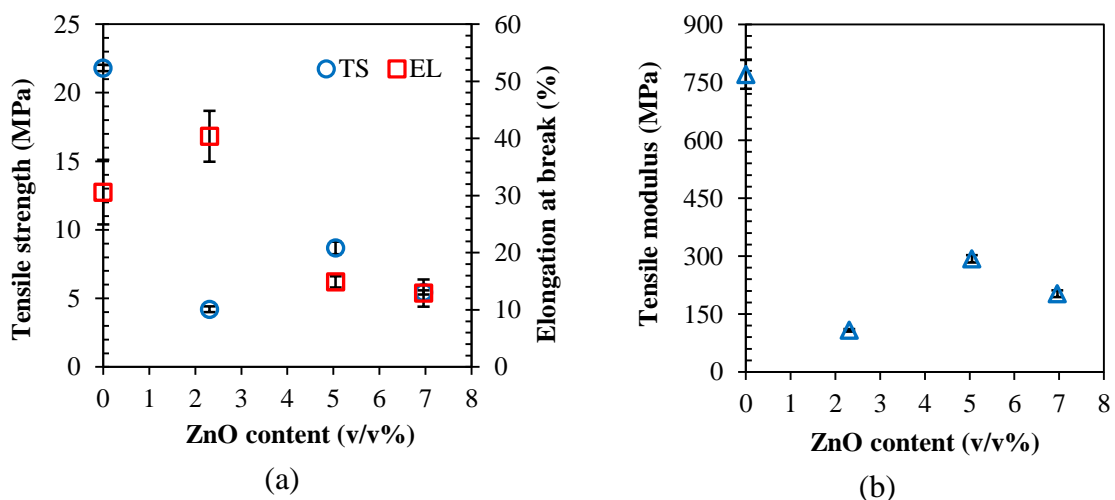


Figure 4.41 Tensile strength, elongation at break (a) and tensile modulus (b) of rigid polyurethane elastomers with different ZnO contents

4.4.3 Thermal properties

DSC curve of both flexible and rigid PUR with ZnO composites was presented in appendix B. DSC curves reveal $T_{g,SS}$ around $-60\text{ }^{\circ}\text{C}$ in both flexible and rigid PUR matrices, this result is similar to loading SiC and MgO fillers. Loading ZnO content has no significant effect on the $T_{g,SS}$. This can demonstrate that ZnO fillers did not affect on polyol segment as well. Broaden endotherms peak when adding high ZnO content can be suggested to a small degree of ordering in hard segment domains for rigid PUR matrix. For flexible PUR and ZnO composites, $T_{g,HS}$ shows at around $44\text{ }^{\circ}\text{C}$ while $T_{g,HS}$ for rigid PUR composites present at around $44\text{ }^{\circ}\text{C}$ as well. Besides, T_{endo} decreased with raising ZnO content because it affects the cross-linking of the hard segment.

4.4.4 Dynamic mechanical properties

DMA thermograms indicated that ZnO influences the mechanical behaviour in both flexible and rigid PUR composites. In case of flexible PUR and ZnO composites, the E' shows slightly raise with adding ZnO fillers as shown in Figure 4.42. This means that a little reinforcement effect of ZnO in the flexible PUR matrix. This result correlates with the increase of the tensile modulus. $T_{g,SS}$ reveals unimportantly decreased as shown in appendix B. The amplitude of $\tan\delta$ peak at low temperature tends to decrease with increasing ZnO content similar to loading SiC and MgO fillers. This due to increasing content of the ZnO and its dispersion influence the polyol segment motion in PUR structure and also indicate the greatly restricted motion of the polyurethane chains. For $T_{g,HS}$, $\tan\delta$ peak shifts to the lower temperatures with adding ZnO except when adding 7.99 v/v% of ZnO. The shift of $T_{g,HS}$ can be indicating that ZnO particles affect the decreasing level of cross-linking in the flexible PUR matrix [125]. The agglomeration of ZnO particles can be evidenced by the high intensity $\tan\delta$ peak and $T_{g,HS}$ not shifting to lower temperatures similarly to the other fillers. This result might correlate to decreasing modulus.

In case of rigid PUR matrix with ZnO composites, the E' decreases after loading ZnO as shown in Figure 4.43. This is because their incompatibility between ZnO fillers and rigid PUR matrix and formation of foam with adding ZnO fillers into rigid PUR matrix as similar to loading MgO fillers. It is also causing a huge decrease in tensile modulus. The $\tan\delta$ shows a very small peak associated at a lower temperature which did not change with increasing ZnO content, it means loading ZnO has no effect $T_{g,SS}$ in rigid PUR matrix. At high temperature, the $\tan\delta$ peak slightly shifts the lower temperatures when ZnO content was increased. This result can confirm the effect of ZnO content on the cross-linking of the hard segment of both PUR matrices from DSC results.

Furthermore, $T_{g,SS}$ and $T_{g,HS}$ from both DSC and DMA technique show similar trend in both PUR matrices. This can imply that ZnO decreases the level of cross-linking in the PUR matrix.

4.4.5 Infrared spectroscopy

As was expected, the IR spectra of ZnO and PUR composites reveal similar results as loading MgO fillers. The result shows ZnO has no significant influence in the main PUR structure in both flexible and rigid PUR and the intensity peaks of all chemical band groups were increased with increasing ZnO content as shown in appendix B. It can be indicated that ZnO particles affect some chemical groups of PUR structure and ZnO also

has a small effect in the amine group in both flexible and rigid PUR matrices. Besides, adding ZnO into both PUR matrices seemingly introduces degradation of the composites. Increasing ZnO content might increase the degradation which is indicated by the increasing the intensity of every bands.

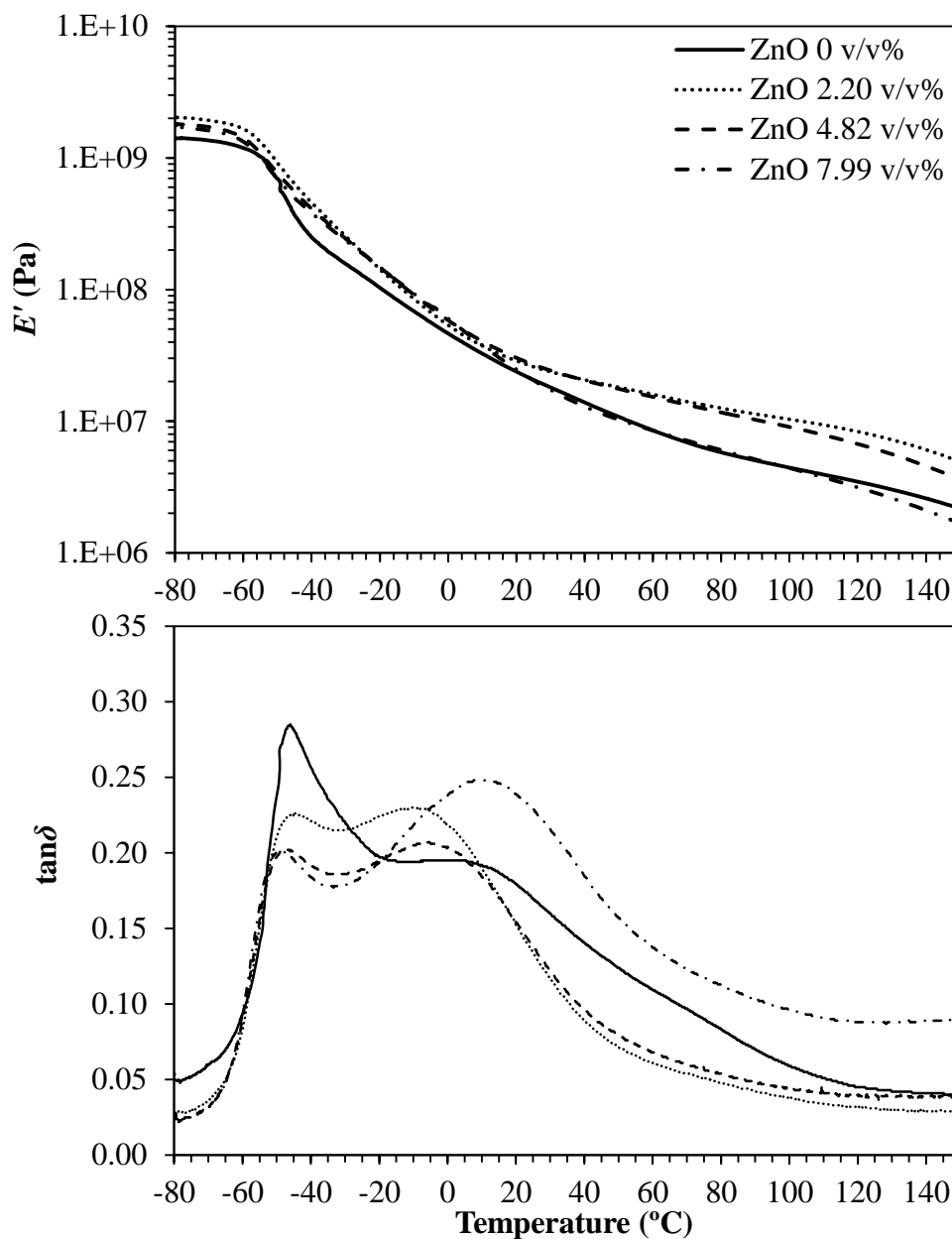


Figure 4.42 Storage modulus and mechanical loss factor from DMA of flexible PUR with different ZnO contents

4.4.6 Morphology

4.4.6.1 Particle size distribution and morphology of ZnO particles

The particle size distribution of ZnO particles showed the two maxima distribution as presented in appendix B. Particle size distribution curve show the particle

median and mean sizes of ZnO are 0.730 and 1.367 μm , respectively. Furthermore, cube-like or flake-like shape particles were revealed in appendix B. SEM images can be clearly seen that it has more aggregated small particles than SiC and MgO fillers.

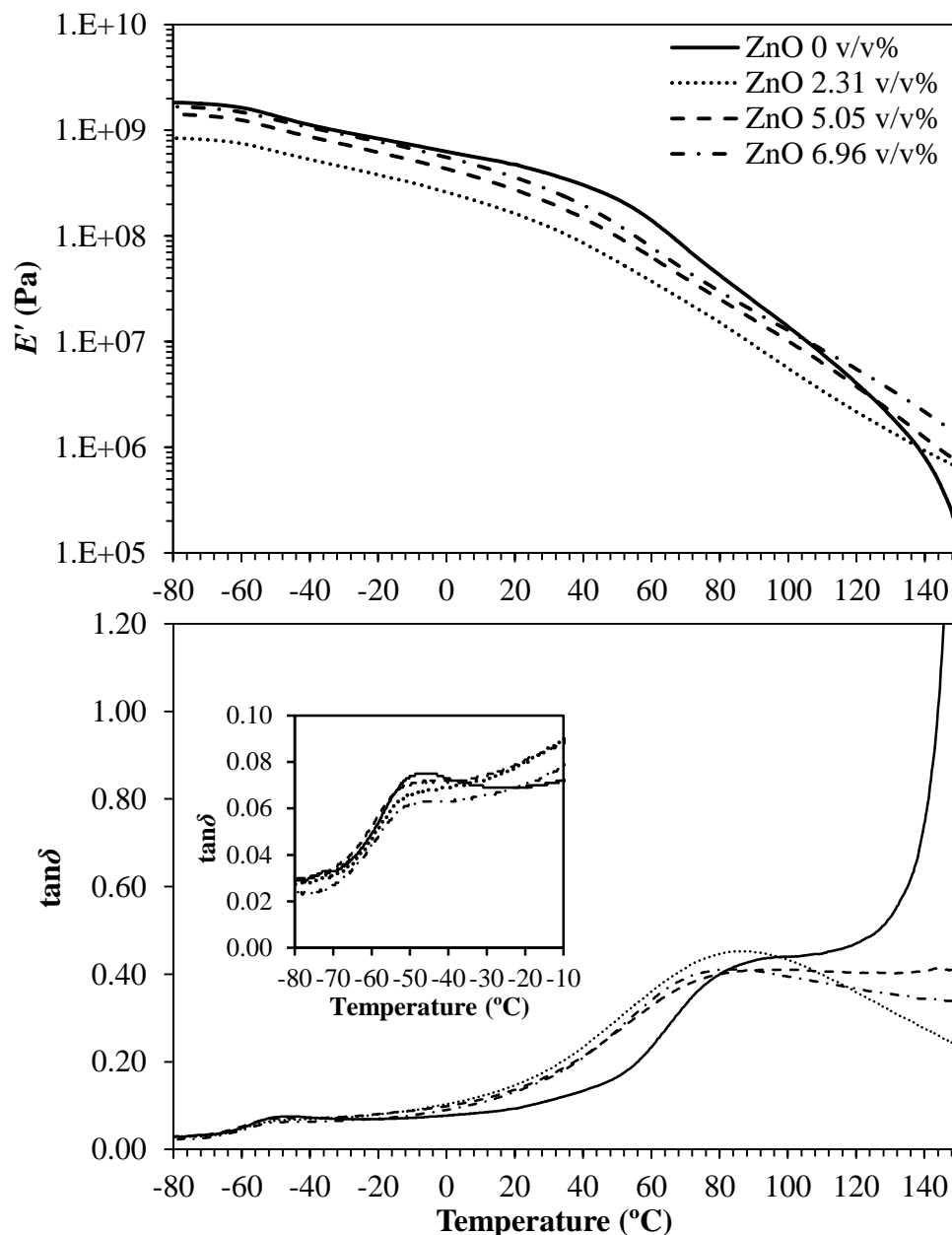
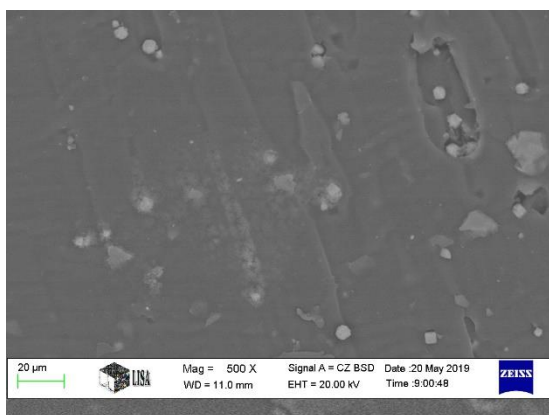


Figure 4.43 Storage modulus and mechanical loss factor from DMA of rigid PUR with different ZnO contents

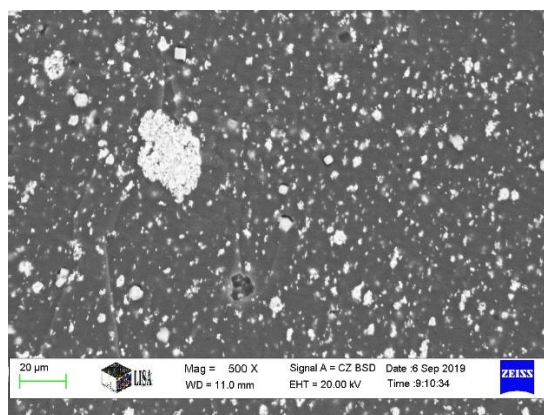
4.4.6.2 Morphology of flexible and rigid polyurethane elastomers with ZnO fillers

In case of flexible PUR matrix, SEM images show ZnO particles have uniformly dispersed in the flexible PUR matrix. The surface area of pure PUR and ZnO with PUR composites specimens reveals a smooth surface as shown in Figure 4.44. For rigid PUR and ZnO composites, the SEM image shows the agglomerated particles of ZnO in rigid PUR matrix at 2.31 v/v% as demonstrated in Figure 4.45 (b). However, the particles

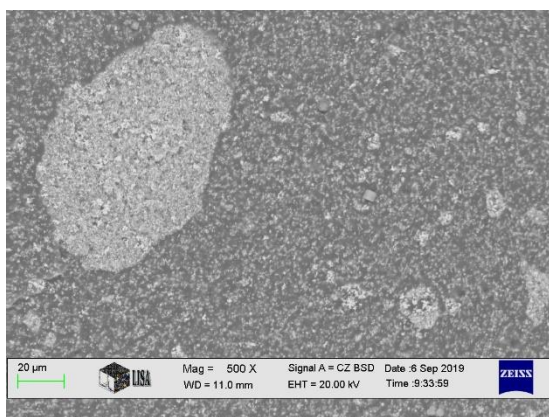
show evenly dispersed in the rigid PUR matrix with adding ZnO content at 6.96 v/v% as revealed in Figure 4.45 (c). Moreover, it can be clearly seen that the particle size of ZnO smaller than 5 μm and it was embedded in both flexible and rigid PUR matrices. EDS results can confirm that ZnO particles can distribute inside both flexible and rigid PUR matrices. The EDS chart present that Zn, O, and Na elements are the main elements as exhibited in Figure 4.44 (d) and Figure 4.45 (d). However, Na element peak obviously shows in the EDS chart which might be created from the synthesis or preparation process of ZnO particles. SEM result can be proving that foam structure of the composites cause the poor thermal conductivity, the lower density, Shore hardness, tensile strength and modulus of the rigid PUR composites.



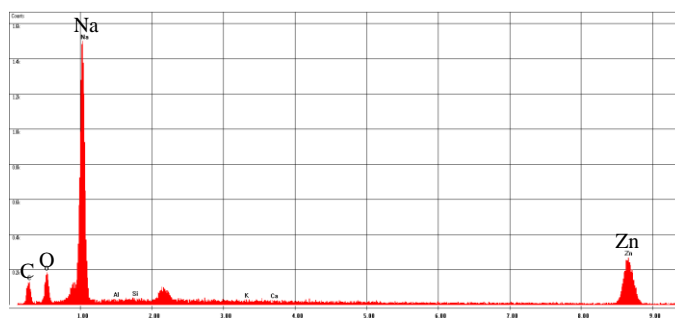
(a)



(b)

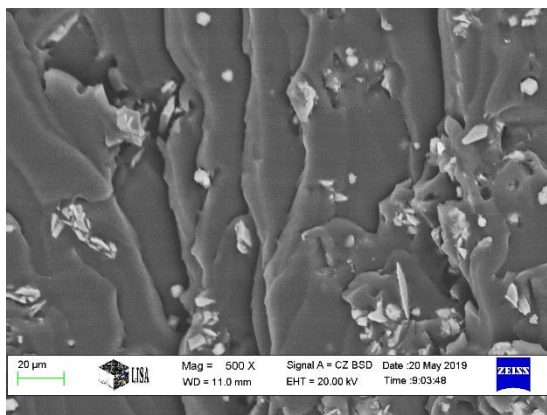


(c)

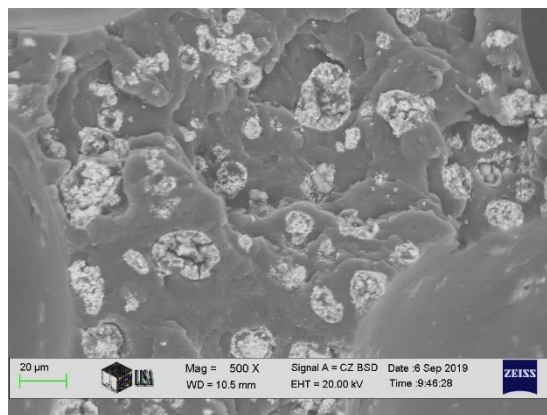


(d)

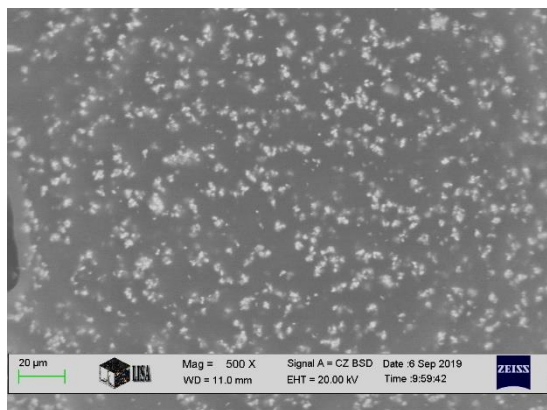
Figure 4.44 SEM image of flexible PUR with different ZnO contents (a) ZnO 0 v/v%, (b) ZnO 2.20 v/v%, (c) ZnO 7.99 v/v% (nominal magnification of 500 \times) and (d) EDS chart



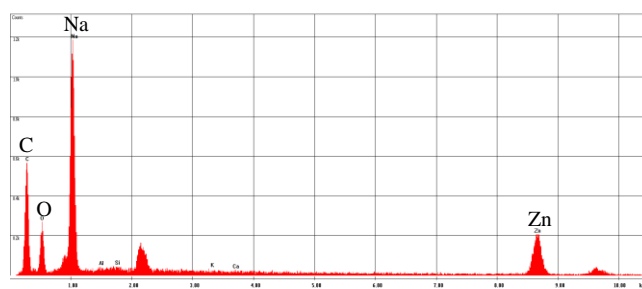
(a)



(b)



(c)



(d)

Figure 4.45 SEM image of rigid PUR with different ZnO contents (a) ZnO 0 v/v%, (b) ZnO 2.31 v/v%, (c) ZnO 6.96 v/v% (nominal magnification of 500 \times) and (d) EDS chart

4.5 Flexible and rigid polyurethane elastomer with copper composites

In this topic, electrolytic copper fillers were choosing to load into both flexible and rigid PUR matrices. It was added between 0 and 2 v/v%. Electrolytic copper has very high thermal conductivity, around 392 W / mK, it is the highest thermal conductive filler in this study. Moreover, it has excellent electrical conductivity, exhibits good strength and formability, has outstanding resistance to corrosion and fatigue.

4.5.1 Thermal conductivity and density

As a result of the flexible PUR matrix, thermal conductivity increased from 0.253 to 0.314 W / mK, it was enhanced by 24 % when compared to pure flexible PUR as shown in Figure 4.46. In case of rigid PUR matrix, thermal conductivity value was enhanced by 47 % from 0.290 to 0.429 W / mK, it is a huge improvement when compared to the other fillers as presented in appendix C. The other reason from promoted phonon propagation to raising the thermal conductivity is the high thermal conductive value of Cu filler also supports the increase of thermal conductivity of this composite.

A graphical representation of the theoretical modeling and experimental data can be found in Figure 4.47. Result show good improvement of the thermal conductivity in both flexible and rigid PUR matrices than the composites containing SiC, MgO, and ZnO fillers. The thermal conductivity from the experiment is following the theoretical modeling line 1, which means it has a very good predicted value in both flexible and rigid PUR matrices. Result show that it is getting close to the upper limit line 0. This result can be explained by the good dispersion of Cu particles and the high thermal conductivity of Cu fillers even though loading low Cu content. It can be revealed in some works where the metallic particles were filled into polymer matrix [49, 47]. The other reason for increasing the thermal conductivity is that adding Cu particles did not create a foam structure or tiny bubbles inside rigid PUR composite as same as adding MgO and ZnO fillers.

The density was raised with increasing Cu content in both flexible and rigid PUR matrices. This can be concluded that the Cu fillers were contained inside the PUR matrix. Besides, the result can correlate to thermal conductivity in both flexible and rigid PUR composites as shown in Figure 4.48.

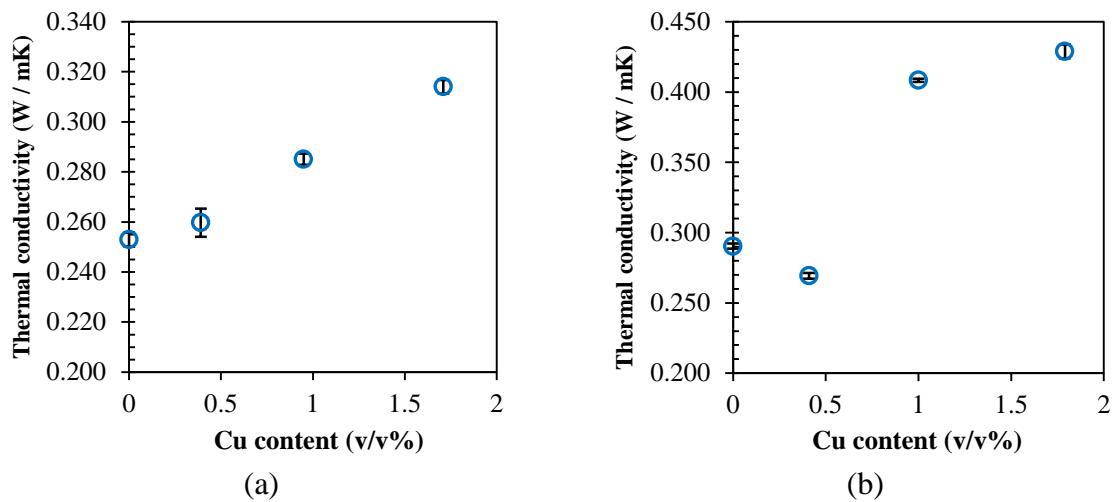


Figure 4.46 Thermal conductivity of flexible (a) and rigid (b) PUR with different Cu contents

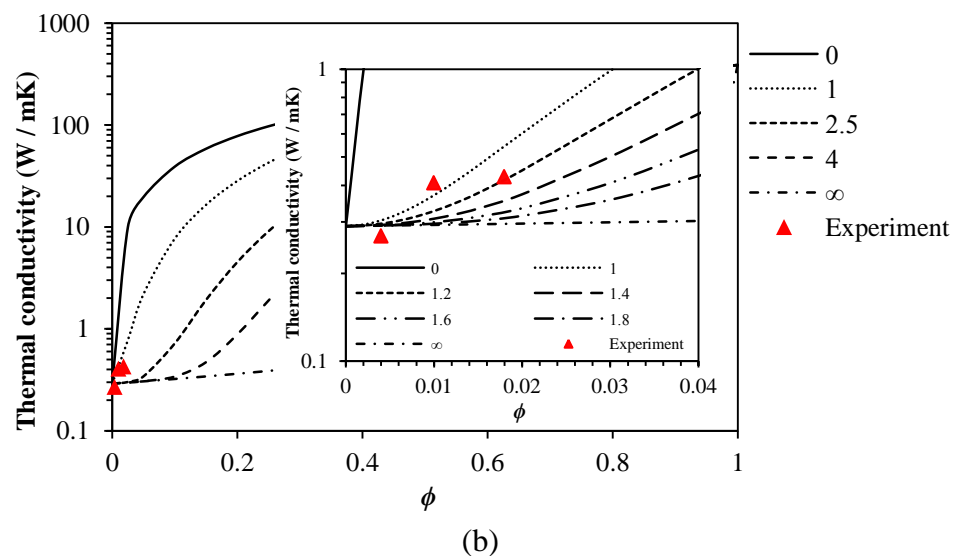
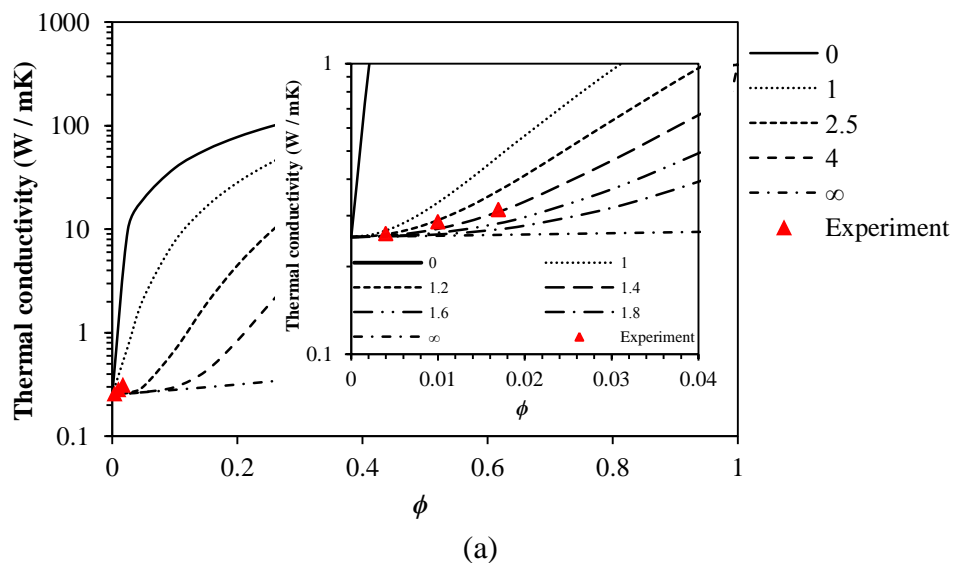


Figure 4.47 Thermal conductivity modelling of flexible (a) and rigid (b) polyurethane elastomers with different electrolytic Cu contents

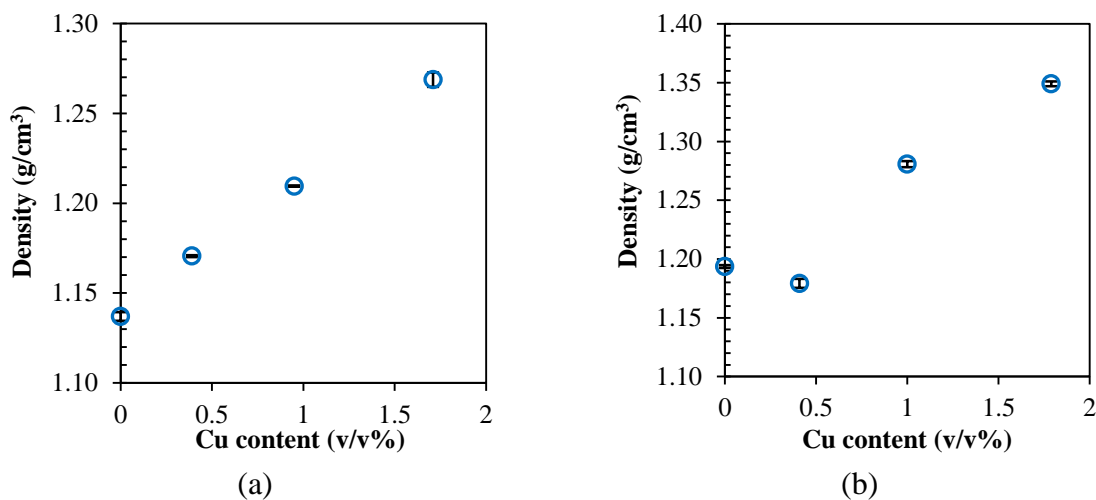


Figure 4.48 Density of flexible (a) and rigid (b) PUR with different Cu contents

4.5.2 Mechanical properties

Mechanical properties (Shore hardness and tensile properties) of Cu and both flexible and rigid PUR composites were presented in this topic. Mechanical properties were plotted as a function of Cu content between 0 and 2 v/v%.

4.5.2.1 Hardness

Shore A and D hardness of flexible and rigid PUR present slightly raising of Shore A and D hardness in both flexible and rigid PUR composites. As a result of the flexible PUR matrix, Shore A hardness increases from 81 to 86 while Shore D hardness increases from 26 to 33. For rigid PUR matrix, Shore A hardness slightly increase from 95 to 98 while Shore D hardness was raised from 65 to 68, as shown in Figure 4.49. This result can be indicated that Cu content influences the stiffness of both PUR composites even though at low content. Moreover, this result indicated that Cu particles can act as active fillers in both flexible and rigid PUR matrices.

4.5.2.2 Tensile properties

The effect of copper filler was also investigated by tensile testing. Results exhibit that tensile strength tends to increase with increasing Cu content while elongation at break decreased in case of flexible PUR composites. Tensile strength was improved from 7 to 10 MPa while tensile modulus was enhanced from 18 to 38 MPa which increasing more than 100%, as shown in Figure 4.50. These results similar to adding Cu into the high-density polyethylene (HDPE) which increasing Cu content can improve tensile strength and tensile modulus of polymer composites [47]. Moreover, this improvement can demonstrate that Cu fillers can act as reinforcement fillers in flexible PUR matrix.

As a result of the rigid PUR matrix, tensile strength and modulus decrease with increasing Cu content from 0 to 1.79 v/v% as shown in Figure 4.51. The decreasing tensile strength and modulus might due to the agglomeration of Cu particles in rigid PUR matrix. Besides, incompatibility between Cu particles and a rigid PUR matrix also effect on decreasing tensile properties when Cu content was increased. The other reason might be due to the copper particle's shape and size might obstruct elastic deformation of the rigid matrix. The composites became more rigid but also brittle as the result of Shore hardness and tensile properties.

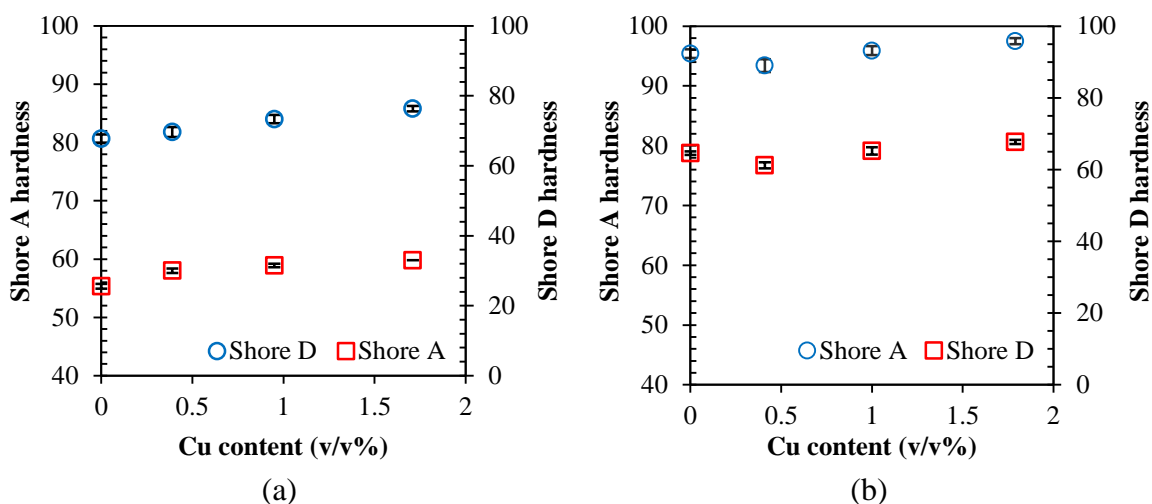


Figure 4.49 Shore A and D hardness of flexible (a) and rigid (b) PUR with different Cu contents

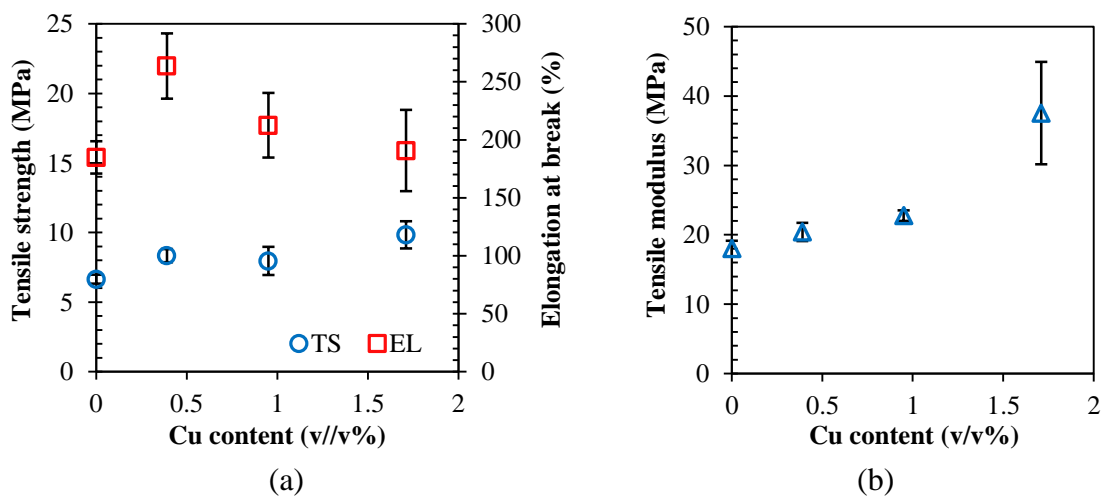


Figure 4.50 Tensile strength and elongation at break (a) and tensile modulus (b) of flexible PUR with different Cu contents

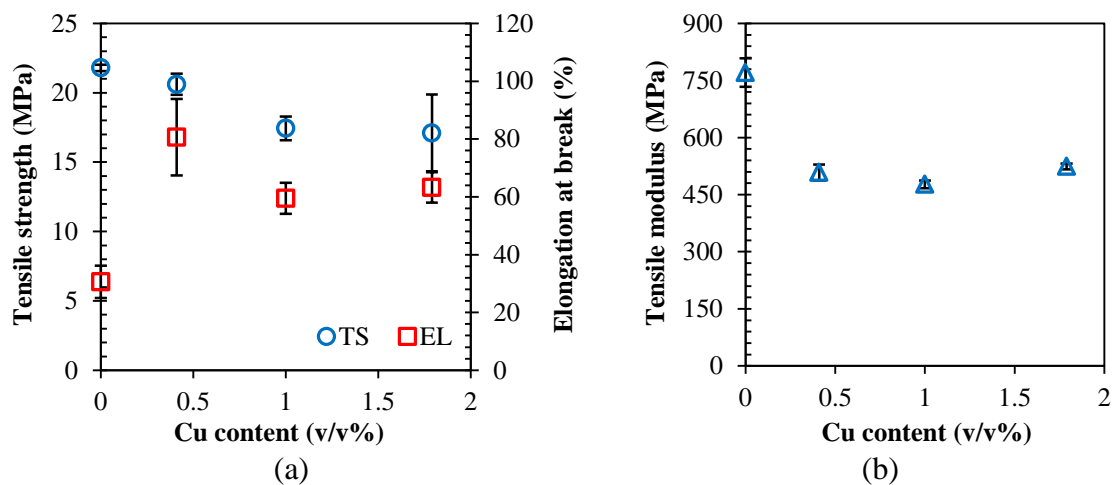


Figure 4.51 Tensile strength and elongation at break (a) and tensile modulus (b) of rigid PUR with different Cu contents

4.5.3 Thermal properties

DSC curves of both flexible and rigid PUR matrices with increasing Cu fillers from 0 to 2 v/v% were presented in appendix C. In case of flexible PUR, increasing Cu content has no significant influence on the $T_{g,SS}$ of the composites. DSC result presents similar trend to the addition of SiC, MgO and ZnO fillers. $T_{g,HS}$ shows slight decrease from 45 to 41 °C. For rigid PUR matrix, $T_{g,HS}$ revealed the same temperature at around 43 °C. Furthermore, the endothermic temperature did not significantly change with adding Cu filler both flexible and rigid PUR matrix. Increasing Cu content also reveals broad endotherms peak. It can be suggested to a small degree of ordering in hard segment domains of both flexible and rigid PUR matrices when Cu content was increased. Besides, endothermic temperature did not significantly change when Cu content was increased.

4.5.4 Dynamic mechanical properties

DMA thermogram result reveals that the addition of Cu has a great effect on the mechanical behavior of the PUR matrix, especially the flexible PUR matrix. E' of the composites improves with raising Cu content as revealed in Figure 4.52, at high temperature (rubbery region). This can be explained that the effect of reinforcement of Cu fillers in the flexible PUR matrix. The amplitude of the $\tan\delta$ peak of the soft segment (at low temperature) decreases with increasing Cu content. It implies the greatly restricted motion of polyurethane chains resulting from the cross-linking function of the filler. However, $T_{g,SS}$ did not significantly change with increasing Cu content, at around -47°C. At the high temperatures, the $\tan\delta$ peak shift to the lower temperatures with

raising Cu content, it means that decreasing $T_{g,HS}$. This result can be explained by the high content of Cu which affects the cross-linking.

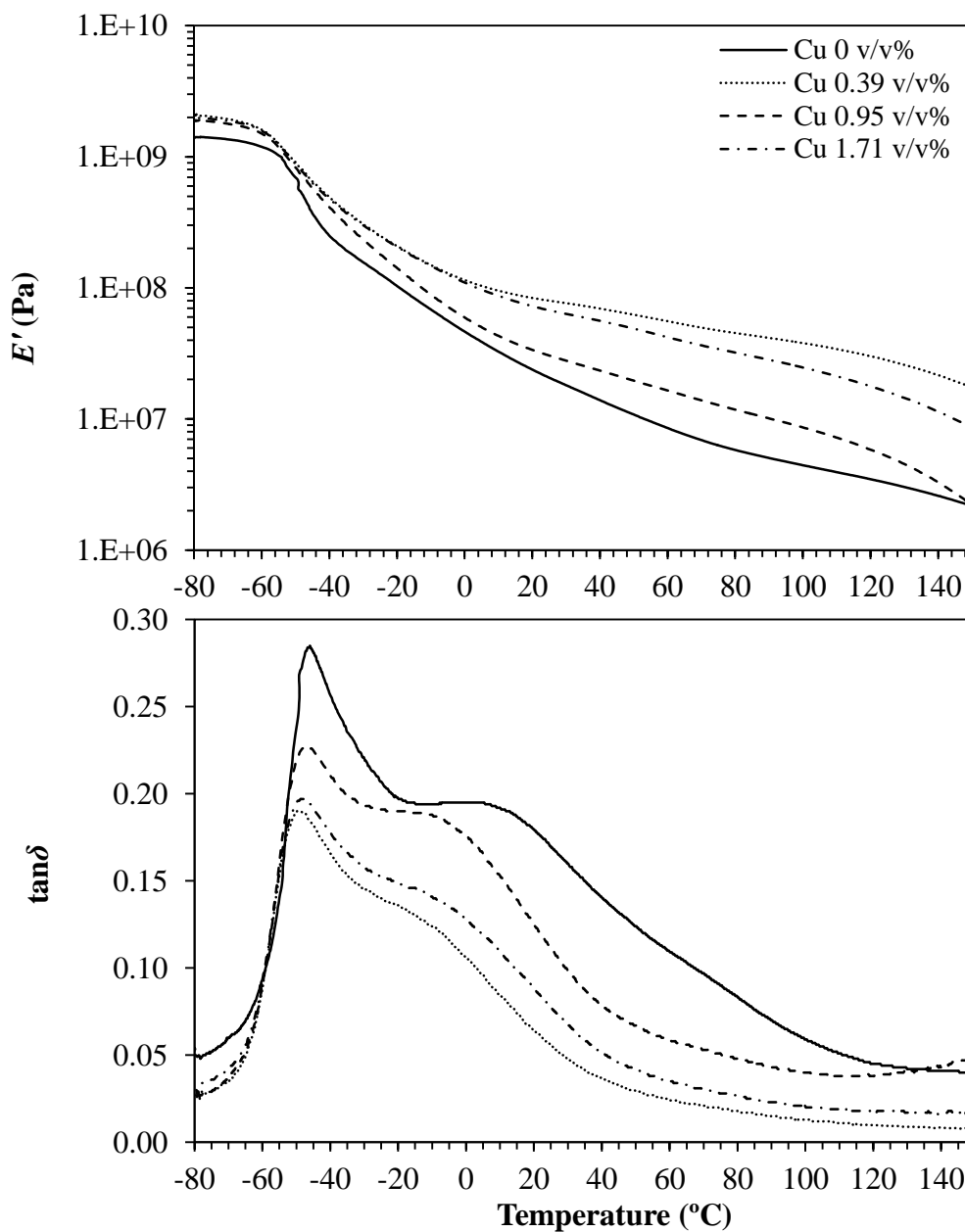


Figure 4.52 Storage modulus and mechanical loss factor from DMA of flexible PUR with different Cu contents

In case of rigid PUR matrix, E' shows slightly increase when Cu was loaded from 0 to 1.79 v/v%. It means that Cu particles have a little reinforcement effect inside rigid PUR matrix. At low temperature, the $\tan \delta$ peak shows a very small intensity which it did not significantly change with increasing Cu content, it reveals at around -51°C (appendix C). At high temperature, the $\tan \delta$ peak shows shoulder transition which could not be clearly seen a peak when adding Cu fillers as shown in Figure 4.53. This may be due to

Cu fillers content, size and shape influences the cross-linking segment motion of the hard segment in a rigid PUR structure. Besides, it has been seen that shoulder transition at the high-temperature shift to a lower temperature which means that $T_{g,HS}$ tends to decrease with raising Cu content.

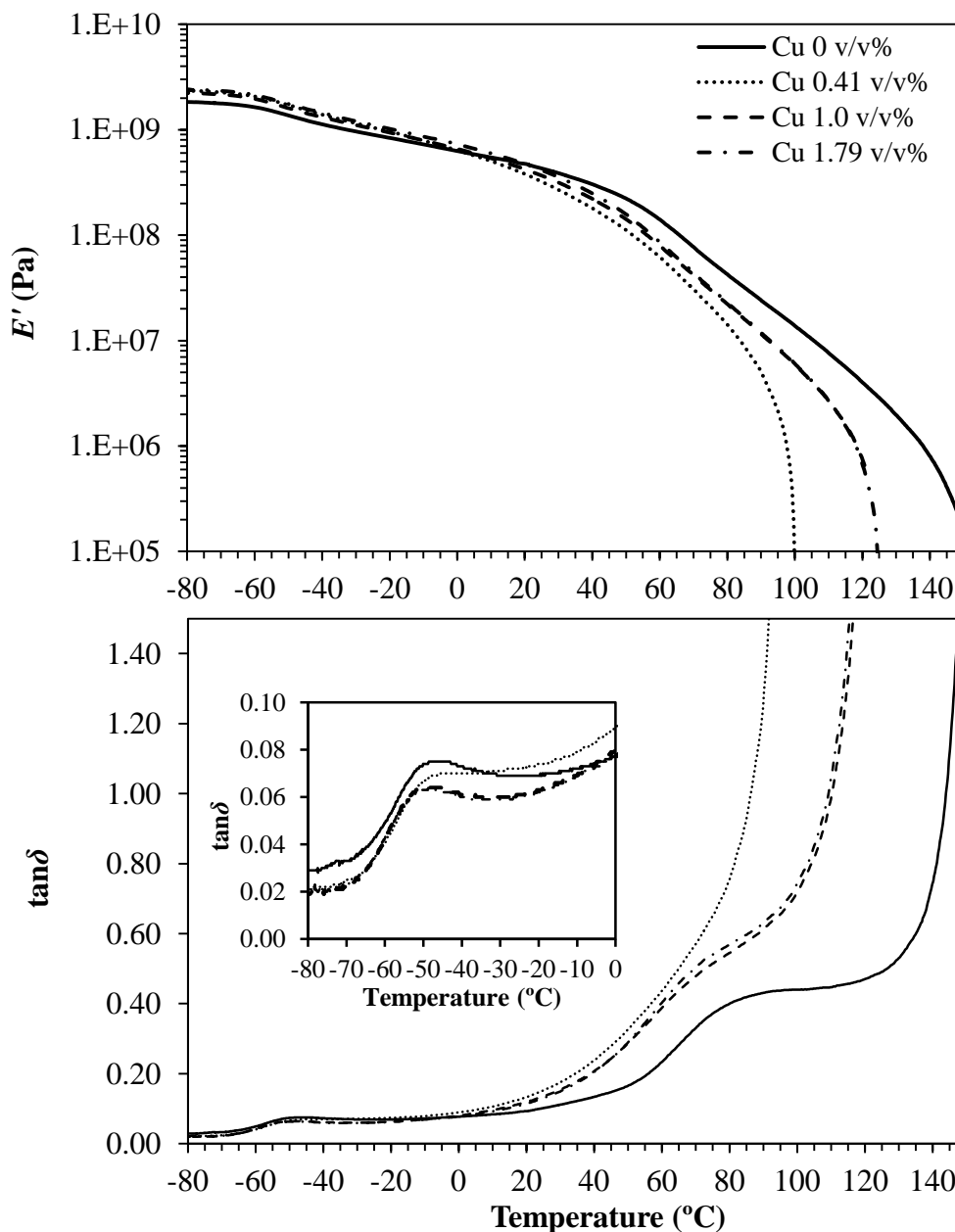


Figure 4.53 Storage modulus and mechanical loss factor from DMA of rigid PUR with different Cu contents

However, DSC and DMA results reveal that $T_{g,SS}$ did not clearly change for the rigid PUR matrix. $T_{g,SS}$ and $T_{g,HS}$ shows no significant change for both techniques.

4.5.5 Infrared spectroscopy

After loading Cu fillers with different contents into both flexible and rigid PUR matrices, the chemical structure of the composites was characterized and shown in appendix C. IR spectra of Cu and both flexible and rigid PUR matrices show a similar result as loading SiC fillers. The result has Cu particles and its content did not significantly affect the main PUR structure in PUR matrix. In case of both flexible and rigid PUR composites, all the intensities peaks of the chemical band's group increased with increasing Cu content. This result can be indicated that Cu particles and its content affect some chemical groups (amine group) of both flexible and rigid PUR structures.

4.5.6 Morphology

For Cu morphology, the electrolytic copper particles are shown in appendix C. SEM image revealed a dendritic shape of Cu particles and did not present agglomerated particles.

4.5.6.1 Particle size distribution and morphology of Cu particles

The particle size distribution of Cu particles was revealed in appendix C. The particle median and mean size are 24.877 and 28.084 μm , respectively. Particle size distribution curve reveal uni-model distribution of particles as similar to SiC and MgO powder. The dendritic shape of electrolytic Cu was presented. As discussed before, particle size and shape of Cu might be the reason of huge improvement of thermal conductivity in both flexible and rigid matrices. Dendritic shape of Cu can easily generate filler networks and it can increase the phonon propagation of the composites.

4.5.6.1 Morphology of flexible and rigid polyurethane elastomers with electrolytic Cu fillers

SEM image also shows the good mixing of Cu fillers with both flexible and rigid PUR matrices. Flexible PUR with Cu composites have clearly revealed the presence of two phases, as shown in Figure 4.54 (b) and (c). Electrolytic Cu particles can disperse in flexible PUR matrix. It can be seen that particles were buried inside PUR matrix. However, a small cavity around Cu particles were exhibited which because of the incompatibility between Cu and matrix and dendritic shape.

In case of rigid PUR composites, SEM image also shows dispersed particles in a rigid PUR matrix as revealed in Figure 4.55 (b) and (c). These morphologies can confirm the properties in both flexible and rigid PUR matrices. For instance, the thermal conductivity value was improved by increasing Cu content which is evenly dispersed in the flexible PUR matrix as describe from morphology. The other reasons might be due to

the dendritic shape of Cu particles and support the phonon propagation in the PUR matrix which improves the thermal conductivity of the composites. EDS result can confirm existing of Cu particle inside PUR matrix.

From previous results, SEM images revealed the agglomeration of fillers and tiny cavities found inside the PUR matrix, especially, adding MgO and ZnO fillers to rigid PUR matrix. Foam formation of rigid PUR as a result of adding MgO and ZnO fillers might be due to their small particle size the fillers can easily agglomerate with each other. Moreover, MgO and ZnO are sensitive to moisture which can be difficult to control during mixing and making the composites.

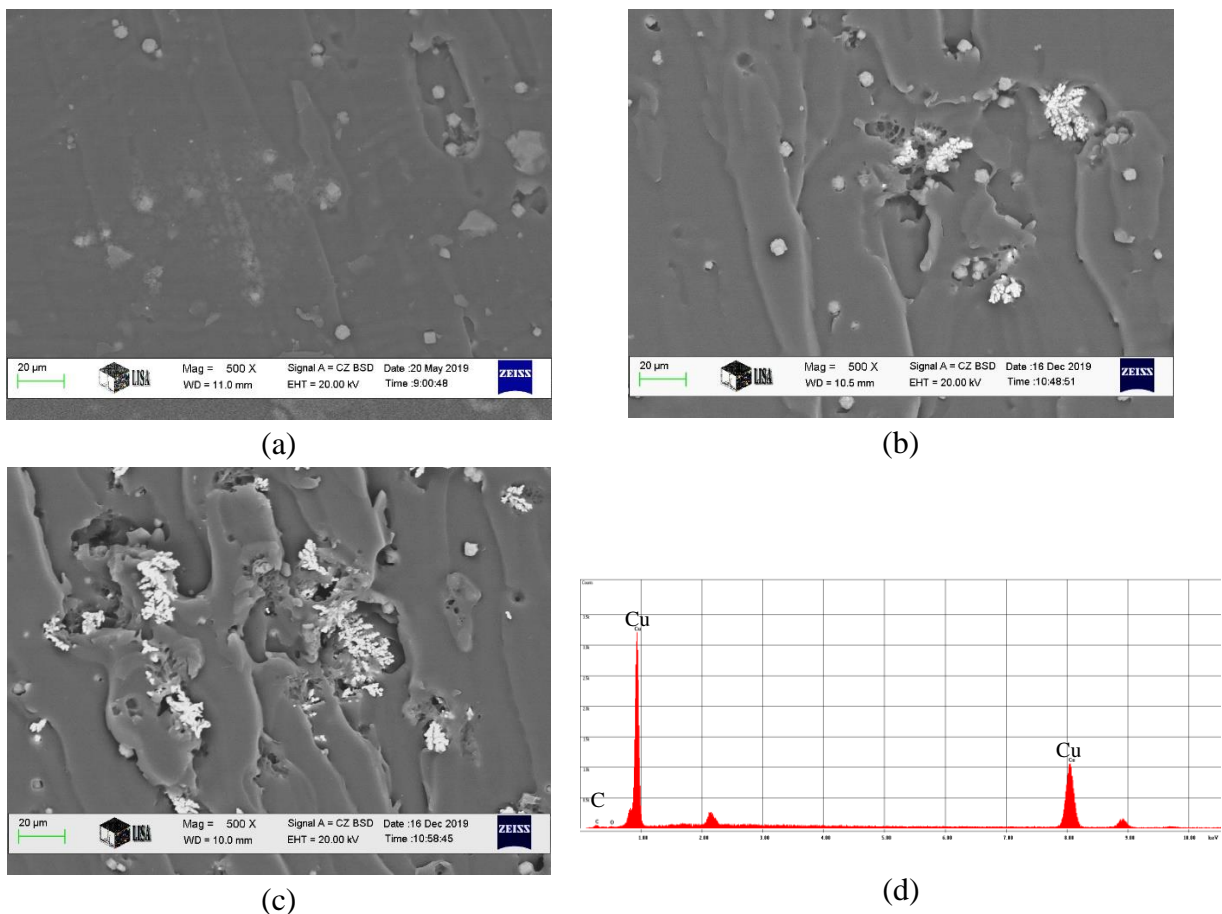
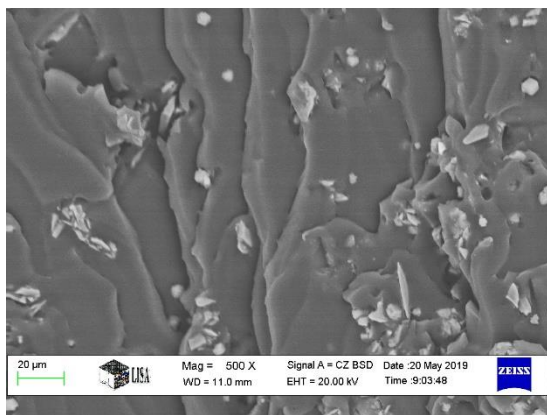
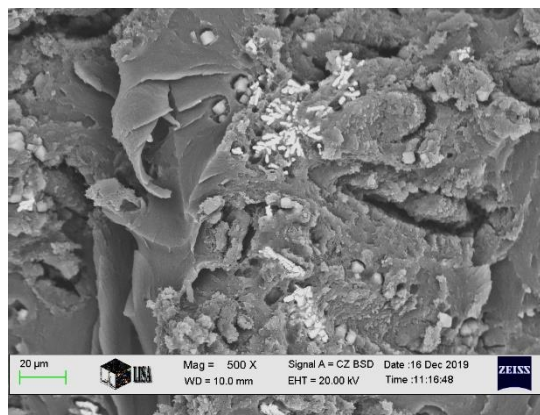


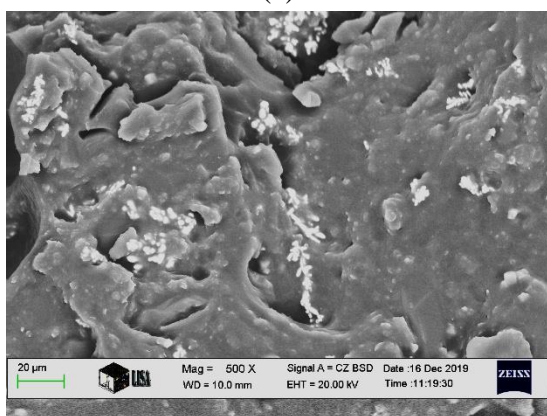
Figure 4.54 SEM image of flexible PUR with different Cu contents (a) Cu 0 v/v%, (b) Cu 0.39 v/v%, (c) Cu 1.71 v/v% (nominal magnification of 500×) and (d) EDS chart



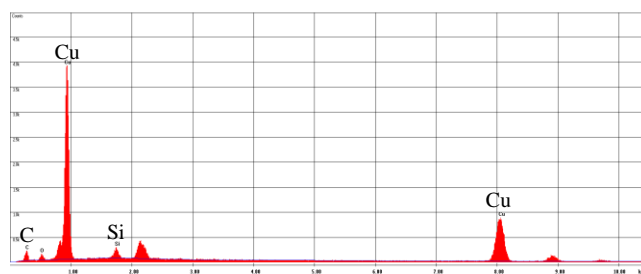
(a)



(b)



(c)



(d)

Figure 4.55 SEM image of rigid PUR with different Cu contents (a) Cu 0 v/v%, (b) Cu 0.41 v/v%, (c) Cu 1.79 v/v% (nominal magnification of 500 \times) and (d) EDS chart

4.6 Comparing properties of polyurethane elastomers with different types and contents of fillers

Properties of both flexible and rigid PUR with different filler types and contents were compared in this topic that consists of results based on measurement of thermal conductivity, density, Shore A and D hardness, tensile strength, modulus and elongation at break.

Thermal conductivity as a function of filler types and contents are presented in Figure 4.56. In case of flexible PUR matrix, loading SiC, MgO, ZnO, and Cu fillers can improve the thermal conductivity of all composites. The result indicates that increasing SiC content increases the thermal conductivity higher than MgO and ZnO fillers when same loadings were compared. In similar trend, raising Cu content also increased thermal conductivity of the composites. Moreover, the value of thermal conductivity changed more significantly by adding Cu fillers than the other fillers. This result is due to the inherent high thermal conductivity of the Cu and SiC fillers and because the uniform dispersion of these fillers inside the flexible PUR matrix. The other reasons may be that the dendritic shape of Cu can easy form filler networks. Filler bridges can be used by the phonons in order to cross the polymer matrix faster. In this case, a huge enhancement of thermal conductivity is shown. In case of rigid PUR matrix, results show that SiC and Cu fillers can enhance the thermal conductivity of the composites only. This result might be due to SiC and Cu particles have a good dispersion inside a rigid PUR matrix more than MgO and ZnO fillers. Furthermore, adding SiC and Cu did not create foam structure during forming while loading MgO and ZnO fillers lead to foam formation. Unfortunately, presence of moisture is not following strictly increase thermal conductive value.

In case of density, the trends found in the results are correlating with the thermal conductivity of both flexible and rigid PUR matrices. It is clearly seen that the increase of density value for the flexible PUR composite with the increase of Cu filler is higher than the other filler. This can be because of the effect of the density value of these fillers ($Cu > ZnO > MgO > SiC$). Furthermore, decreasing of density found for the rigid PUR composites can be correlated to decreasing thermal conductivity of the composites with adding MgO and ZnO fillers as exhibited in Figure 4.57. This can confirm influence of foam formation on thermal conductivity result.

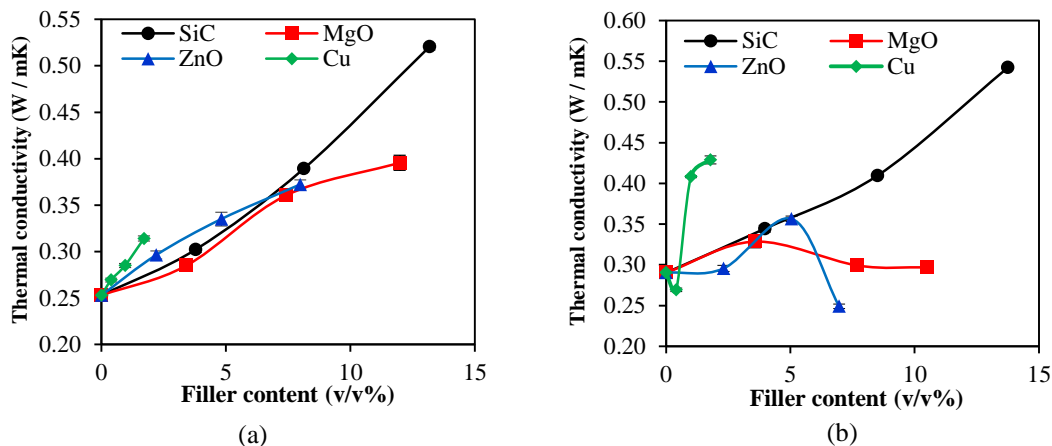


Figure 4.56 Comparing thermal conductivity of flexible PUR (a) and rigid PUR (b) with different the high thermal conductive fillers

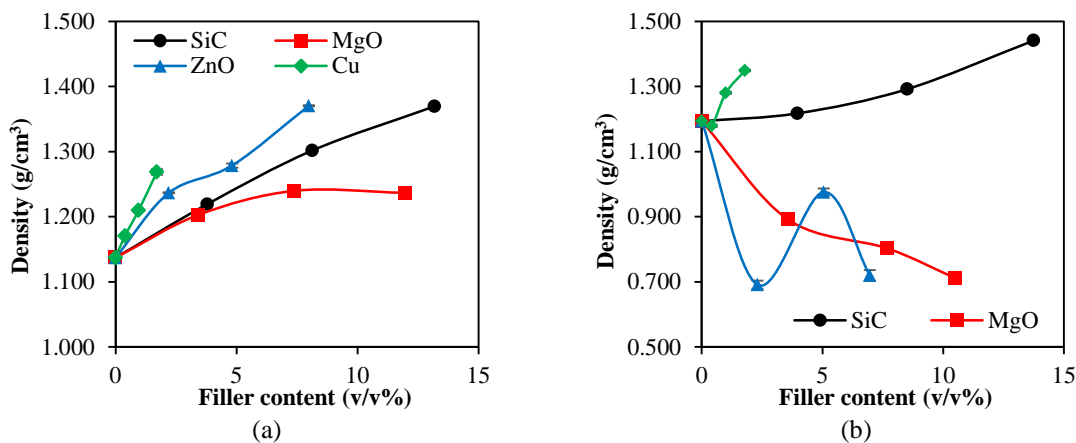


Figure 4.57 Comparing density of flexible PUR (a) and rigid PUR (b) with different the high thermal conductive fillers

Shore A and D hardness clearly shown that SiC, MgO, and Cu fillers are acting as active fillers in flexible PUR matrix by improving of Shore A and D hardness when these filler's content were increased, especially, adding Cu filler as presented in Figure 4.58 (a) and (b). This result is due to good dispersion of fillers in flexible PUR matrix even at high content of fillers. For rigid PUR matrix, Shore A and D hardness did not significant change when the content of fillers was increased as shown in Figure 4.58 (c) and (d). The cause for this result is that the high viscosity of rigid PUR matrix affects the dispersion of fillers and because of their incompatibility between these fillers and rigid PUR matrix. Moreover, foam formation provided a large scattering of hardness values due to adding MgO and ZnO rigid PUR matrix.

For tensile properties, Figure 4.59 shows increasing of tensile strength with rising SiC, MgO, and Cu content in flexible PUR matrix. This is due to evenly dispersion of these three fillers inside flexible PUR matrix and these fillers act as reinforcement fillers

in PUR matrix. The fillers might help the molecular chain of PUR against the deformation when the composites were forced. As a result of rigid PUR matrix, tensile strength did not significant changed with increasing filler content. This result occurs due to presence fillers agglomeration in the high viscosity matrix and the poor adhesion between the fillers and rigid PUR matrix which it can be confirmed by SEM image.

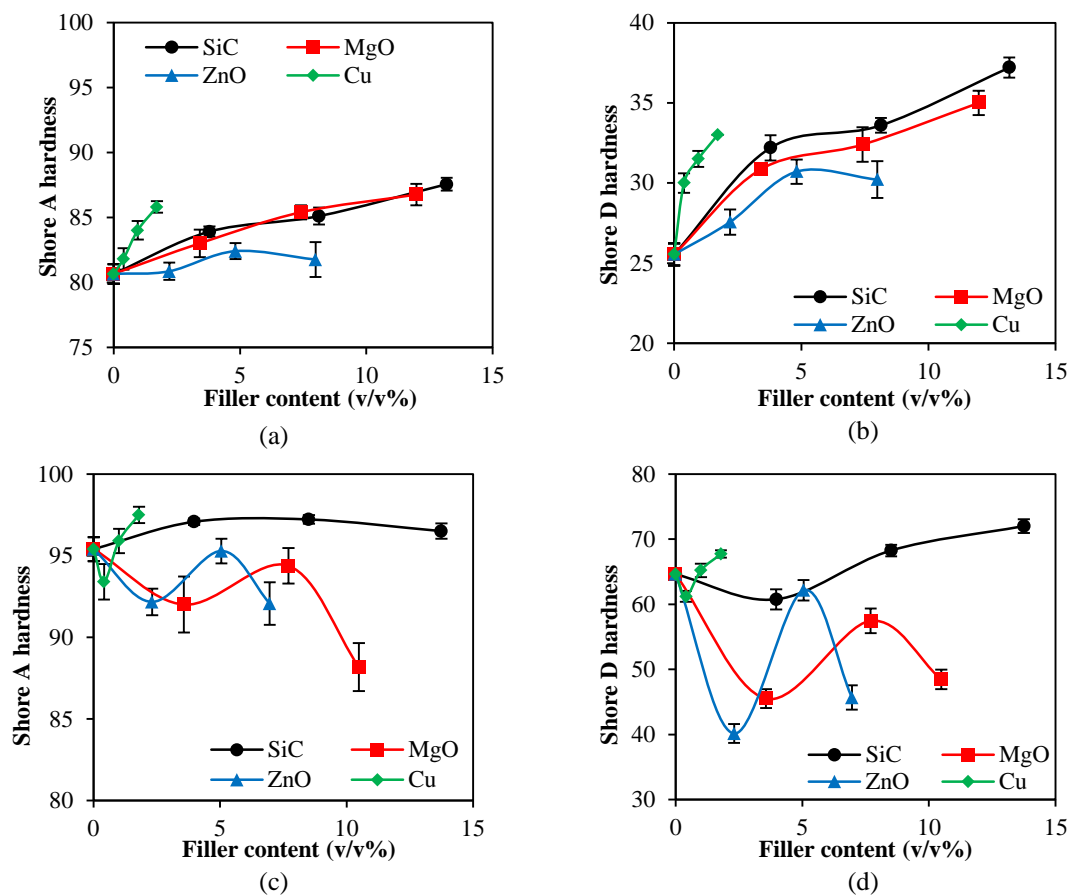


Figure 4.58 Comparing Shore A (a), Shore D hardness of flexible PUR and Shore A (c) and Shore D (d) of rigid PUR with different the high thermal conductive fillers

Tensile modulus was enhanced with increasing SiC, MgO and Cu contents as presented in Figure 4.60. It can be improved by 1.7 times (SiC and MgO) and 2.1 times (Cu) for flexible PUR composites. This increasing can be demonstrated that these fillers act as reinforcement fillers in flexible PUR matrix. This also can be assumed that filler can dissipate applied force to matrix. For rigid PUR matrix, tensile modulus did not significant change with increasing filler content except adding SiC filler. This result can confirm the effect of the dispersion of SiC particles and its content on the stiffness and elastic deformation of PUR composites.

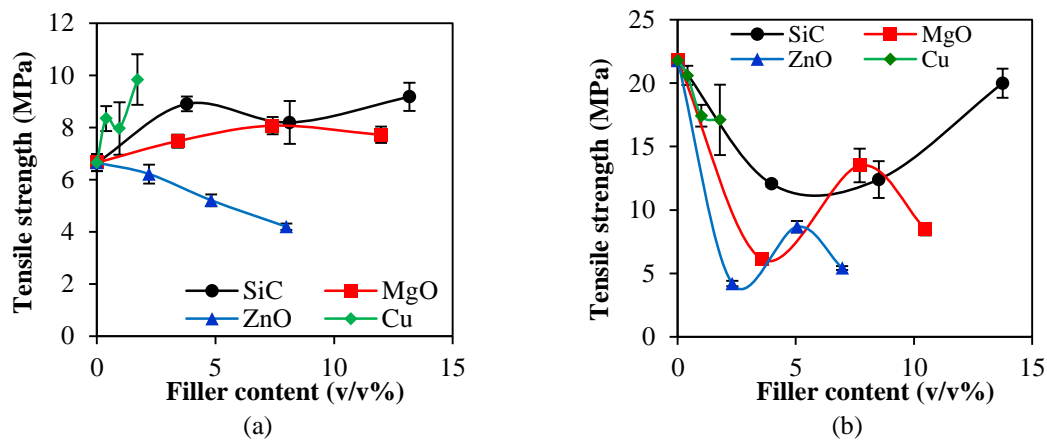


Figure 4.59 Comparing tensile strength of flexible PUR (a) and rigid PUR (b) with different the high thermal conductive fillers

As expected the elongation at break, results reveal that elongation of all composites was decreased with raising filler contents (Figure 4.61). Main reason is PUR composites indicate hindrance by these fillers to molecular mobility of PUR chain or deformability of composites which causes the matrix to lose its elastic deformation ability.

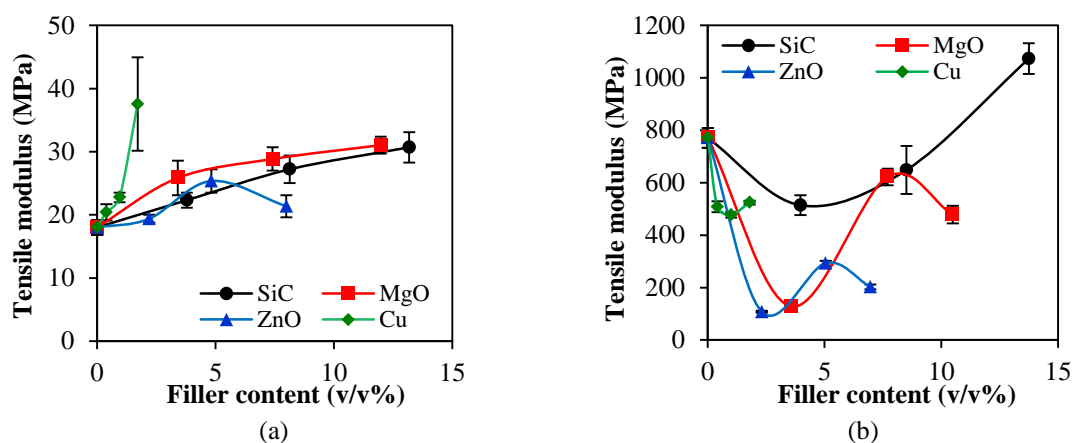


Figure 4.60 Comparing tensile modulus of flexible PUR (a) and rigid PUR (b) with different the high thermal conductive fillers

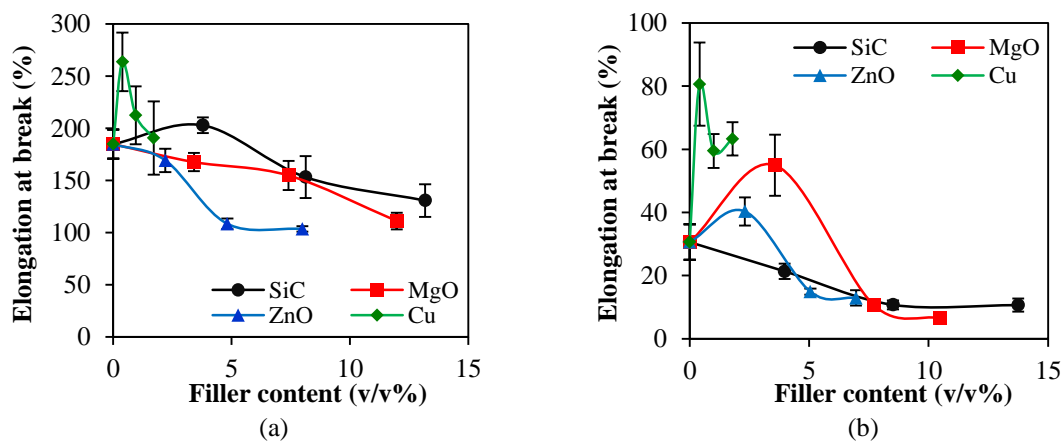


Figure 4.61 Comparing elongation at break of flexible PUR (a) and rigid PUR (b) with different the high thermal conductive fillers

CHAPTER 5

Conclusions

5.1 Effect of chain extender content on polyurethane elastomers matrix

Increasing the chain extender content in polyurethane elastomers (PUR) formula from 7 to 34 phr can enhance the thermal conductivity by 1.3 times. The density, Shore A and D hardness, tensile strength and tensile modulus were also improved when the chain extender content was increased. Increasing the chain extender content has provided high reactivity with MDI and polyol that leads to high physical cross-linking within the structure and the formation of phase-separated hard segment. Adjusting the chain extender content has no influence on $T_{g,SS}$ and T_{endo} of PUR while $T_{g,HS}$ slightly decreased. E' was improved with increasing the chain extender content, especially in the rubbery region. $T_{g,SS}$ slightly decreases which did not significantly change while $T_{g,HS}$ increases with increasing the chain extender content by DMA technique. This increase is due to increase in the number of higher length hard segment chains in the hard segment domains that occur as the hard segment content of the polymer increased and attributed to increasing hard segment crystallinity and phase separation. The intensity peak of all chemical band groups from IR spectra decrease with raising chain extender content which means the chemical structure of PUR shows more aggregated hard segments to form domains in the PUR block copolymer. Thermally stimulated discharge spectroscopic and swelling degree results can confirm affect increasing of the chain extender content in PUR structure.

5.2 Flexible and rigid polyurethane elastomer with silicon carbide composites

Adding silicon carbide (SiC) fillers from 0 to 14 v/v% into flexible and rigid PUR composites can improve the thermal conductivity of both flexible and rigid PUR composites when compared to pure PUR by 2 and 1.9 times, respectively. Applied mechanical model provided good prediction on thermal conductivity both PUR matrices. Besides, increasing Shore A and D hardness, tensile strength, modulus, and E' of the composites can indicate that good dispersion of SiC and it is acting as active and reinforcement fillers in both matrices. SiC did not influence on polyol segment motion in PUR matrix. At high amount of SiC obstructed the molecular chain movement in the physical cross-linking structure. The crystalline phase was increased with increasing SiC

content and improved the hard segment phase separation in flexible PUR. E' was increased with adding SiC in flexible PUR because of effect of reinforcement fillers. Decreasing amplitude of $\tan\delta$ peak implied that SiC content and its dispersion influence the degree of polyol segment motion. The shift to low temperature of $T_{g,HS}$ indicated the decreasing level of cross-linking in both PUR matrices. Loading SiC particles did not significantly affect thermal properties but it affects the hard segment cross-linking. IR spectra show that SiC content has no significant effect in the main PUR structure while increasing SiC content might be affect degradation both PUR matrices. Furthermore, SiC particles show evenly dispersed and embedded into both flexible and rigid PUR matrices.

5.3 Flexible and rigid polyurethane elastomer with magnesium oxide composites

Thermal conductivity can improve only by adding magnesium oxide (MgO) fillers in flexible PUR matrix by 1.6 times. Uniform dispersion of MgO fillers might be acting as network fillers that the phonon can easily cross the PUR matrix. Moreover, applied model reveal fairly good fitting to thermal conductivity. MgO is acting as active fillers in flexible PUR matrix. Loading MgO created some foaming within the rigid PUR matrix which decreasing thermal conductivity and mechanical properties. MgO particles did not influence the polyol segment motion. Small degrees of ordering in hard segment in both PUR matrices were exhibited with adding MgO fillers. Furthermore, loading MgO did not significantly change $T_{g,SS}$, $T_{g,HS}$, and T_{endo} in both PUR matrices. Adding MgO filler can obstruct the physical cross-linking level in PUR matrix by the shifting of $T_{g,HS}$ to lower temperature from DMA curve. IR spectra show that MgO content affects the increase in the intensity peak of IR spectra that might increase the rate of degradation in PUR matrix. MgO particles can disperse and embedded inside flexible and rigid PUR matrices. However, the agglomeration of MgO particles and cavities clearly seen in rigid PUR matrix with addition of 3.57 v/v% MgO content.

5.4 Flexible and rigid polyurethane elastomer with zinc oxide composites

Thermal conductivity is also improved with loading zinc oxide (ZnO) fillers from 0 to 7.99 v/v% into flexible matrix, by 1.5 times. Adding ZnO in flexible PUR matrix exhibited a little better fitting to applied model than SiC and MgO. Smaller particle size of ZnO can create more network fillers that result in faster phonon transportation. Foam structure of rigid composites decreases thermal conductive value. On the other hand, ZnO filler did not improve the mechanical properties of both PUR matrices. This result proved that ZnO fillers are inactive fillers and non-reinforcement. From DSC result,

loading ZnO fillers did not influence on thermal properties of both flexible and rigid PUR matrices. However, ZnO content affects the cross-linking of hard segment. $T_{g,SS}$ from DMA result has no significant change with adding ZnO fillers into both PUR matrices while $T_{g,HS}$ is decreased with loading ZnO fillers in rigid matrix. IR spectra show similar effect to adding MgO fillers. SEM images reveal some agglomeration of ZnO particles and cavities in rigid PUR matrix.

5.5 Flexible and rigid polyurethane elastomer with copper composites

Electrolytic copper (Cu) was incorporated into both flexible and rigid PUR matrices from 0 to 2 v/v%. Results show that the thermal conductivity of flexible PUR and rigid PUR composites were enhanced by 1.2 and 1.5 times, respectively. Applied model reveals a very good predicted value for both PUR matrices by getting close the upper limit line. Good dispersion and dendritic shape of Cu can easily create filler networks that can accelerate the phonon transportation. Electrolytic Cu fillers are acting as an active and reinforcement filler in flexible PUR matrix. Loading Cu filler has no influence on the thermal properties of the composites as confirmed by DSC curves. E' of the composites improves with raising Cu content in flexible PUR matrix. $T_{g,SS}$ did not significantly change both PUR matrices while $T_{g,HS}$ tends to decrease in case of flexible composites. The $\tan\delta$ peak shows a shoulder on the transition for rigid PUR matrix. This may be due to the Cu filler's content, size and shape influences the cross-linking segment motion of the hard segment. As was expected, loading Cu has no significant influence on the main chemical structure of PUR. However, increasing Cu content may be causing degradation in both PUR matrices. SEM images show the dendritic shape of Cu particles and it can be dispersed inside both flexible and rigid PUR matrices. Dendritic shape like of electrolytic Cu can be a clue that it has improved the thermal conductivity of the composites more than the other fillers.

5.6 Comparing properties of polyurethane elastomers with different types and contents of fillers

In case of the flexible PUR matrix, adding SiC, MgO, ZnO, and Cu fillers can improve the thermal conductivity of the composites. Increasing SiC content increases the thermal conductivity more than MgO and ZnO. However, adding Cu fillers has resulted in the largest increase in the value of thermal conductivity. This is most probably due to the uniformly dispersion of fillers, filler content, size and shape affect the phonon transportation. In case of rigid PUR matrix, loading SiC and Cu fillers can enhance the

thermal conductivity of the composites. Density results show a same trend to thermal conductivity both flexible and rigid PUR matrices. Shore A and D hardness results exhibited that SiC, MgO, and Cu fillers are acting as active filler in flexible PUR matrix. For rigid PUR matrix, Shore A and D hardness did not significant change when the content of fillers was increased. High viscosity of rigid PUR matrix affects the dispersion of fillers which influence the hardness value. Tensile strength and modulus with rising SiC, MgO, and Cu content in flexible PUR matrix were improved. As expected from the other results, adding Cu provided the highest improvement. This can confirm that these fillers act as reinforcement fillers in PUR matrix. Tensile strength and modulus did not significant changed with increasing filler content in rigid PUR matrix. This result is due to filler agglomeration and the poor adhesion between the fillers and rigid PUR matrix. Moreover, foam formation provided a large scattering of mechanical properties value with loading MgO and ZnO in the rigid PUR matrix.

NEW SCIENTIFIC RESULTS

Thesis 1. It has been revealed that increasing the chain extender content in the range of 7 to 34 phr can provide higher thermal conductivity and improve the mechanical properties of polyurethane elastomers. Adjusting the chain extender content can enhance thermal conductivity, Shore A and Shore D hardness, tensile strength, and tensile modulus of polyurethane elastomers by 1.3, 1.5, 3.4, 5.5, and 79.1 times, respectively.

Thesis 2. I showed that the thermal conductivity of flexible polyurethane elastomers can be enhanced by preparing a new composition of the chain extender content at 10 phr and different filler types and content. I have examined this new composition and provided a quantitative description of the changing of the thermal conductivity as a function of the applied filler and its content. The thermal conductivity of the composites resulted in different improvements such as 2.1 times by loading 13.18 v/v% silicon carbide, 1.6 times by loading 11.98 v/v% magnesium oxide, 1.5 times by loading 7.99 v/v% zinc oxide, and 1.2 times by loading 1.71 v/v% copper.

Thesis 3. I demonstrate that new flexible polyurethane elastomer composites of the chain extender content at 10 phr and all of the tested high thermal conductive fillers by different composition that were not prepared before, but can improve the mechanical behavior, namely, increasing the Shore A and D hardness, tensile modulus, and storage modulus. I have also shown that the highest improvement of Shore A and D hardness are 1.1 and 1.5 times by loading 13.18 v/v% silicon carbide and the tensile modulus is 2.1 times by loading 1.71 v/v% copper.

Thesis 4. I proved that the thermal conductivity of polyurethane elastomer composites can be described using the equation below. Where λ_u and λ_l are the upper and lower limiting value of the thermal conductivity. This model is similar to the model developed for mechanical properties of the composites described by Coran and Patel (1976) but never used before for thermal conductivity.

$$\lambda_c = \lambda_l + \phi_2^n (n\phi_1 + 1)(\lambda_u - \lambda_l)$$

LIST OF PUBLICATIONS

International Journal articles

1. Somdee P., Marossy K., Lassú-Kuknyó T. and Kónya C.: Polyurethane Elastomers with Improved Thermal Conductivity Part I: Elaborating Matrix Material for Thermal Conductive Composites. *International Journal of Mechanical and Production Engineering (IJMPE)*, 6(6), 1-5 (2018).
2. Somdee P., Lassú-Kuknyó T., Kónya C., Szabó T. and Marossy K.: Thermal analysis of polyurethane elastomers matrix with different chain extender contents for thermal conductive application. *Journal of Thermal Analysis and Calorimetry*, 138, 1003-1010 (2019). doi : <https://doi.org/10.1007/s10973-019-08183-y>
3. Somdee P., Lassú-Kuknyó T., Kónya C., Szabó T. and Marossy K.: Investigating the Properties and Structure of Polyurethane Elastomers with Monoethylene Glycol Chain Extender. *Materials Science Forum*, 986, 18-23 (2020). doi : <https://doi.org/10.4028/www.scientific.net/MSF.986.18>
4. Somdee P., Lassú-Kuknyó T., Kónya C., Ibrahim J.F.M. and Marossy K.: Investigation of the rubber elasticity and properties of polyurethane elastomers with different silicon carbide contents. *Journal of Physics: Conference Series*, 1527, 012038 (2020). doi : 10.1088/1742-6596/1527/1/012038

National Journal articles

1. Somdee P., Lassú-Kuknyó T., Kónya C., Szabó T. and Marossy K.: Influence of Chain Extender on Soft and Hard Segment of Polyurethane Elastomers. *Materials Science and Engineering: A Publication of the University of Miskolc*, 43(1), 98-107 (2018).

Conference Proceeding

1. Somdee P., Marossy K., Lassú-Kuknyó T. and Kónya C.: Polyurethane elastomers with improved thermal conductivity part I: Elaborating matrix material for thermal conductive composites. ISER international conference, Poland (2018).

Oral Presentations

1. Somdee P., Polyurethane Elastomer Composites of Increased Thermal Conductivity Part I: Magnesium Oxide, DOKTORANDUSZOK FÓRUMA, Miskoci Egyetem, Miskolc, Hungary, 15 November 2017.

2. Somdee P., Polyurethane elastomers with improved thermal conductivity part I: elaborating matrix material for thermal conductive composites, ISER international conference, Krakow, Poland, 15 April 2018.
3. Somdee P., Effect of Chain Extender on Hard Segment in Polyurethane Elastomers Structure. 5th International Conference on Competitive Materials and Technology Processes, Miskolc, Hungary, 11 October 2018.
4. Somdee P., Chemical structure and thermal properties of flexible polyurethanes with silicon carbide, 18 Österreichische Chemietage, Linz, Austria, 24-27 September 2019.
5. Somdee P., Investigation of the rubber elasticity and properties of polyurethane elastomers with different silicon carbide contents. 4th International Conference on Rheology and Modeling of Materials (ic-rmm4), Miskolc, Hungary, 9 October 2019.

Poster Presentation

1. Somdee P., Effect of Magnesium Oxide on Flexible and Rigid Polyurethanes, ANM2019 conference, Aveiro, Portugal, 17-19 July 2019.

REFERENCES

- [1] Osswald TA, Baur E, Brinkmann S, et al. International plastics handbook. The resource for plastics engineers. Cincinnati: Hanser Gardner Publications; 2006. p. 1–901.
- [2] Chakraborty BC and Ratna D. *Design of polymer systems for vibration damping. Polymer for vibration damping applications*. Netherlands, 2020, p. 143-201.
- [3] Chung DDL. Review materials for vibration damping. *J Mater Sci* 2001; 36: 5733-5737.
- [4] Santos WN. Modified split column technique for the experimental determination of thermal conductivity of polymers. *Polym Test* 2015; 41: 40-43.
- [5] dos Santos WN, de Sousa JA and Gregorio Jr R. Thermal conductivity behaviour Of polymers around glass transition and crystalline melting temperatures, *Polym Test* 2013; 32: 987-994.
- [6] Petrovic ZS and Ferguson J. Polyurethane elastomers, *Prog Polym Sci* 1991; 16: 695-836.
- [7] Anasari S and Muralidharan MN. *Electronic applications of polyurethane and its composites*. Ponnamma D, Sadasivuni KK, Wan C, et al. *Flexible and stretchable electronic composites*. Springer, Switzerland, 2016, p. 87-123.
- [8] Chen H, Ginzburg VV, Yang J, et al. Thermal conductivity of polymer-based composites: Fundamentals and applications, *Prog Polym Sci* 2016; 59: 41-85.
- [9] Zhao Y, Zhai Z and Drummer D. Thermal conductivity of aluminosilicate and aluminum oxide filled thermoset for injection molding: effect of filler content, filler size and filler geometry, *Polymers* 2018; 10: 457.
- [10] Sato K, Ijuin A and Hotta Y. Thermal conductivity enhancement of alumina/polyamide composites via interfacial modification, *Ceram Int* 2015; 41: 10314-10318.
- [11] Si W, He X, Huang Y et al. Polydimethylsiloxane/aluminum oxide composites prepared by spatial confining forced network assembly for heat conduction and dissipation, *RSC Adv* 2018; 8: 36007-36014.
- [12] Tommalieh MJ, Zihlif AM and Ragosta G. Electrical and thermal properties of polyimide/silica nanocomposite, *J Exp Nanosci* 2011; 6(6): 652-664.
- [13] Talib SFA, Azmi WH, Zakaria I, et al. Thermophysical properties of silicon dioxide (SiO₂) in ethylene glycol/water mixture for proton exchange membrane fuel cell cooling application, *Energy Procedia* 2015; 79: 366-371.

- [14] Khan H, Amin M, Ali M, et al. Effect of micro/nano-SiO₂ on mechanical, thermal, and electrical properties of silicon rubber, epoxy, and EPDM composites for outdoor electrical insulations, *Turk J Elec Eng & Comp Sci* 2017; 25: 1426-1435.
- [15] Turko BI, Kapustianyk VB, Rudyk VP, et al. Thermal conductivity of zinc oxide micro- and nanocomposites, *J Nano- Electron Phys* 2016; 8: 02004.
- [16] ERSOY S and TAŞDEMİR M. Zinc oxide (ZnO), magnesium hydroxide [Mg(OH)₂] and calcium carbonate (CaCO₃) filled HDPE polymer composites: Mechanical, thermal and morphological properties, *Fen Bilimleri Dergisi* 2012; 24: 93-104.
- [17] Ebadi-Dehaghani H, Reiszadeh M, Chavoshi A, et al. The effect of zinc oxide and calcium carbonate nanoparticles on the thermal conductivity of polypropylene, *J macromol sci Phys* 2014; 53: 93-107.
- [18] Guo L, Zhang Z, Kang R, et al. Enhanced thermal conductivity of epoxy composites Filled with tetrapod-shaped ZnO, *RSC Adv* 2018; 8: 12337-12343.
- [19] Mu Q, Feng S and Diao G. Thermal conductivity of silicone rubber filled with ZnO, *Polym Composite* 2007; 28(2): 125-130.
- [20] Celebi H, Bayram G and Dogan A. Influence of zinc oxide on thermoplastic elastomer-based composites: synthesis, processing, structural and thermal characterization, *Polym Composite* 2015; 37(8): 2369-2376.
- [21] Li L, Chen Y and Stachurski AH. Boron nitride nanotube reinforced polyurethane composites, *Prog Nat Sci-Mater* 2013; 23(2): 170-173.
- [22] Wang L, Han D, Luo J, et al. Highly efficient growth of boron nitride nanotubes and the thermal conductivity of their polymer composites, *J Phys Chem C* 2018; 122(3): 1867-1873.
- [23] Sharma S, Setia P, Chandra R, et al. Experimental and molecular dynamics study of boron nitride nanotube-reinforced polymethyl methacrylate composites, *J Compos Mater* 2019; 54(1): 3-11.
- [24] Yu C, Zhang J, Tian W, et al. Polymer composites based on hexagonal boron nitride and their application in thermally conductive composites, *RSC Adv* 2018; 8: 21948-21967.
- [25] Su Z, Wang H, He J, et al. Fabrication of thermal conductivity enhanced polymer composites by constructing an oriented three-dimensional staggered interconnected network of boron nitride platelets and carbon nanotube, *ACS Appl Mater Interfaces* 2018; 10(42): 36342-36351.
- [26] Jung J, Kim J, Uhm YR, et.al. Preparations and thermal properties of micro- and nano-BN dispersed HDPE composites, *Thermochim Acta* 2010; 499: 8-14.

- [27] Zhou W, Qi S, Li H, et. al. Study on insulating thermal conductive BN/HDPE composites, *Thermochim Acta* 2007; 452: 36-42.
- [28] Kemaloglu S, Ozkoc G and Aytac A. Thermally conductive boron nitride/SEBS/EVA ternary composites: “processing and characterization”, *Polym Compos.* Epub ahead of print 16 June 2020. DOI:<https://doi.org/10.1002/pc.20925>.
- [29] Cheewawuttipong W, Fuoka D, Tanoue S, et. al. Thermal and mechanical properties of polypropylene/boron nitride composites, *Energy Procedia* 2013; 34: 808-817.
- [30] Shen D, Zhan Z, Liu Z, et al. Enhanced thermal conductivity of epoxy composites filled with silicon carbide nanowires, *Science Reports* 2017; 7: 2606.
- [31] Huang Y, Hu J, Yao Y, et al. Manipulating orientation of silicon carbide nanowire in polymer composites to achieve high thermal conductivity, *Adv Mater Interfaces* 2017; 4(17): 1700446.
- [32] Zhou T, Wang X, Cheng P, et al. Improving the thermal conductivity of epoxy resin by the addition of a mixture of graphite nanoplatelets and silicon carbide microparticles, *Express Polym Lett* 2013; 7(7): 585-594.
- [33] Yao Y, Zhu X, Zeng X, et al. Vertically aligned and interconnected SiC nanowire networks leading to significantly enhanced thermal conductivity of polymer composites, *ACS Appl Mater Interfaces* 2018; 10(11): 9669-9678.
- [34] Panda A. *Effect of Shape, Size and Content on the Effective Thermal Conductivity of BeO Filled Polymer Composites*. B. Tech Project Report, National Institute of Technology Rourkela, India, 2013.
- [35] Alwaan IM, Hassan A and Piah MAM. Effect of zinc borate on mechanical and dielectric properties of metalocene linear low-density polyethylene/rubber/magnesium oxide composite for wire and cable applications, *Iran Polym J* 2015; 24: 279-288.
- [36] De Silva RT, Mantilaka MMMGPG, Ratnayake SP, et al. Nano-MgO reinforced chitosan nanocomposites for high performance packaging applications with improved mechanical, thermal and barrier properties, *Carbohydr Polym* 2017; 157: 739-747.
- [37] Pattanshetti VV, Shashidhara GM and Veena MG. Dielectric and thermal properties of magnesium oxide/poly(aryl ether ketone) nanocomposites, *Sci Eng Compos Mater* 2018; 25(5): 915-925.
- [38] Takahashi S, Imai Y, Kan A, et al. Preparation and characterization of isotactic polypropylene/MgO composites as dielectric materials with low dielectric loss, *J Ceram Soc JAPAN* 2013; 121(8): 606-610.

- [39] Wereszczak AA, Morrissey TG, Volante CN, et al. Thermally conductive MgO-filled epoxy molding compounds, *IEEE T Comp Pack Man* 2013; 3(12): 1994-2004.
- [40] Abbas ZA and Aleabi SH. Studying some of mechanical properties (tensile, impact, hardness) and thermal conductivity of polymer blend reinforce by magnesium oxide, *AIP Conference Proceedings*, 2019.
- [41] Yaman K and Taga O. Thermal and electrical conductivity of unsaturated polyester resin filled with copper filler composites, *Int J Polym Sci*. Epub ahead of print 29 April 2018. DOI: <https://doi.org/10.1155/2018/8190190>.
- [42] Tekce HS, Kumlutas D and Tavman IH. Effect of particle shape on thermal conductivity of copper reinforced polymer composites, *J Reinf Plast Compos* 2007; 26(1): 113-121.
- [43] Mamunya YP, Davydenko VV, Pissis P, et al. Electrical and thermal conductivity of polymers filled with metal powders, *Eur Polym J* 2002; 38: 1887-1897.
- [44] Saini A and Aseer JR. Experimental and theoretical thermal conductivity analysis of copper/aluminium reinforced epoxy polymer composites. *J Mat Sci Mech Eng* 2015; 2: 34-36.
- [45] Janković Z, Pavlović MM, Pantović MR, et al. Electrical and thermal properties of poly(methyl metacrylate) composites filled with electrolytic copper powder, *Int J Electrochem Sci* 2018; 13: 45-57.
- [46] Luyt AS, Molefi JA and Krump H. Thermal, mechanical and electrical properties of copper powder filled low-density and linear low-density polyethylene composites, *Polym Degrad Stab* 2006; 91: 1629-1636.
- [47] Tavman IH. Thermal and mechanical properties of copper powder filled poly(ethylene) composites. *Powder Technol* 1997; 91: 63-67.
- [48] Jouni M, Boudenne A, Boiteux G, et al. Electrical and thermal properties of polyethylene/silver nanoparticle composites, *Polym Compos* 2013; 34: 778.
- [49] Bjorneklett A, Halbo L and Kristiansen H. Thermal conductivity of epoxy adhesives filled with silver particles. *Int J Adhes Adhes* 1992; 12: 99-104.
- [50] Kubat J, Kužel R, Křivka I, et al. New conductive polymeric systems, *Synthetic metals* 1993; 54(1-3): 187-194.
- [51] Li F, Qi L, Yang J, et al. Polyurethane/conducting carbon black composites: structure, electric conductivity, strain recovery behavior, and their relationships. *J Appl Polym Sci* 2000; 75: 68-73.
- [52] Leng JS, Huang WM, Lan X, et al. Significantly reducing electrical resistivity by forming conductive Ni chains in a polyurethane shape-memory polymer/carbon black composite. *Appl Phys Lett* 2008; 92: 204101.

- [53] Gunes IS, Jimenez GA and Jana SC. Carbonaceous fillers for shape memory actuation of polyurethane composites by resistive heating. *Carbon* 2009; 47: 981–997.
- [54] Petit L, Guiffard B, Seveyrat L, et al. Actuating abilities of electroactive carbon nanopowder/polyurethane composite films. *Sens Actuator A-Phys* 2008;148: 105–110.
- [55] Furtado CA, de Souza PP, Goulart Silva G, et al. Electrochemical behavior of polyurethane ether electrolytes: carbon black composites and application to double layer capacitor. *Electrochim Acta* 2001; 46: 1629–1634.
- [56] Chen J, Zhang Z, Huang W, et al. Carbon nanotube network structure induced strain sensitivity and shape memory behavior changes of thermoplastic polyurethane. *Mater Des* 2015; 69: 105–113.
- [57] Liu Z, Bai G, Huang Y, et al. Reflection and absorption contributions to the electromagnetic interference shielding of single-walled carbon nanotube/polyurethane composites. *Carbon* 2007; 45: 821–827.
- [58] Cho JW, Kim JW, Jung YC, et al. Electroactive shape-memory polyurethane composites incorporating carbon nanotubes. *Macromol Rapid Commun* 2005; 26: 412–416
- [59] Luo H, Li Z, Yi G, et al. Multistimuli responsive carbon nanotube–shape memory polymeric composites. *Mater Lett* 2014;137: 385–388.
- [60] Luo H, Li Z, Yi G, et al. Temperature sensing of conductive shape memory polymer composites. *Mater Lett* 2015; 140: 71–74.
- [61] Putson C, Lebrun L, Guyomar D, et al. Effects of copper filler sizes on the dielectric properties and the energy harvesting capability of nonpercolated polyurethane composites. *J Appl Phys* 2011; 109: 024104.
- [62] Jung YC, Kim JH, Hayashi T, et al. Fabrication of transparent, tough, and conductive shape-memory polyurethane films by incorporating a small amount of high-quality graphene. *Macromol Rapid Commun* 2012; 33: 628–634.
- [63] Choi JT, Dao TD, Oh KM, et al. Shape memory polyurethane nanocomposites with functionalized graphene. *Smart Mater Struct* 2012; 21: 075017.
- [64] Park JH, Dao TD, Lee H, et al. Properties of graphene/shape memory thermoplastic polyurethane composites actuating by various methods. *Materials* 2014; 7: 1520–1538.
- [65] Ebadi-Dehaghani H and Nazempour M. Thermal conductivity of nanoparticles filled polymers. Shahreza Branch, Islamic Azad University, Iran.

- [66] Majumdar A. *Microscale transport phenomena*. Rohsenow WM, Hartnett JR and Cho YI. *Handbook of heat transfer*. New York, 1998, p. 8.1-8.9.
- [67] Agari Y and Ueda A. Thermal diffusivity and conductivity of PMMA/PC blends. *Polym* 1997; 4: 801-807.
- [68] Huang C, Qian X and Yang R. Thermal conductivity of polymers and polymer nanocomposites Epub ahead of print 1 June 2020.DOI: 10.1016/j.mser.2018.06.002.
- [69] Khan MO. Thermally Conductive Polymer Composites for Electronic Packaging Applications. The degree of Master of Applied Science, Mechanical and Industrial Engineering, University of Toronto, 2012.
- [70] Li A, Zhang C and Zhang YF. Thermal conductivity of graphene-polymer composites: mechanisms, properties, and applications, *Polymers* 2017; 9: 437.
- [71] Huang X and Zhi C. *Polymer nanocomposites: Electrical and thermal properties*. Switzerland, 2016, p. 285.
- [72] Kumlutas D and Tavman IH. A numerical and experimental study on thermal conductivity of particle filled polymer composites. *J Thermoplast Compos Mater* 2006; 19: 441-455.
- [73] Prisacariu C. *Polyurethane Elastomers: From Morphology to Mechanical Aspects*. New York: Springer, 2011.
- [74] Kim K, Kim M and Kim J. Enhancement of the thermal and mechanical properties of a surface-modified boron nitride polyurethane composite, *Polym Adv Technol* 2014; 25: 791-798.
- [75] Clemitson IR. *Castable polyurethane elastomers*. New York: CRC Press, 2015, p. 13-14.
- [76] Korodi T, Marcu N and Tirnaveanu A. Polyurethane microcellular elastomers: 2. Effect of chain extender on the mechanical properties. *Polymer* 1984; 25: 1211-1213.
- [77] Oprea S. The effect of chain extenders structure on properties of new polyurethane elastomers. *Polym Bull* 2010; 65: 753-766.
- [78] Auten KL and Petovic ZS. Synthesis, structure characterization, and properties of polyurethane elastomers containing various degree of unsaturation in the chain extenders. *J Polym Sci B Polymer Phys* 2002; 40: 1316-1333.
- [79] Barikani M and Barmar M. Thermoplastic polyurethane elastomers: synthesis, and study of effective structural parameters. *Iran Polym J* 1996; 5: 231-235.
- [80] Abderrazak H and Bel Hadj Hmida ES. Silicon carbide: synthesis and properties. Epub ahead of print 22 May 2020.DOI: 10.5772/15736.

- [81] Vlasov AS, Zakharov AI, Sarkisyan OA, et al. Obtaining silicon carbide from rice husks. *Refract Ind Ceram* 1991; 32: 521–523.
- [82] Wang Z and Zhi C. Chapter 11 Thermally conductive electrically insulation polymer nanocomposites. In: Springer International Publishing Switzerland *Polymer Nanocomposites*, pp. 281-321.
- [83] Izhevskiy VA, Genova LA, Bressiani JC, et.al. Review article: silicon carbide. Structure, properties and processing, *Cerâmica* 2000; 46(297).
- [84] Hachani SE, Meghezzi A, Nebbache N, et.al. Impact of magnesium oxide incorporation on tensile and hardness properties of polystyrene/magnesium oxide composites. *J Chem Pharm Sci* 2016; 9(4): 2664-2667.
- [85] Ropp RC. Group 16 (O, S, Se, Te) alkaline earth compounds, in *Encyclopedia of The Alkaline Earth Compounds*, 2013.
- [86] Shand MA. Physical and chemical properties of magnesium oxide. In: John Wiley and Sons. *The chemistry and technology of magnesia*, pp. 121-131.
- [87] Wang ZL. Zinc oxide nanostructures: growth, properties and applications, *J Phys: Condens Matter* 2004; R829-R858.
- [88] Parihar V, Raja M and Paulose R. A brief review of structural, electrical and electrochemical properties of zinc oxide nanoparticles, *Rev Adv Mater Sci* 2018; 53: 119-130.
- [89] Siddiqi KS, ur Rahman A, Tajuddin and Husen A. Properties of zinc oxide nanoparticles and their activity against microbes, *Nanoscale Res Lett* 2018; 13: 141.
- [90] Kołodziejczak-Radzimska A and Jesionowski T. Zinc oxide-from synthesis to application: a review, *Materials* 2014; 7: 2833-2881.
- [91] Tjong SC, Liang GD and Bao SP. Electrical properties of low density polyethylene/ZnO nanocomposites: the effect of thermal treatments, *J Appl Polym Sci* 2006; 102: 1436-1444.
- [92] Copper development association, John L. Everhart, *Copper and copper alloy powder metallurgy properties and applications*, New York, NY 10017
- [93] Copper development association, Madison Avenue, *The copper advantage: a guide to working with copper and copper alloys*, New York, NY 10016-2401
- [94] Guo Z, Kim TY, Pereira T, et al. Strengthening and thermal stabilization of polyurethane nanocomposites with silicon carbide nanoparticles by a surface-initiated-polymerization approach. *Compos Sci Technol* 2008; 68: 164–170.

- [95] Selvam R, Ravi S and Raja R. Fabrication of SiC particulate reinforced polyester matrix composite and investigation. *IOP Conf Series: Materials Science and Engineering* 2017; 197: 012052.
- [96] Ishimoto K, Kanegae E, Ohki Y, et.al. Superiority of dielectric properties of LDPE/MgO nanocomposites over microcomposites. *IEEE T Dielect El In* 2009; 16(6): 1735-1742.
- [97] Pandey GP, Agrawal RC and Hashmi SA. Magnesium ion-conducting gel polymer electrolytes dispersed with nanosized magnesium oxide. *J Power Sources* 2009; 190: 563-572.
- [98] Żyła G. Viscosity and thermal conductivity of MgO-EG nanofluids experimental results and theoretical models predictions. *J Therm Anal Calorim* 2017; 129: 171-180.
- [99] Koerner H, Kelley J, George J, et al. ZnO Nanorod-Thermoplastic polyurethane nanocomposites: Morphology and Shape Memory Performance. *Macromolecules* 2009; 42: 8933-8942.
- [100] ISO 527-1:2012(E). Plastics-Determination of tensile properties-Part 1: General principles.
- [101] Sienkiewicz A, Krasucka P, Charmas B, et.al. Swelling effects in cross-linked polymers by thermogravimetry. *J Therm Anal Calorim* 2017; 130: 85-93.
- [102] Wintle HJ, Pepin MP. Decay of surface charge between electrodes on insulator surfaces. *J of Electrostat* 2000; 48: 115-126.
- [103] Matsui K, Tanaka Y, Takada T, et.al. Space charge behavior in low density polyethylene at pre-breakdown. *IEEE Dielectr Electr Insul* 2005; 12: 406-415.
- [104] Lee KY, Lee KW, Choi YS et. al. Improved thermal, structure and electrical properties of epoxy for use at high voltages. *IEEE Dielectr Electr Insul* 2005; 12: 566-572.
- [105] Liszkowska J, Czuprynski B and Paciorek-Sadowska J. Thermal properties of polyurethane-polyisocyanurate (PUR-PIR) foams modified with tris(5-hydroxypentyl) citrate. *J Adv Chem Eng* 2016; 6: 1000148.
- [106] Zamzam MM. *A study on the thermal degradation resistance of thermoplastic Polyurethane coating*. Master Thesis, United Arab Emirates University, UAE, 2005.
- [107] Seymour RW and Cooper SL. Thermal analysis of polyurethane block polymers. *Macromolecules* 1973; 6(1): 48-52.
- [108] Liaw DJ. The relative physical and thermal properties of polyurethane elastomers: effect of chain extenders of bisphenols, diisocyanate, and polyol structures. *J Appl Polym Sci* 1997; 66(7): 1251-1265.

- [109] Oprea S. Effect of the diisocyanate and chain extenders on the properties of the cross-linked polyetherurethane elastomers. *J Mater Sci* 2008; 43: 5274-5281.
- [110] Auten KL and Petrovic ZS. Synthesis, structural characterization, and properties of polyurethane elastomers containing various degrees of unsaturation in the chain extenders. *J Polym Sci B Polym Phys* 2002; 40: 1316-1333.
- [111] Hsu JM, Yang DL and Huang SK. Characterization of the relaxation transitions in toluene diisocyanate-based polyurethanes with poly(propylene glycol) as the soft segment by thermally stimulated current depolarization with relaxation mapping analysis. *J Appl Polym Sci* 1999; 73(4): 527–545.
- [112] Marossy K. Practical approach to thermally stimulated discharge (TSD) method on polymers. *J Therm Anal Calorim* 2017; 129(1): 161–170.
- [113] Raj P, Lal S, Mahna SK, et.al. Dielectric relaxation investigations in NCO-terminated liquid crystalline polyurethane: thermally stimulated depolarization current technique. *Int J Polymer Anal Char* 2012; 17(3): 235-245.
- [114] Pardini FM and Amalvy JI. Synthesis and swelling behavior of pH-responsive polyurethane/poly[2-(diethylamino)ethyl methacrylate] hybrid Materials. *J Appl Polym Sci* 2013; 39799.
- [115] Barlkanl M and Hepburn C. Determination of crosslink density by swelling in the castable polyurethane elastomer based on 1/4- cyclohexane diisocyanate and para-phenylene diisocyanate. *Iranian Journal of Polymer Science & Technology* 1992; 1(1): 1-5.
- [116] Somani KP, Patel NK, Kansara SS, et. al. Effect of chain length of polyethylene glycol and crosslink density (NCO/OH) on properties of castor oil based polyurethane elastomers. *J Macromol Sci A* 2006; 43: 797-811.
- [117] Cheng SC and Vachon RI. The prediction of the thermal conductivity of two and three phase solid heterogeneous mixtures. *Int J Heat Mass Transfer* 1969; 12: 249-267.
- [118] Lewis TB and Nielsen LE. Dynamic mechanical properties of particulate-filled composites. *J Appl Polym Sci* 1970; 14: 1449-1471.
- [119] Coran AY and Patel R. Predicting elastic moduli of heterogeneous polymer compositions. *J Appl Polym Sci* 1976; 20: 3005-3016.
- [120] Tsekmes IA, Kochetov R, Morshuis PHF, et. al. Thermal conductivity of polymeric composites: a review. In: 2013 IEEE International Conference on Solid Dielectrics, Bologna, Italy, 30 June – 4 July, 2013. pp. 678-681.
- [121] Agarwal G, Patnaik A and Sharma RK. Thermo-mechanical properties of silicon carbide-filled chopped glass fiber-reinforced epoxy composites. *Int J Adv Struct Eng* 2013; 5:21.

- [122] Gu SY, Liu LL and Yan BB. Effects of ionic solvent-free carbon nanotube nanofluid on the properties of polyurethane thermoplastic elastomer. *J Polym Res* 2014; 21:356.
- [123] Ramdani N, Wang J and Liu WB. Preparation and thermal properties of polybenzoxazine/TiC hybrids. *Adv Mater Res* 2014; 887-888: 49-52.
- [124] Mariana C, Sorin I, Constantin NC, et.al. Dynamic mechanical analysis of polyurethane-epoxy interpenetrating polymer networks. *High Perform Polym* 2009; 21: 608-623.
- [125] Głowinska E and Datta J. Structure, morphology and mechanical behavior of novel bio-based polyurethane composites with microcrystalline cellulose. *Cellulose* 2015; 22: 2471-2481.
- [126] Pokharel P, Choi S and Lee DS. The effect of hard segment length on the thermal and mechanical properties of polyurethane/graphene oxide nanocomposites. *Compos Part A Appl Sci Manuf* 2015; 69: 168-177.
- [127] Kwiatkowski K and Nachman M. The abrasive wear resistance of the segmented linear polyurethane elastomers based on a variety of polyol as soft segments. *Polymers* 2017; 9(12): 705.
- [128] Liszkowska J, Moraczewski K, Borowicz M, et al. The Effect of accelerated aging conditions on the properties of rigid polyurethane-polyisocyanurate foams modified by cinnamon extract. *Appl Sci* 2019; 2663.

APPENDIX A

Flexible and rigid polyurethane elastomers with magnesium oxide composites

Table 4.12 Thermal conductivity and density of flexible and rigid polyurethane elastomers with different MgO contents

MgO content (v/v%)	Flexible PUR		MgO content (v/v%)	Rigid PUR	
	Thermal conductivity (W / mK)	Density (g/cm ³)		Thermal conductivity (W / mK)	Density (g/cm ³)
0.00	0.253±0.003	1.137±0.002	0.00	0.290±0.002	1.194±0.001
3.41	0.285±0.004	1.203±0.001	3.57	0.329±0.008	0.892±0.014
7.36	0.360±0.003	1.240±0.001	7.70	0.299±0.005	0.803±0.010
11.98	0.396±0.008	1.237±0.001	10.49	0.297±0.006	0.712±0.015

Table 4.13 Mechanical properties of flexible PUR with different MgO contents

MgO content (v/v%)	Shore A hardness	Shore D hardness	Tensile strength (MPa)	Elongation at break (%)	Tensile modulus (MPa)
0.00	81±0.7	26±0.7	7±0.3	185±14	18±1
3.41	83±1.1	31±0.2	7±0.3	168±9	26±3
7.36	85±0.5	32±1.1	8±0.3	155±14	29±2
11.98	87±0.8	35±0.8	8±0.3	111±8	31±1

Table 4.14 Mechanical properties of rigid PUR with different MgO contents

MgO content (v/v%)	Shore A hardness	Shore D hardness	Tensile strength (MPa)	Elongation at break (%)	Tensile modulus (MPa)
0.00	95±0.7	65±0.5	22±0.2	31±5.6	771±38
3.57	92±1.7	46±1.4	6±0.3	55±9.6	128±7
7.70	94±1.1	57±1.9	14±1.3	11±1.8	622±32
10.49	88±1.5	48±1.5	8±0.5	7±0.5	478±34

Table 4.15 Thermal properties of flexible and rigid polyurethane elastomers with different MgO contents

Flexible Polyurethane				Rigid Polyurethane			
MgO content (v/v%)	T _{g,SS} (°C)	T _{g,HS} (°C)	T _{endo} (°C)	MgO content (v/v%)	T _{g,SS} (°C)	T _{g,HS} (°C)	T _{endo} (°C)
0.00	-60	45	68	0.00	-60	44	67
3.41	-60	40	63	3.57	N/A	40	61
7.36	-59	40	61	7.70	N/A	41	59
11.98	-58	39	65	10.49	N/A	41	63

Table 4.16 The glass transition temperature of soft and hard segment of polyurethane elastomers with different MgO contents from DMA technique

MgO content (v/v%)	Flexible PUR		MgO content (v/v%)	Rigid PUR	
	T _{g,SS} (°C)	T _{g,HS} (°C)		T _{g,SS} (°C)	T _{g,HS} (°C)
0.00	-46	11	0.00	-48	83
3.41	-45	-2	3.57	-50	82
7.36	-44	1	7.70	-50	71
11.98	-46	1	10.49	-51	75

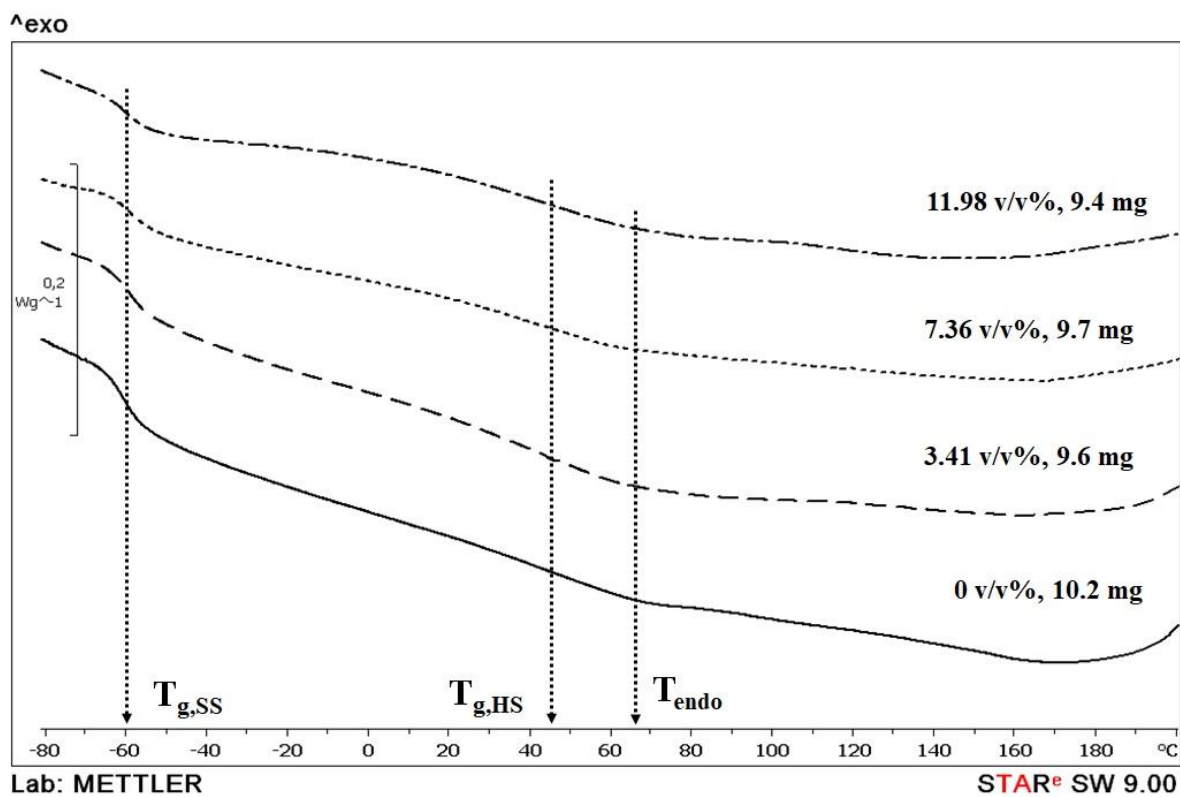


Figure 4.62 DSC curve of flexible polyurethane elastomers with different MgO contents

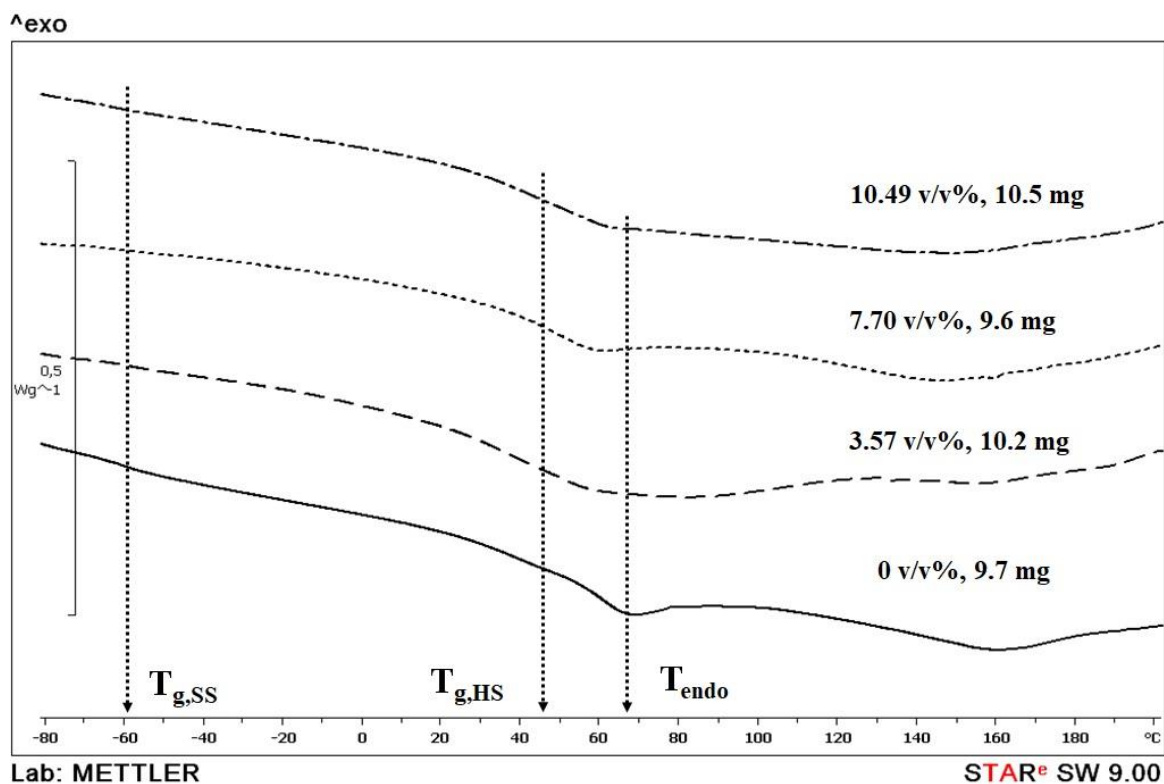


Figure 4.63 DSC curve of rigid polyurethane elastomers with different MgO contents

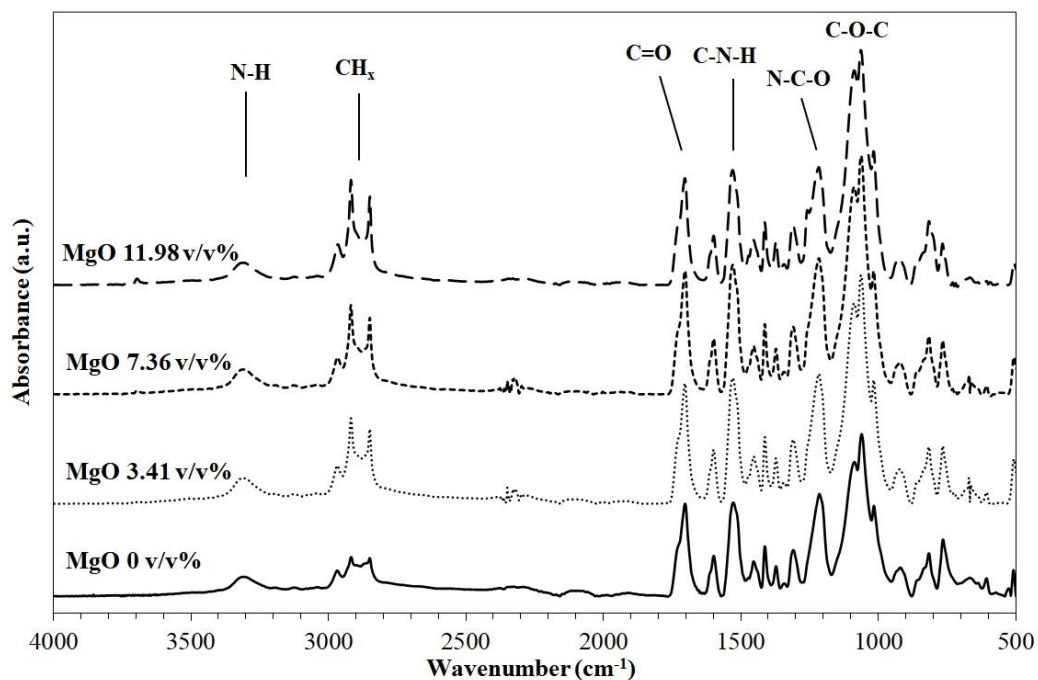


Figure 4.64 IR spectra of flexible polyurethane elastomers with different MgO contents

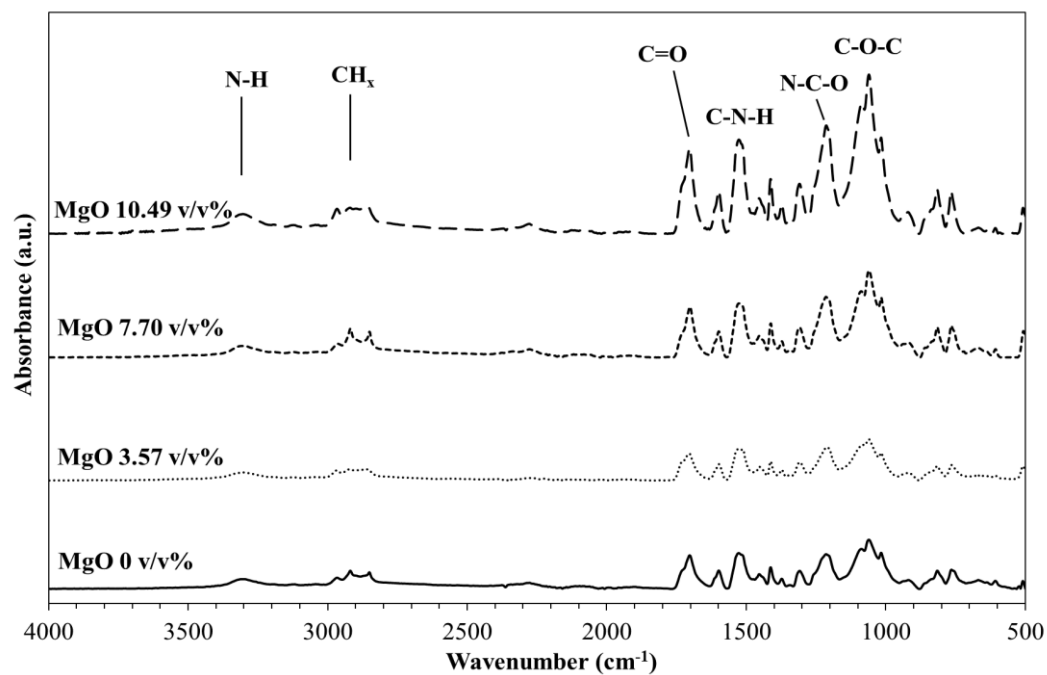


Figure 4.65 IR spectra of rigid polyurethane elastomers with different MgO contents

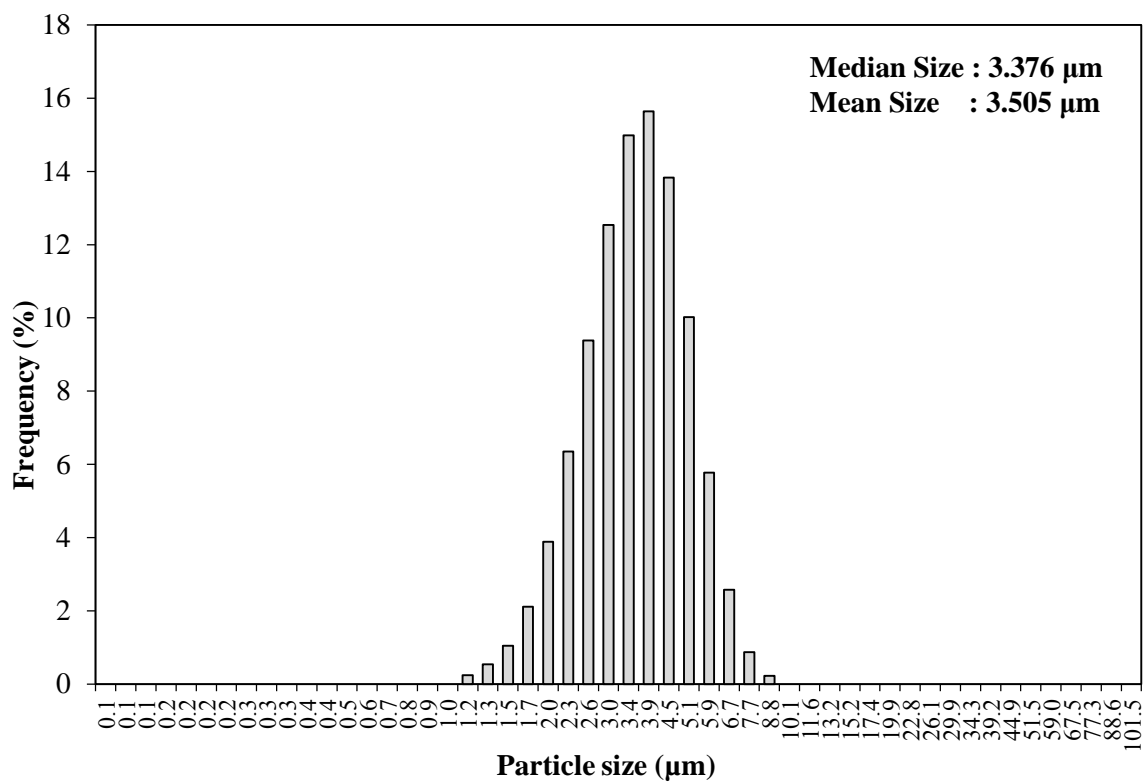


Figure 4.66 Particle size distributions of MgO particles

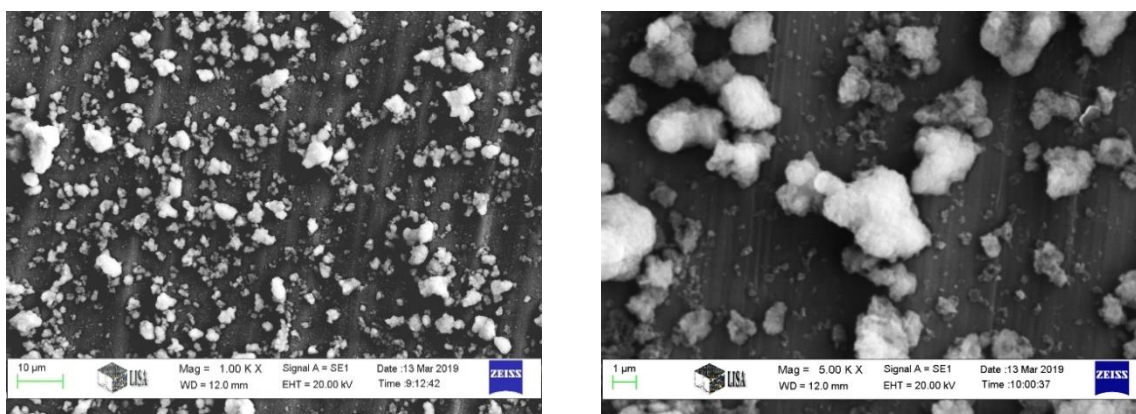


Figure 4.67 SEM image of MgO particles (nominal magnification of 1000× and 5000×)

APPENDIX B

Flexible and rigid polyurethane elastomers with zinc oxide composites

Table 4.17 Thermal conductivity and density of flexible and rigid polyurethane elastomers with different ZnO contents

ZnO content (v/v%)	Flexible PUR		ZnO content (v/v%)	Rigid PUR	
	Thermal conductivity (W / mK)	Density (g/cm ³)		Thermal conductivity (W / mK)	Density (g/cm ³)
0.00	0.253±0.003	1.137±0.002	0.00	0.290±0.002	1.194±0.001
2.20	0.296±0.004	1.237±0.001	2.31	0.296±0.004	0.691±0.013
4.82	0.335±0.007	1.279±0.003	5.05	0.357±0.003	0.976±0.011
7.99	0.372±0.005	1.370±0.001	6.96	0.249±0.003	0.720±0.016

Table 4.18 Mechanical properties of flexible PUR with different ZnO contents

ZnO content (v/v%)	Shore A hardness	Shore D hardness	Tensile strength (MPa)	Elongation at break (%)	Tensile modulus (MPa)
0.00	81±0.7	26±0.7	7±0.3	185±14	18±1.1
2.20	81±0.7	28±0.8	6±0.4	169±11	19±0.6
4.82	82±0.6	31±0.8	5±0.2	109±5	25±1.9
7.99	82±1.3	30±1.1	4±0.1	104±3	21±1.8

Table 4.19 Mechanical properties of rigid PUR with different ZnO contents

ZnO content (v/v%)	Shore A hardness	Shore D hardness	Tensile strength (MPa)	Elongation at break (%)	Tensile modulus (MPa)
0.00	95±0.7	65±0.5	22±0.2	31±6	771±38
2.31	92±0.8	40±1.5	4±0.2	40±4	108±3
5.05	95±0.8	62±1.6	9±0.5	15±1	293±9
6.96	92±1.3	46±1.9	5±0.2	13±2	203±9

Table 4.20 Thermal properties of flexible and rigid polyurethane elastomers with different ZnO contents

Flexible Polyurethane				Rigid Polyurethane			
ZnO content (v/v%)	T _{g,SS} (°C)	T _{g,HS} (°C)	T _{endo} (°C)	ZnO content (v/v%)	T _{g,SS} (°C)	T _{g,HS} (°C)	T _{endo} (°C)
0.00	-60	45	68	0.00	-60	44	67
2.20	-60	44	72	2.31	N/A	45	62
4.82	-61	43	67	5.05	N/A	45	59
7.99	-60	45	63	6.96	N/A	44	58

Table 4.21 The glass transition temperature of soft and hard segment of polyurethane elastomers with different ZnO contents from DMA technique

ZnO content (v/v%)	Flexible PUR		ZnO content (v/v%)	Rigid PUR	
	T _{g,SS} (°C)	T _{g,HS} (°C)		T _{g,SS} (°C)	T _{g,HS} (°C)
0.00	-46	11	0.00	-48	83
2.20	-45	-5	2.31	-52	87
4.82	-47	1	5.05	-52	78
7.99	-49	14	6.96	-52	77

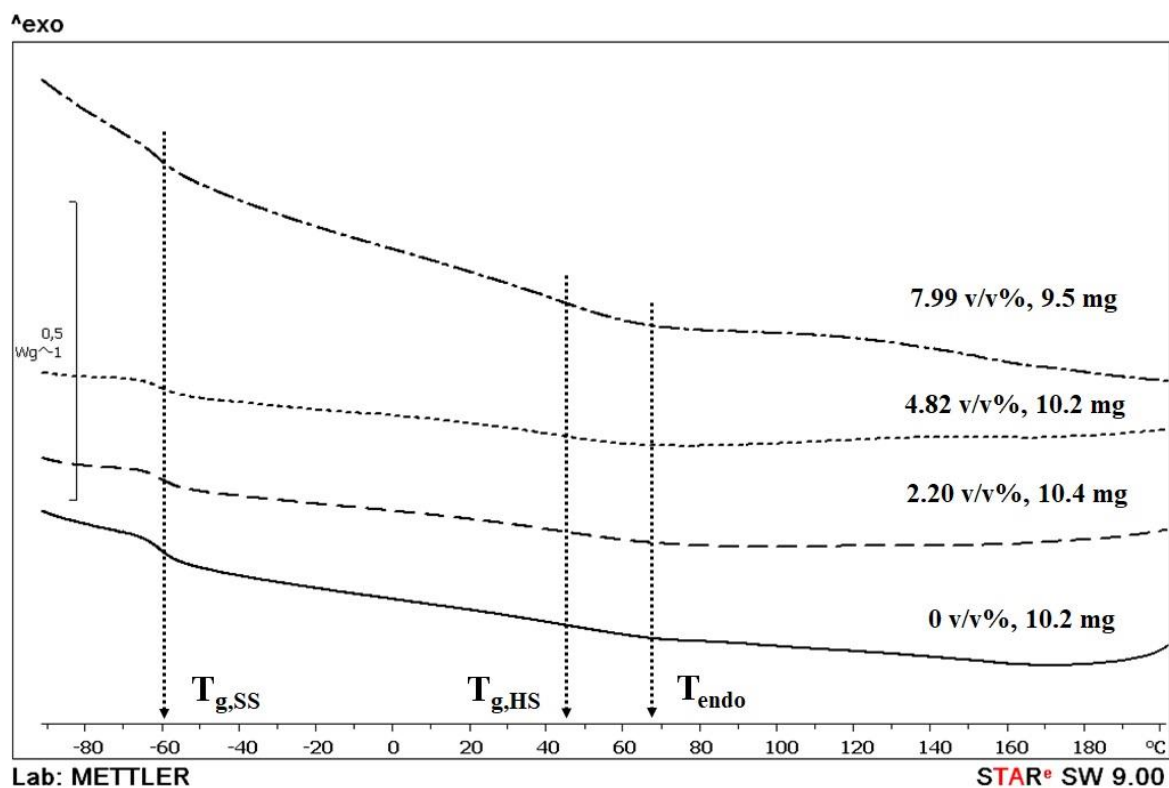


Figure 4.68 DSC curve of flexible polyurethane elastomers with different ZnO contents

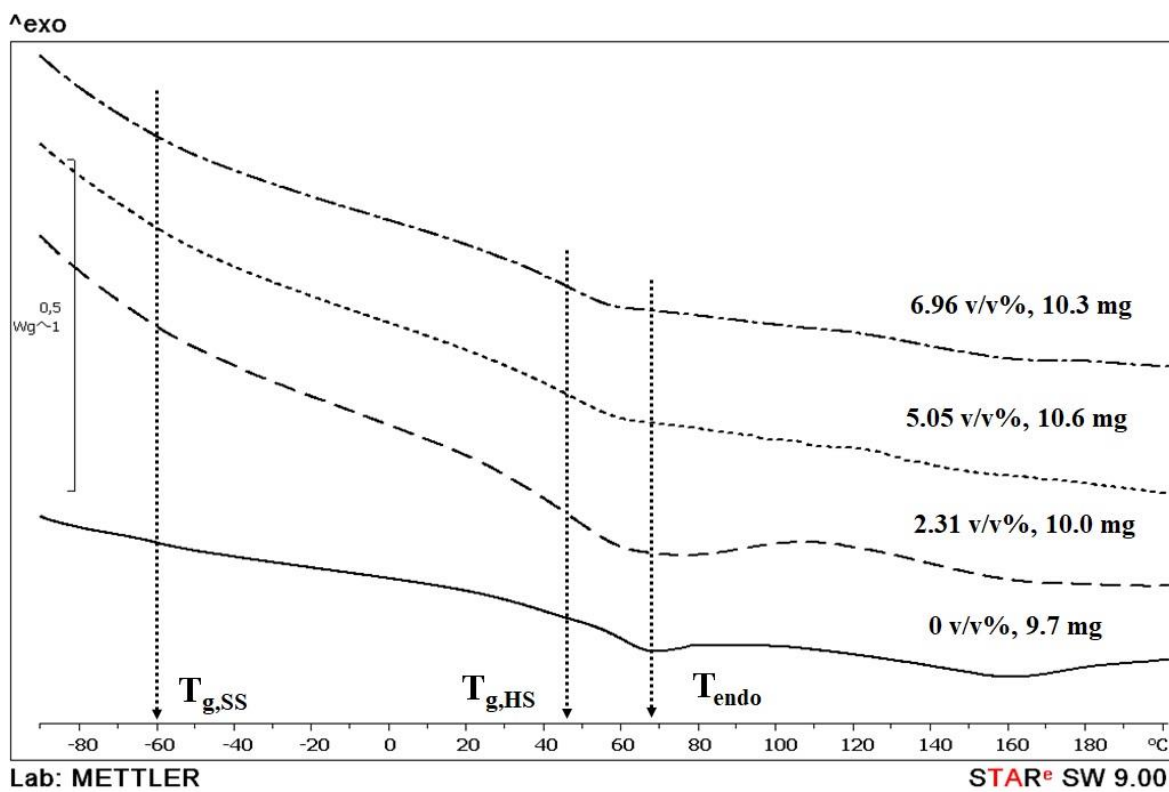


Figure 4.69 DSC curve of rigid polyurethane elastomers with different ZnO contents

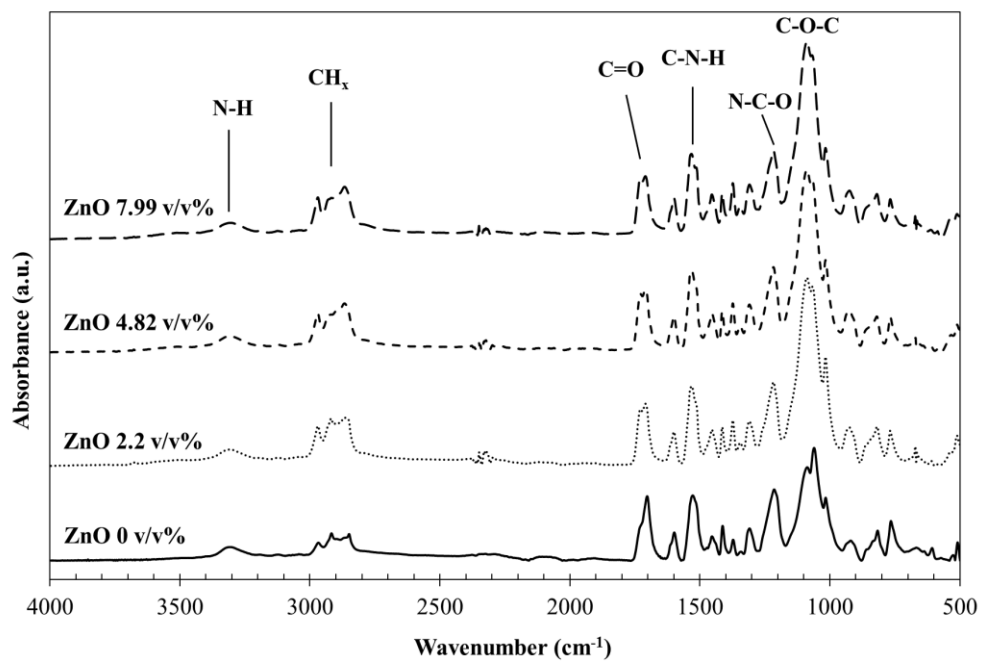


Figure 4.70 IR spectra of flexible polyurethane elastomers with different ZnO contents

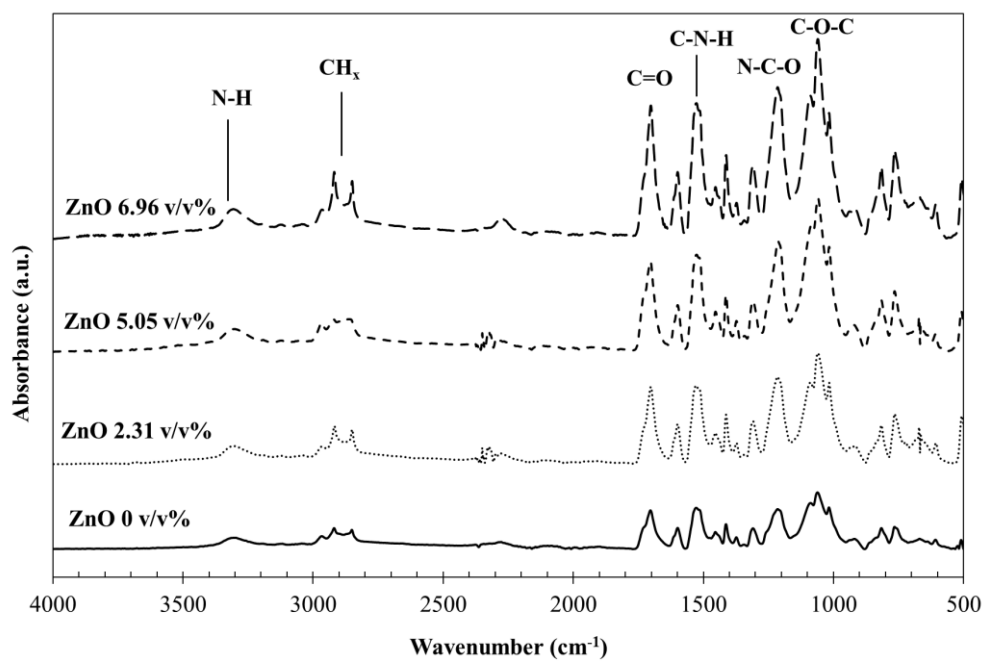


Figure 4.71 IR spectra of rigid polyurethane elastomers with different ZnO contents

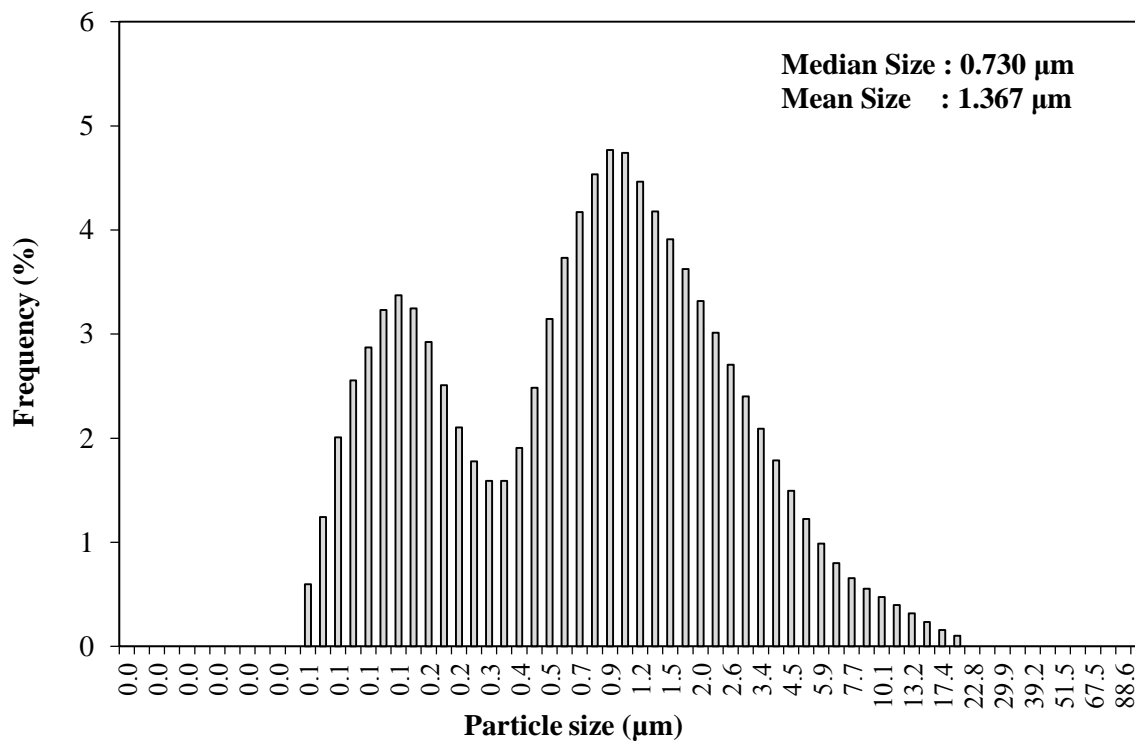


Figure 4.72 Particle size distribution of zinc oxide particles

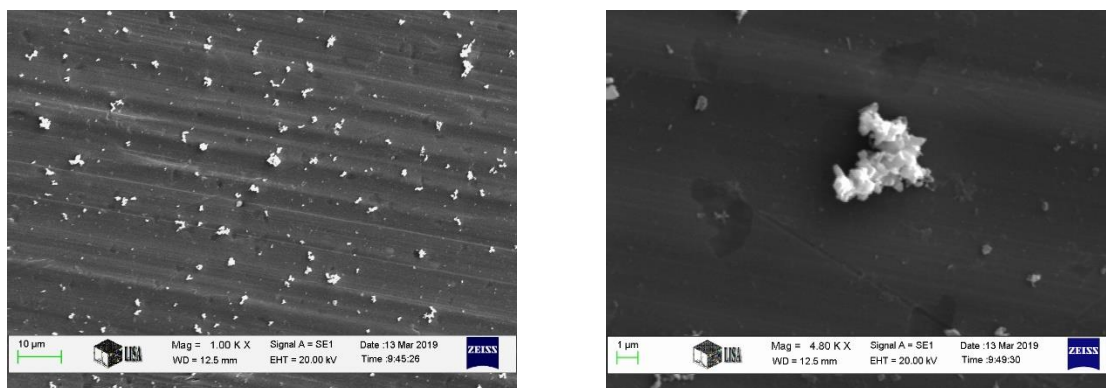


Figure 4.73 SEM image of zinc oxide particles
(nominal magnification of 1000 \times and 4800 \times)

APPENDIX C

Flexible and rigid polyurethane elastomers with copper composites

Table 4.22 Thermal conductivity and density of flexible and rigid polyurethane elastomers with different Cu contents

Cu content (v/v%)	Flexible PUR		Cu content (v/v%)	Rigid PUR	
	Thermal conductivity (W / mK)	Density (g/cm ³)		Thermal conductivity (W / mK)	Density (g/cm ³)
0.00	0.253±0.003	1.137±0.002	0.00	0.290±0.002	1.194±0.001
0.39	0.260±0.006	1.171±0.001	0.41	0.269±0.002	1.179±0.004
0.95	0.285±0.002	1.210±0.000	1.00	0.408±0.001	1.281±0.003
1.71	0.314±0.003	1.269±0.004	1.79	0.429±0.005	1.349±0.002

Table 4.23 Mechanical properties of flexible PUR with different Cu contents

Cu content (v/v%)	Shore A hardness	Shore D hardness	Tensile strength (MPa)	Elongation at break (%)	Tensile modulus (MPa)
0.00	81±0.7	26±0.7	7±0.3	185±14	18±1.1
0.39	82±0.8	30±0.6	8±0.5	264±28	20±1.3
0.95	84±0.7	32±0.5	8±1.0	212±28	23±0.8
1.71	86±0.4	33±0.0	10±1.0	191±35	38±7.4

Table 4.24 Mechanical properties of rigid PUR with different Cu contents

Cu content (v/v%)	Shore A hardness	Shore D hardness	Tensile strength (MPa)	Elongation at break (%)	Tensile modulus (MPa)
0.00	95±0.7	65±0.5	22±0.2	31±6	771±38
0.41	93±1.1	61±0.8	21±0.8	81±13	508±21
1.00	96±0.7	65±1.0	17±0.9	59±5	477±10
1.79	98±0.5	68±0.6	17±2.8	63±5	524±8

Table 4.25 Thermal properties of flexible and rigid polyurethane elastomers with different Cu contents

Flexible Polyurethane				Rigid Polyurethane			
Cu content (v/v%)	T _{g, SS} (°C)	T _{g, HS} (°C)	T _{endo} (°C)	Cu content (v/v%)	T _{g, SS} (°C)	T _{g, HS} (°C)	T _{endo} (°C)
0.00	-60	45	68	0.00	-60	44	67
0.39	-60	45	77	0.41	N/A	42	60
0.95	-58	43	65	1.00	N/A	43	64
1.71	-60	41	66	1.79	N/A	44	60

Table 4.26 The glass transition temperature of soft and hard segment of polyurethane elastomers with different Cu contents from DMA technique

Cu content (v/v%)	Flexible PUR		Cu content (v/v%)	Rigid PUR	
	T _{g,SS} (°C)	T _{g,HS} (°C)		T _{g,SS} (°C)	T _{g,HS} (°C)
0.00	-46	11	0.00	-48	83
0.39	-49	-8	0.41	-50	N/A
0.95	-47	-2	1.00	-52	N/A
1.71	-48	3	1.79	-52	N/A

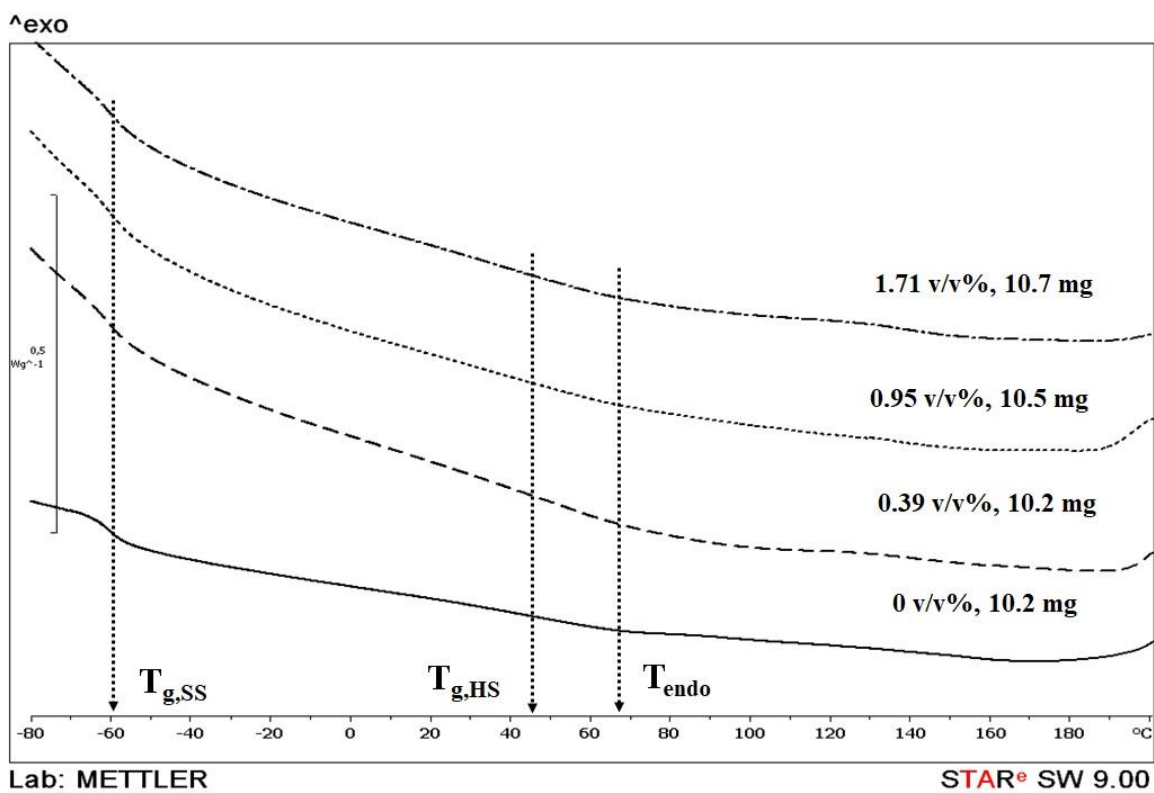


Figure 4.74 DSC curve of flexible PUR with different Cu contents

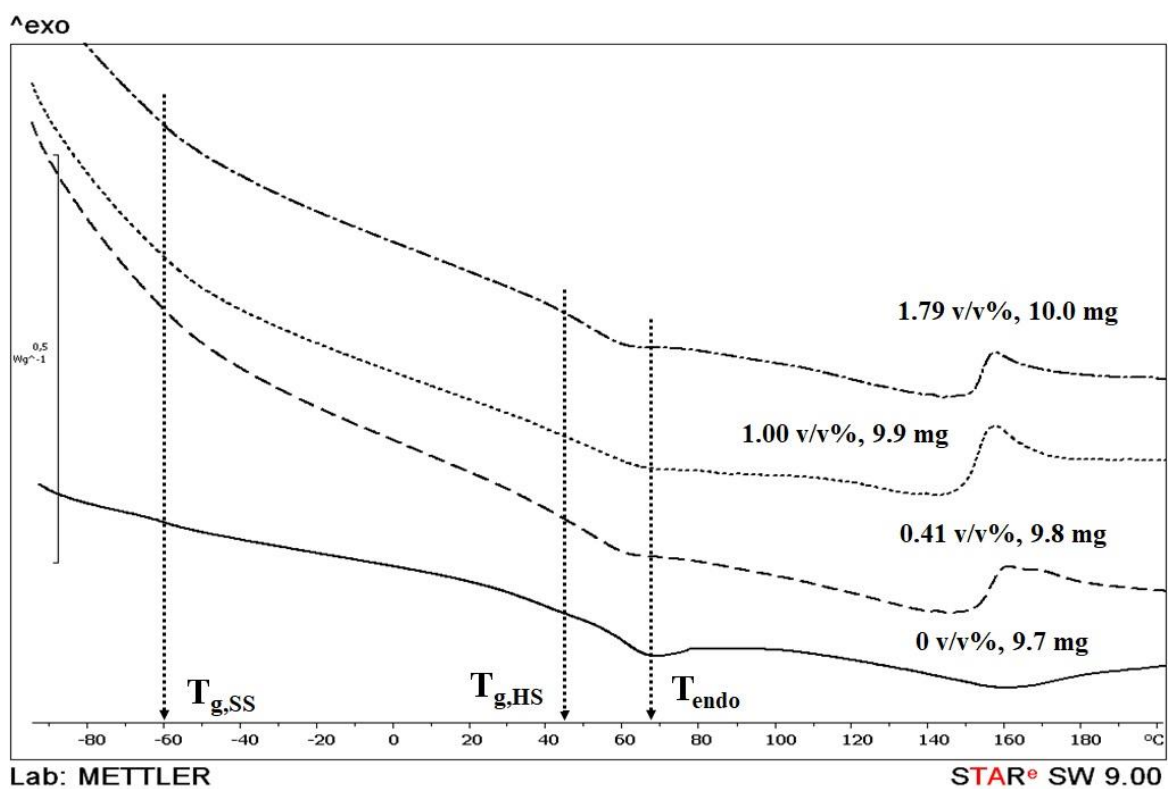


Figure 4.75 DSC curve of rigid PUR with different Cu contents

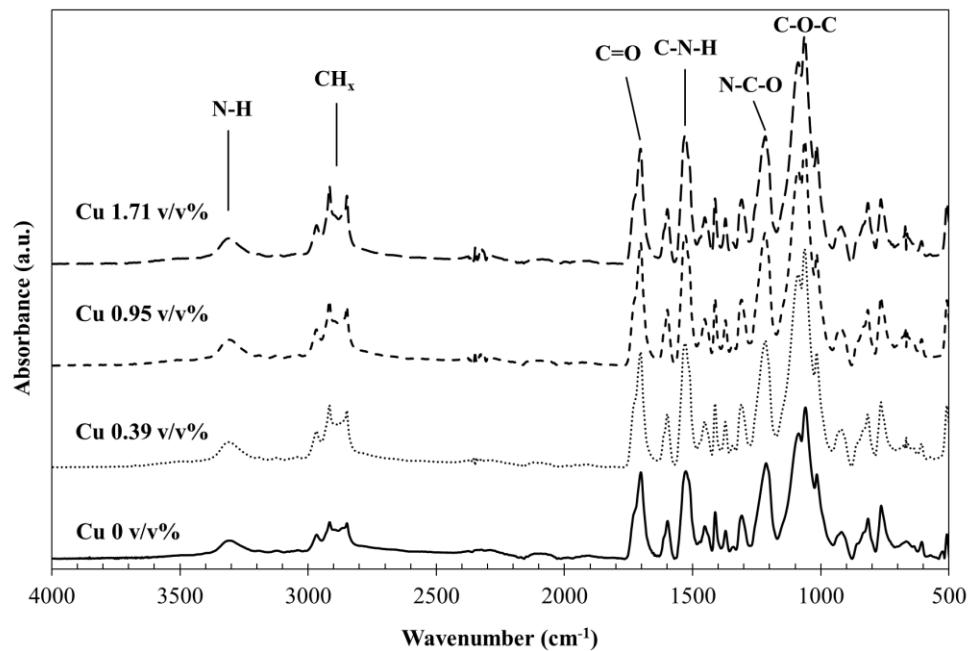


Figure 4.76 IR spectra of flexible polyurethane elastomers with different Cu contents

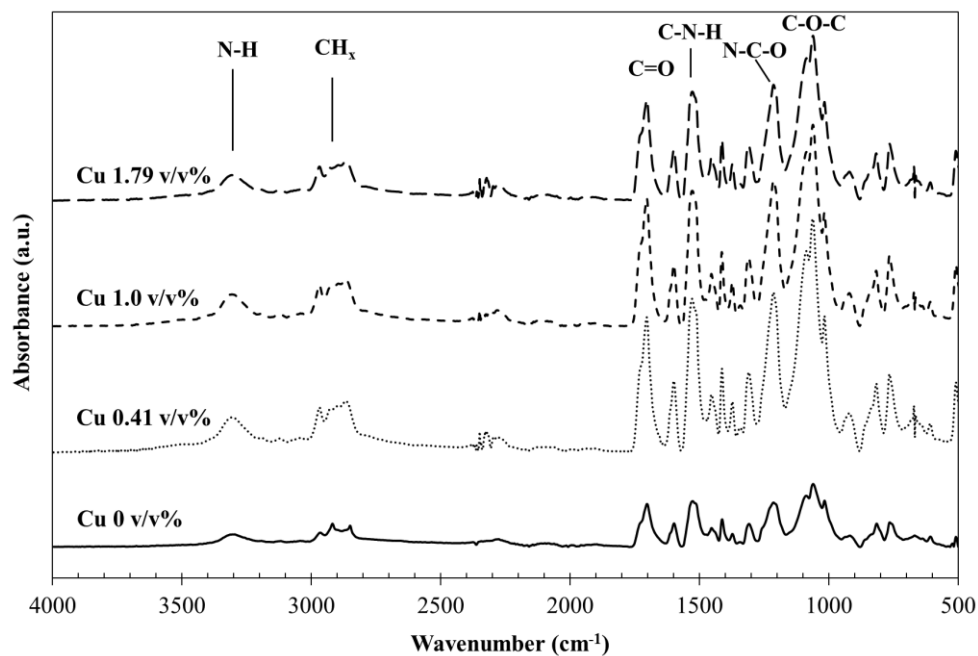


Figure 4.77 IR spectra of rigid polyurethane elastomers with different Cu contents

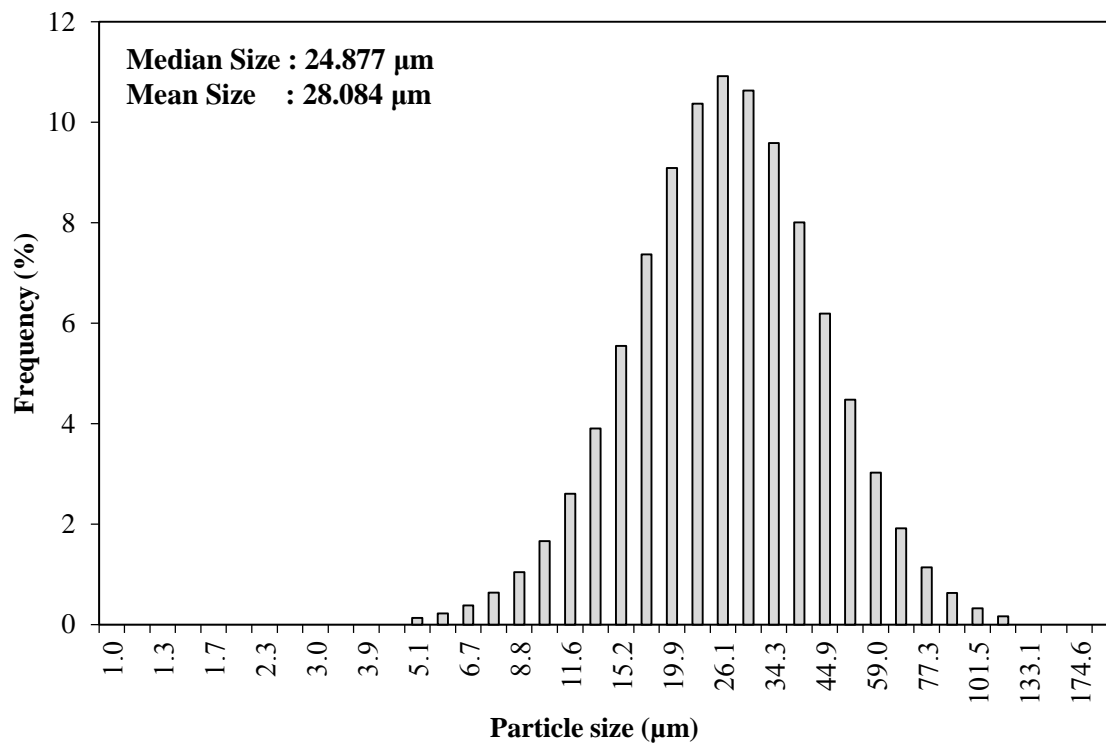


Figure 4.78 Particle size distribution of copper particles

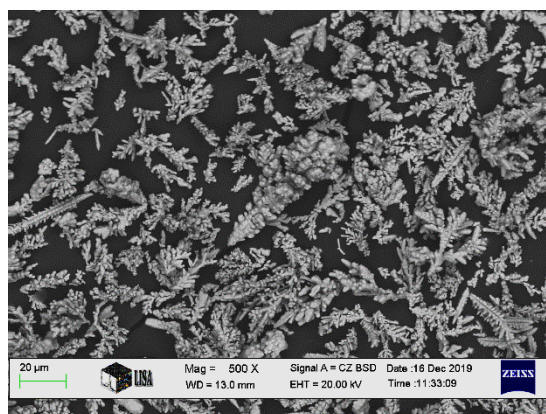


Figure 4.79 SEM image of electrolytic copper particles (nominal magnification of 500 \times)

APPENDIX D

Components and variation of polyurethane elastomer composites samples

Table 4.27 Components and fraction of polyurethane elastomers with different the chain extender contents

Components	Weight fraction (g)				
	7	10	22	30	34
Polyether polyol	100	100	100	100	100
Polypropylene glycol	5	5	5	5	5
Monoethylene glycol	7	10	22	30	34
Amine Catalyst	0.6	0.6	1.2	1.2	1.2
Moisture scavenger	5	5	5	5	5
4,4' diphenylmethane diisocyanate (MDI)	25.76	30.80	44.30	49.83	52.02

Table 4.28 Components and fraction of polyurethane elastomers with different silicon carbide contents

Components	Weight fraction (g)					
	SiC/Flexible PUR composites			SiC/Rigid PUR composites		
	3.79 v/v%	8.13 v/v%	13.18 v/v%	3.97 v/v%	8.51 v/v%	13.75 v/v%
Polyether polyol	100	100	100	100	100	100
Polypropylene glycol	5	5	5	5	5	5
Monoethylene glycol	10	10	10	30	30	30
Amine Catalyst	0.3	0.3	0.3	2.4	1.2	0.9
Moisture scavenger	5	5	5	5	5	5
4,4' diphenylmethane diisocyanate (MDI)	27.76	24.73	21.75	45.33	40.26	35.35
SiC	21	45	75	32	71	121

Table 4.29 Components and fraction of polyurethane elastomers with different magnesium oxide contents

Components	Weight fraction (g)					
	MgO/Flexible PUR composites			MgO/Rigid PUR composites		
	3.41 v/v%	7.36 v/v%	11.98 v/v%	3.57 v/v%	7.70 v/v%	10.49 v/v%
Polyether polyol	100	100	100	100	100	100
Polypropylene glycol	5	5	5	5	5	5
Monoethylene glycol	10	10	10	30	30	30
Amine Catalyst	0.3	0.3	0.3	2.4	0.6	0.6
Moisture scavenger	5	5	5	5	5	5
4,4' diphenylmethane diisocyanate (MDI)	27.76	24.73	21.75	45.33	40.19	37.14
MgO	21	45	75	32	71	100

Table 4.30 Components and fraction of polyurethane elastomers with different zinc oxide contents

Components	Weight fraction (g)					
	ZnO/Flexible PUR composites			ZnO/Rigid PUR composites		
	2.20 v/v%	4.82 v/v%	7.99 v/v%	2.31 v/v%	5.05 v/v%	6.96 v/v%
Polyether polyol	100	100	100	100	100	100
Polypropylene glycol	5	5	5	5	5	5
Monoethylene glycol	10	10	10	30	30	30
Amine Catalyst	0.3	0.3	0.3	0.6	0.6	0.6
Moisture scavenger	5	5	5	5	5	5
4,4' diphenylmethane diisocyanate (MDI)	27.76	24.73	21.75	45.17	40.19	37.14
ZnO	21	45	75	32	71	100

Table 4.31 Components and fraction of polyurethane elastomers with different copper contents

Components	Weight fraction (g)					
	Cu/Flexible PUR composites			Cu/Rigid PUR composites		
	0.39 v/v%	0.95 v/v%	1.71 v/v%	0.41 v/v%	1.00 v/v%	1.79 v/v%
Polyether polyol	100	100	100	100	100	100
Polypropylene glycol	5	5	5	5	5	5
Monoethylene glycol	10	10	10	30	30	30
Amine Catalyst	0.3	0.3	0.3	0.3	0.3	0.3
Moisture scavenger	5	5	5	5	5	5
4,4' diphenylmethane diisocyanate (MDI)	30.07	28.94	27.34	48.70	46.62	44.15
Cu	6	13	24	9	22	39